



3

LIBRARY  
Michigan State  
University



This is to certify that the

dissertation entitled

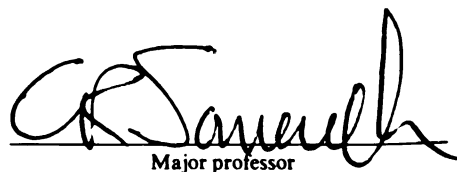
Genetic Analysis of Wax Ester and Tri-  
acylglycerol Biosynthesis in Acinetobacter  
calcoaceticus Strain BD413

presented by

Steven E. Reiser

has been accepted towards fulfillment  
of the requirements for

Ph.D. degree in Biochemistry

  
Major professor

Date 3/18/96

**PLACE IN RETURN BOX to remove this checkout from your record.  
TO AVOID FINES return on or before date due.**

DATE DUE	DATE DUE	DATE DUE
<del>OCT 24 2000</del>	_____	_____
_____	_____	_____
_____	_____	_____
_____	_____	_____
_____	_____	_____
_____	_____	_____
_____	_____	_____

**MSU Is An Affirmative Action/Equal Opportunity Institution**

c:\circ\datedue.pm3-p.1

**GENETIC ANALYSIS OF WAX ESTER AND TRIACYLGLYCEROL  
BIOSYNTHESIS IN *ACINETOBACTER CALCOACETICUS* STRAIN BD413**

**By**

**Steven Edward Reiser**

**A DISSERTATION**

**Submitted to  
Michigan State University  
in partial fulfillment of the requirements  
for the degree of**

**DOCTOR OF PHILOSOPHY**

**Department of Biochemistry**

**1996**



## ABSTRACT

### GENETIC ANALYSIS OF WAX ESTER AND TRIACYLGLYCEROL BIOSYNTHESIS IN *ACINETOBACTER CALCOACETICUS* STRAIN BD413

By

Steven Edward Reiser

The phenomena I have investigated is the accumulation of wax esters and triacylglycerol in the form of intracellular inclusions in the gram negative aerobic bacterium *Acinetobacter calcoaceticus* strain BD413. This strain of *A. calcoaceticus* accumulates both wax esters and triacylglycerol as a means of carbon storage when it undergoes nutrient starvation.

Mutants of strain BD413 were induced using both chemical and transposon mutagenesis methods. By screening colonies for wax accumulation by staining with the lipophilic dye, Sudan black B, followed by TLC, a total of 8 transposon mutants and 21 chemically induced mutants were isolated. These mutants were separated into 3 general categories:  $wax^{+}tag^{+}$ ,  $wax^{+}tag^{-}$  and  $wax^{-}tag^{-}$ .

Nutritional supplementation experiments on the  $wax^{+}tag^{+}$  mutant, *Wow15*, indicated that this mutants genetic lesion was an inability to catalyze the conversion of acyl-CoA to fatty aldehyde. Complementation of this mutant with a cosmid from a cosmid genomic library allowed the identification of an open reading frame encoding the *wow15* gene. The open reading frame shared considerable similarity to an open reading frame described in *Mycobacterium tuberculosis* called ORF2. It is believed that ORF2 acts as a  $\beta$ -keto reductase involved in mycolic acid biosynthesis based on its similarity to a known  $\beta$ -keto reductase.

By expressing the identified open reading frame from *A. calcoaceticus* in *E. coli*, and assaying for the encoded protein's activity, the gene's enzymatic activity was identified. The gene product was observed to catalyze the formation of fatty alcohol from acyl-CoA via a fatty aldehyde intermediate. The isolated gene has been named *acr1* for *acyl-CoA reductase*.

A second aspect of the research described herein concerns mutants isolated following transposon mutagenesis with mini-Tn10PttKm. Flanking sequence surrounding a transposon insertion in strain 11-C7, a *wax<sup>+</sup> tag<sup>-</sup>* mutant, was cloned by inverse PCR (IPCR). DNA sequencing of this DNA allowed the identification of an open reading frame that shares considerable homology to *glnE*, glutamate-ammonia-ligase adenylyltransferase, from *E. coli*. This gene is involved in the regulation of glutamine synthetase (GS), an important enzyme involved in amino acid biosynthesis. Examination of the open reading frames found near the disrupted *glnE* gene indicated that one of these had significant homology to a branched-chain-amino-acid transaminase and a third open reading frame that did not share homology to anything in GenBank, release 92.0. It seems likely that the putative mutation in this line disrupts the ability of the mutant to respond properly to nitrogen concentrations surrounding it.

**Copyright by  
Steven Edward Reiser  
1996**

I dedicate this work to my wife, Sharon. What is that elusive "something" that allows us to love each other forever? You are my effervescent soda bubble, my risotto, in short, my Boopie. This is also for my parents, I love you both. I also dedicate this to rockin' music from the likes of Pearl Jam and the Violent Femmes. Sometimes the situation calls for music with an attitude.

## ACKNOWLEDGMENTS

I would like to thank Dr. Chris Somerville for his tutelage and for providing an environment for independent thought and growth. I really enjoyed our conversations about things like TIGR, biotechnology and the like. Looking at the future through your eyes has been very exciting. I would also like to thank Dr. Christoph Benning, whose guidance as a mentor helped this project really get off the ground. You are a good friend. I also owe thanks to Dr. Jan Jaworski who helped me put some Biochemistry in my Biochemistry degree. Thank you, Amy Stroven who endeavored to screen through thousands of bacterial colonies looking for mutants, and then went back for more to see if they were complemented. I would like to thank Dr. Joe Ogas for providing the pileup which was used to clone a partial acyltransferase. Additional thanks goes to Dr. Michele Nikoloff who took time out to review this manuscript. Special thanks to my committee members Dr. Green, Dr. Kaguni, Dr. McIntosh, Dr. Ohlroggee and Dr. Zeikus for providing guidance and their time. This work was supported by the United States Department of Energy grant DE-FG02-94-ER-20133. Thank you DOE!

RESULTS AND DISSCUSION .....	70
CONCLUSIONS .....	106
REFERENCES .....	108
CHAPTER 4: ISOLATION AND CHARACTERIZATION OF TRANSPOSON MUTANTS FROM <i>A. CALCOACETICUS</i> STRAIN BD413 .....	111
ABSTRACT .....	111
INTRODUCTION .....	112
MATERIALS AND METHODS .....	114
RESULTS AND DISCUSSION .....	126
CONCLUSION .....	141
REFERENCES .....	145
CHAPTER 5: CONCLUSIONS AND PERSPECTIVES .....	146
APPENDIX A: DNA SEQUENCE INFORMATION AND CONTIG MAPS ....	155
APPENDIX B: CONSTRUCTION OF A TRANSCRIPTIONAL EXPRESSION VECTOR FOR <i>A. CALCOACETICUS</i> AND <i>E. COLI</i> .....	174
REFERENCES .....	188
APPENDIX C: CLONING OF A PARTIAL DNA FRAGMENT OF SN-1 ACYLTRANSFERASE FROM <i>A. CALCOACETICUS</i> .....	189
REFERENCES .....	194

## LIST OF TABLES

Table 1-1: A comparison of some naturally occurring wax esters . . . . .	3
Table 1-2: Relative concentrations of neutral lipids in hexadecane inclusions. . . . .	9
Table 1-3: Lipid composition of intracellular inclusions isolated from hexadecanol and hexadecane-grown <i>Acinetobacter</i> sp. strain HO1-N . . . . .	9
Table 1-4: Quantitation of <i>Acinetobacter</i> sp. HO1-N cellular lipids . . . . .	12
Table 1-5: Quantitation of <i>Acinetobacter</i> sp. HO1-N extracellular lipids . . . . .	12
Table 1-6: Energy yields in moles of ATP per mole of energy source . . . . .	14
Table 1-7: Relative changes in the amounts of aliphatic compounds comprising the epicuticular waxes of 20 <i>eceriferum</i> ( <i>cer</i> ) mutants compared to wild type levels . . . . .	15
Table 2-1: Bacterial strains from Chapter 2 . . . . .	25
Table 2-2: Effect of inclusion of hexadecane (0.3% w/v) and hexadecanol (0.3% w/v) on neutral lipid composition of various mutants . . . . .	41
Table 3-1: Bacterial strains used in Chapter 3 . . . . .	53
Table 3-2: Plasmid sources and derivations for Chapter 3 . . . . .	55
Table 3-3: List of synthetic oligonucleotides used in Chapter 3 . . . . .	63
Table 3-4: Cosmids that share homology to 1A-3F . . . . .	74
Table 4-1: Bacterial strains used in Chapter 4 . . . . .	115
Table 4-2: Plasmid sources and derivations for Chapter 4 . . . . .	117
Table 4-3: List of synthetic oligonucleotides used in this Chapter 4 . . . . .	123

Table B-1: Plasmid sources and derivations for Appendix B . . . . .	175
Table B-2: $\beta$ -Galactosidase content of cells transformed with pSER120 constructs . . . . .	181
Table C-1: Synthetic degenerate oligonucleotides used in Appendix C . . . . .	191



## LIST OF FIGURES

Figure 1-1: Structure of a generic wax ester . . . . .	2
Figure 1-2: Proposed pathway for wax ester biosynthesis in <i>Acinetobacter calcoaceticus</i> strain BD413 . . . . .	6
Figure 2-1: A comparison of wax ester accumulation from four strains of <i>A. calcoaceticus</i> . . . . .	31
Figure 2-2: Effect of duration of NTG treatment on cell viability over time following NTG mutagenesis and induced number of Rif <sup>r</sup> colonies . . . . .	33
Figure 2-3: Example of staining for mutants affected in neutral lipid accumulation using the lipophilic dye Sudan black B . . . . .	35
Figure 2-4: TLC plate illustrating the three general classes of mutants . . . . .	36
Figure 2-5: Qualitative TLC analysis of the mutants isolated following NTG mutagenesis . . . . .	37
Figure 2-6: Proposed pathway for wax ester biosynthesis in <i>Acinetobacter calcoaceticus</i> strain BD413 . . . . .	39
Figure 2-7: Chemical complementation of class I and class III mutants grown under nitrogen starvation (wax inducing) conditions in the presence of 0.3% hexadecanol . . . . .	40
Figure 2-8: Chemical complementation of the <i>Wow15</i> mutant . . . . .	43
Figure 3-1: Detailed restriction map of pLA2917 (taken from Allen, 1985) . . . .	71
Figure 3-2: Complementation of <i>Wow1</i> . . . . .	73
Figure 3-3: Restriction map of cosmid 4A-55 and locations of the transposon insertions . . . . .	76
Figure 3-4: Restriction map of cosmid 1A-3F . . . . .	77

Figure 3-5: EcoRV digestions of 4A-55 and transposon containing derivatives . .	80
Figure 3-6: Southern analysis of transposon mutagenized cosmids . . . . .	81
Figure 3-7: Map showing sequence ID#1-9 in respect to one another . . . . .	82
Figure 3-8: DNA and protein sequence of the region containing <i>acr1</i> . . . . .	85
Figure 3-9: Optimized FASTA alignment between <i>acr1</i> and ORF2 . . . . .	87
Figure 3-10: Three-way alignment of <i>acr1</i> (ACAR1.AMI), ORF2 from <i>Mycobacterium tuberculosis</i> (ORF2.AMI) and ActIII from <i>Streptomyces</i> <i>cinnamomensis</i> (ACT3.AMI) . . . . .	89
Figure 3-11: Optimized FASTA alignment between <i>acr1</i> and ActIII . . . . .	90
Figure 3-12: Proposed pathway for wax ester biosynthesis in <i>Acinetobacter</i> <i>calcoaceticus</i> strain BD413 . . . . .	91
Figure 3-13: Complementation of the mutant <i>Wow15</i> with pSER2: <i>acr1</i> . . . . .	93
Figure 3-14: Kyte and Doolittle plots of the protein sequence from <i>acr1</i> . . . . .	94
Figure 3-15: SDS-PAGE gel showing protein induction . . . . .	96
Figure 3-16: <i>In vitro</i> acyl-CoA reductase assay . . . . .	97
Figure 3-17: Demonstration of an <i>in vitro</i> assay showing reductase activity of <i>acr1</i> with different radiolabelled substrates . . . . .	98
Figure 3-18: Cofactor dependence of acyl-CoA reductase . . . . .	99
Figure 3-19: <i>In vitro</i> acyl-CoA reductase timecourse . . . . .	101
Figure 3-20: <i>In vitro</i> enzyme assay testing for reductase activity using 1- <sup>14</sup> C- palmitoyl aldehyde . . . . .	102
Figure 3-21: Secondary structure prediction for <i>acr1</i> and conserved amino acid residues specific to the family of short chain alcohol dehydrogenases . . . .	103
Figure 3-22: <i>In vitro</i> acyl-CoA reductase assay carried out in the presence of unlabelled <i>cis</i> -11-hexadecenal . . . . .	105
Figure 4-1: Positional mapping of the BglIII fragment in the cosmid 5A-F1 . . . .	125

Figure 4-2: Southern blot analysis of 9 random colonies following mutagenesis with mini-Tn10PttKm transposon . . . . .	127
Figure 4-3: Southern analysis of isolated mutants carrying mini-Tn10PttKm . . . .	129
Figure 4-4: Southern analysis of genomic DNA from 30-F10 and 11-C7 . . . . .	131
Figure 4-5: Extended IPCR of 11-C7 and 30-F10 . . . . .	132
Figure 4-6: Southern analysis of 11-C7 with pSER10 . . . . .	133
Figure 4-7: Southern analysis of 5A-F1 cosmid DNA . . . . .	135
Figure 4-8: Southern analysis of 11-C7 with pSR11 . . . . .	137
Figure 4-9: Map showing sequence ID#10-14 in respect to one another . . . . .	138
Figure 5-1: DNA Sequence of <i>Arabidopsis</i> EST T21872 . . . . .	149
Figure 5-2: Optimized FASTA alignment between Acr1 and the <i>Arabidopsis</i> EST, T21872 . . . . .	150
Figure A-1: Sequence ID#1 . . . . .	156
Figure A-2: Sequence ID#2 . . . . .	157
Figure A-3: Sequence ID#3 . . . . .	158
Figure A-4: Sequence ID#4 . . . . .	159
Figure A-5: Sequence ID#5 . . . . .	159
Figure A-6: Sequence ID#6 . . . . .	160
Figure A-7: Sequence ID#7 . . . . .	161
Figure A-8: Sequence ID#8 . . . . .	162
Figure A-9: Sequence ID#9 . . . . .	163
Figure A-10: Sequence ID#10 . . . . .	164
Figure A-11: Sequence ID#11 . . . . .	166
Figure A-12: Sequence ID#12 . . . . .	167

Figure A-13: Sequence ID#13 .....	168
Figure A-14: Sequence ID#14 .....	169
Figure A-15: Sequencing contigs of pSR6 .....	170
Figure A-16: Sequencing contigs of pSR2 .....	171
Figure A-17: Sequencing contigs of pSR11 .....	172
Figure A-18: Sequencing contigs of pSR12 .....	173
Figure B-1: Restriction maps of pBR322, pWH1274, pSER1 and pSER2 .....	176
Figure B-2: Illustration of the steps taken to constuct pSER200-1 and pSER200-4 transcriptional expression vectors for use in <i>A. calcoaceticus</i> ..	178
Figure B-3: Sequence ID#15 .....	183
Figure B-4: Sequence ID#16 .....	183
Figure B-5: Best known restriction map of <i>A. calcoaceticus</i> / <i>E. coli</i> transcriptional expression vector pSER200-1 .....	184
Figure B-6: Results of BLASTX alignment using sequence ID#17 as a query sequence .....	186
Figure B-7: Sequence ID#17 .....	186
Figure B-8: Best known restriction map of <i>A. calcoaceticus</i> / <i>E. coli</i> transcriptional expression vector pSER200-4 .....	187
Figure C-1: Pileup of known and putative acyltransferases .....	190
Figure C-2: Sequence ID#18 .....	193
Figure C-3: BLASTX alignment between a putative acyltransferase from <i>A.</i> <i>calcoaceticus</i> and Sn-1 acyltransferase from <i>E. coli</i> .....	193

## LIST OF ABBREVIATIONS

ATP	Adenosine triphosphate
cfu	Colony forming unit
EDTA	(Ethylenedinitilo)tetraacetic acid
IPCR	Inverse polymerase chain reaction
NADH	Nicotinamide adenine dinucleotide (reduced form)
NADPH	Nicotinamide adenine dinucleotide phosphate (reduced form)
NTG	Nitrosoguanidine
PCR	Polymerase chain reaction
TLC	Thin layer chromatography

## CHAPTER 1

### INTRODUCTION

Wax esters are found in a number of very different organisms. Over a century ago, Melville wrote about wax esters as a liquid gold hunted by whalers in his eighteenth century novel, Moby Dick (Melville, 1851). Referred to as spermaceti oil, these wax esters are stored in the heads of the sperm whale and have the general chemical structure that is shared by all wax esters (Figure 1-1). The North American shrub, jojoba, is a new source of wax esters that is cultivated in the southwestern portion of the United States. In jojoba (*Simmondsia chinensis*), wax esters are stored in the seeds of the plant where they serve as a means of energy and carbon storage for developing seedlings. Wax esters have also been found in a number of microbial organisms such as *Acinetobacter calcoaceticus* strain BD413, a gram negative aerobic bacteria that was first isolated by Juni et. al. (Juni & Janik, 1969) as an unencapsulated form of *A. calcoaceticus* strain BD4. *A. calcoaceticus* strain BD413 accumulates wax esters when grown under nitrogen limited conditions (Fixter et al., 1986). Although these organisms are very diverse, examination of the chemical structures of the waxes they produce reveals that these waxes are very similar to each other structurally, in terms of their fatty acid and fatty alcohol components, carbon chain lengths and degree of saturation (Table 1-1)(Ervin et al., 1984).

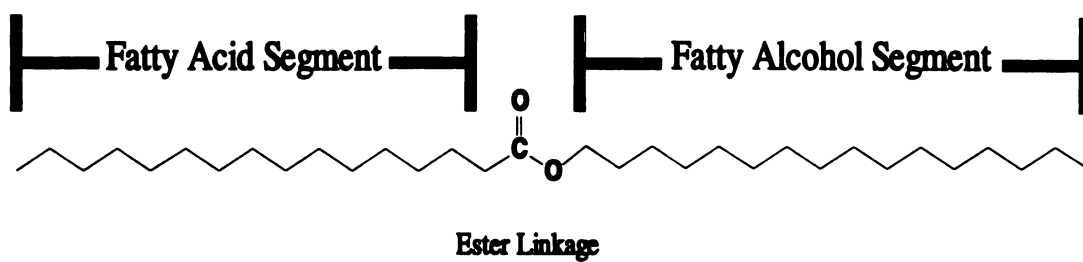


Figure 1-1: Structure of a generic wax ester. The fatty acid, or acyl segment and the fatty alcohol, or alkoxy segment are shown.

Table 1-1: A comparison of some naturally occurring wax esters<sup>a</sup>

	<b>Sperm whale oil</b>	<b>Microbial wax esters</b>	<b>Jojoba oil</b>
Carbon number of intact wax esters	28-40	32-40 <sup>b</sup>	36-44
Fatty acid segments:			
Carbon number	14-22	16-20 <sup>b</sup>	16-24
Number of unsaturations	0 or 1	0 or 1 <sup>c</sup>	1
Fatty alcohol segments:			
Carbon number	16-20	16-20 <sup>b</sup>	18-24
Number of unsaturations	0 or 1	0 or 1 <sup>c</sup>	1
Predominant sites of unsaturation <sup>d</sup>	$\omega$ 7, $\omega$ 9 and $\omega$ 11	$\omega$ 7 and $\omega$ 9	$\omega$ 9

<sup>a</sup>Adopted from Ervin et al., 1984

<sup>b</sup>Carbon numbers dependent on n-alkane used as substrate for growth.

<sup>c</sup>Degree of unsaturation is dependent on growth temperature.

<sup>d</sup>Position of double bond is indicated relative to the end carbon position.

The characterization of wax esters that occur in *Acinetobacter* species has previously been described by several different researchers (Gallagher, 1971; Fixter, 1986). It was observed that when cells of different strains of *A. calcoaceticus* were grown with carbon in abundance but some other nutrient limiting, wax esters accumulated both intracellularly and extracellularly (Makula, 1975; Scott, 1976). Wax esters were also observed when cells were grown under nutrient rich conditions, but to a lesser extent. Cells can be starved for nitrogen, sulphur or phosphorous, and if carbon is in abundance, wax esters will accumulate (Fixter, 1991). The amount of wax ester accumulation was found to be highly variable depending on the strain examined. Wax contents ranged from 0.6 mg to 141.1 mg per gram of bacteria dry



weight (Fixter, 1986).

Wax composition of *A. calcoaceticus* species has been extensively studied. Thirty two carbon length waxes make up the majority (roughly 50%) of waxes produced by *A. calcoaceticus* species (Fixter et al., 1986), while 34 carbon length waxes make up about 40% of the total wax ester content. The remaining 10% can be found in the form of 30 and 36 carbon waxes. These waxes are typically greater than 80% saturated. Examination of the isomeric composition of wax ester species by gas liquid chromatography/mass spectrometry in terms of fatty acid-fatty alcohol combinations was observed to be, what would be expected if one assumed random combination of available fatty acids with fatty alcohols (Fixter & Sherwani, 1991). The degree of desaturation of wax esters can be altered by changing growth temperature. Ervin et. al. report that when *Acinetobacter* species were grown at 30°C, 80% of the wax esters produced were saturated with 18% being monounsaturated and 2% being diunsaturated (Ervin et al, 1984). When the growth temperature was dropped to 24°C, 61% of the waxes were saturated, but the amount of monosaturated waxes climbed to 31% and diunsaturated waxes composed 8% of the total. Finally, when cultures were incubated at 17°C, the amount of saturated wax esters fell to 50%, monounsaturated waxes hovered near 35% and diunsaturated wax esters jumped to 15%. In all of these measurements, diunsaturated compounds were the result of one unsaturation in the acyl segment, and the other unsaturation in the alkoxy segment. Monounsaturated wax esters were the result of an unsaturation in either segment. Finally, unsaturations occurred at the  $\omega 7$  and  $\omega 9$  sites (when numbering from the terminal methyl carbon of the carbon chain) on the acyl segments, and at the  $\omega 7$  site

only in the alkoxy segment.

Wax composition can also be altered by varying the composition of the medium (Dewitt & Ervin, 1982). When cultures are grown in minimal mineral medium with succinate or acetate as a carbon source, wax compositions are observed to be what was previously described, i.e. 50% of the waxes are 32 carbons in length and another 40% being 34 carbons in length. By growing the bacteria in minimal mineral medium with hexadecane (a 16 carbon alkane) as a carbon source 100% of the waxes were 32 carbons in length. Incubation of cultures in longer chain alkanes was found to give rise to wax ester compositions of  $C_{2n}$ ,  $C_{2n-2}$  and  $C_{2n-4}$  (Dewitt & Ervin, 1982). The alcohol segment of the wax esters derived from alkanes was always the same length as the substrate, indicating that the variation observed was due to the length of the fatty acid.

Very little research has been aimed at understanding the biochemistry of wax ester production. Most ideas are based on observed enzymatic activities involved in hydrocarbon oxidation, with the leap in reasoning that what is observed for the degradation of alkanes might be running backwards and be responsible for wax biosynthesis (Fixter et al., 1991). This has given rise to the proposed pathway for wax ester biosynthesis in *A. calcoaceticus* that is illustrated in Figure 1-2. In the production of wax esters *de novo*, it is believed that the starting substrate is either acyl-ACP or acyl-CoA. Acyl-ACP is generally regarded as being the substrate of choice. This is because in many bacteria, particularly *E. coli*, fatty acid biosynthesis typically involves acyl-ACPs rather than CoA derivatives (Rock & Cronan, 1985). In the first committed step of wax ester biosynthesis, acyl-ACP is thought to be reduced

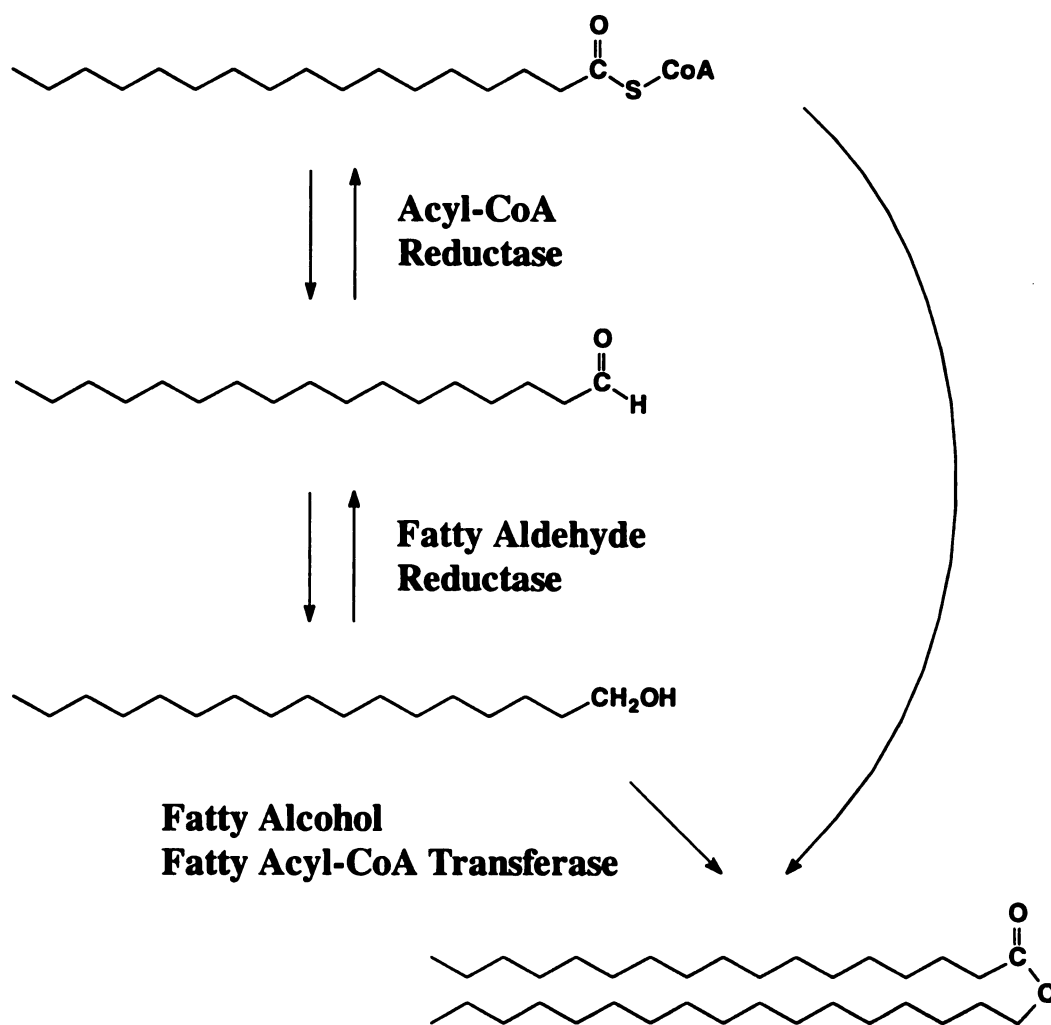


**Figure 1-2:** Proposed pathway for wax ester biosynthesis in *Acinetobacter calcoaceticus* strain BD413.

to the corresponding aldehyde. An aldehyde intermediate is proposed to occur based of the observation of a constitutive NAD-dependent long chain alkanal dehydrogenase and an inducible (induced in the presence of alkanes) NADP-dependent alkanal dehydrogenase in the *Acinetobacter* strain HO1-N (Fox et al., 1992; Singer & Finnerty, 1985c). These activities were detected when strain HO1-N was investigated in relation to its ability to oxidize hexadecane and hexadecanol as carbon sources. With the observed activity of these two enzymes, the idea was put forth that one, or both, of the enzymes might be catalyzing the reverse reaction, reducing acyl-ACP to the corresponding aldehyde. There was no experimental evidence put forth to support this idea. The second step in wax ester formation involves the reduction of the fatty aldehyde to its corresponding fatty alcohol. Here again, the same logic was proposed. Two independent reports describe cofactor dependent and independent fatty alcohol dehydrogenases, and again it is believed that these enzymes may play a role in wax ester biosynthesis (Fox et al., 1992; Singer & Finnerty, 1985b). In this instance also, no experimental evidence was put forth to support the model. No experimental evidence has been presented on the third and final step proposed in wax ester biosynthesis, the formation of wax esters from either an acyl-ACP, or acyl-CoA, and fatty alcohol by acyl-CoA (or ACP):alcohol transferase.

In contrast to *A. calcoaceticus*, the enzymes involved in wax ester biosynthesis of jojoba have been extensively studied and characterized. In this organism it is known that there are two enzymes that directly catalyze the formation of wax esters (Pollard & Metz, 1995; Metz et al., 1995). The first enzyme that was characterized was a fatty acyl-CoA reductase. This enzyme is known to be highly substrate specific

for tetracosenoyl-CoA (a 24 carbon acyl-CoA), and is known to catalyze the formation of a long chain alcohol directly from this substrate via an aldehyde intermediate (Pollard & Metz, 1995). The second enzyme, an acyl-CoA-fatty alcohol transferase catalyzes the formation of an ester linkage between acyl-CoA and a fatty alcohol to yield a wax ester. Assays on this enzyme, found it to be acyl-CoA specific, preferring C<sub>20</sub>-monounsaturated acyl-CoA's and C<sub>14</sub> and C<sub>18</sub> mono- and di- unsaturated fatty alcohols (Metz et al., 1995).

It has been observed for *A. calcoaceticus* that when cellular concentrations of wax esters reach concentrations of 20 mg/g dry weight, inclusion bodies are formed (Fixter et al., 1991). Characterization of these inclusion bodies has never been performed on cells grown in plain, unsupplemented minimal mineral medium. Rather, our knowledge of the composition of inclusion bodies comes from examination of cells grown in minimal mineral medium, supplemented with hexadecane. Table 1-2 recapitulates the neutral lipid profile of inclusion bodies isolated from cells grown under such conditions (Scott & Finnerty, 1976). In a different report put out by the same group 9 years later, the lipid composition of inclusion bodies grown on hexadecane and hexadecanol had the compositions shown in Table 1-3 (Singer & Finnerty, 1985a). These data appear to be contradictory, but represent the only data available. It is also important to note that these studies, along with many others, use *A. calcoaceticus* strain HO1-N. This strain may be very different from other *A. calcoaceticus* species. It was first isolated as *Micrococcus cerificans* by enrichment on hexadecane (Finnerty et al., 1962). It was later reclassified as an *A. calcoaceticus* species. During growth of this culture on alkanes, it was observed that it could

Table 1-2: Relative concentrations of neutral lipids in hexadecane inclusions.<sup>a</sup>

Neutral Lipid	Relative Percentage (%)
Wax ester	50.5
Free fatty acid	5.8
Free fatty alcohol	17.6
Triglyceride	5.7
Diglyceride	6.9
Monoglyceride	1.3
Hexadecane	12

<sup>a</sup>Adapted from Scott & Finnerty, 1976Table 1-3: Lipid composition of intracellular inclusions isolated from hexadecanol and hexadecane-grown *Acinetobacter* sp. strain HO1-N.<sup>a</sup>

Lipid component	Wax ester inclusions (%)	Hydrocarbon inclusions (%) <sup>b</sup>
Phospholipid	9.6	4.7
Wax ester	85.6	1.3
Fatty alcohol	4.8	0.4
Hexadecane	0.0	93.3
Other lipids <sup>c</sup>	0.0	0.3

<sup>a</sup>Taken from Singer et al., 1985a.<sup>b</sup>This data is reported to be derived from the same data presented in Table 1-2.<sup>c</sup>Fatty acid and mono-, di- and triglycerides.

produce up to 4.3 g of wax esters per liter of culture, and most of these waxes were extracellular (Fixter et al., 1991). This is different in respect to other *A. calcoaceticus* species where wax ester accumulation is observed to be intracellular. Mutants of *A. calcoaceticus* strain HO1-N were isolated that were unable to grow on cetyl palmitate (a 32 carbon wax ester) as a sole carbon source. Examination of the amount of wax esters produced by these mutants showed an increase in extracellular wax accumulation. This has led to the speculation that wax ester content in *Acinetobacter* is dependant on the rate of wax ester degradation, rather than the rate of wax ester synthesis (Geigert et al., 1984; Fixter et al., 1991).

Wax ester inclusions of *A. calcoaceticus* strain HO1-N have been examined by electron microscopy where it was observed that they appeared to be surrounded by a monolayer phospholipid membrane. Analysis of this monolayer found it to be composed of phospholipid and proteins. At least five major polypeptide bands were observed when proteins from the membranes were separated on an SDS-PAGE gel (Scott & Finnerty, 1976). Unfortunately, size standards were not included with this data so it is not possible to tell what sizes the proteins are. The lipid and protein composition of the membranes surrounding the vesicles was compared with other membrane fractions of the cell. Their different phospholipid composition, and the banding pattern of proteins isolated from the inclusion membranes led the author to suggest that the membranes arise *de novo*, rather than being derivatives of the cytoplasmic or outer membrane (Fixter et al., 1991). When cells were grown in the presence of hexadecane and hexadecanol, some cells exhibited intracytoplasmic membranes which the author states appeared as lamellar sheaths extending through the

cytoplasm (Scott & Finnerty, 1976; Singer et al., 1985a). Intracellular membranes were also observed in cells grown in the presence of hexadecanol. Examination of succinate grown cultures by electron microscopy never showed the presence of such structures, suggesting that their formation may have something to do with growing the cultures in hydrocarbons.

As indicated in Tables 1-2 and 1-3, in addition to the formation of wax esters, *A. calcoaceticus* also accumulates triacylglycerol (TAG) and other neutral lipids when grown under nitrogen deficient conditions. There has been no investigation of TAG biosynthesis in *Acinetobacter* species other than to note its presence when measuring neutral lipid profiles of cultures grown to induce wax ester biosynthesis. Intracellular and extracellular lipid composition have been measured for *A. calcoaceticus* strain HO1-N grown in nutrient rich NBYE medium versus minimal mineral medium containing hexadecane as a carbon source. The results of these experiments by Makula, et. al. (Makula et al., 1975), are shown in Tables 1-4 and 1-5. Based on these observations it might be assumed that other *Acinetobacter* strains also accumulate triacylglycerol. TAG may be serving as another form of energy storage, in addition to the accumulation of wax esters. Although no biochemical characterization of triacylglycerol biosynthesis has been presented, it could be proposed that, under nitrogen limited conditions, a diacylglycerol-acyltransferase is expressed, leading to an increase in the conversion of diacylglycerol to triacylglycerol. Alternatively, the accumulation of TAG may be the result of a reduction in the conversion of TAG to free fatty acids and glycerol. Based on the data presented in Table 1-2 from Scott et. al. (Scott & Finnerty, 1976) which describes the neutral lipid content of inclusion



Table 1-4: Quantitation of *Acinetobacter* sp. HO1-N cellular lipids.<sup>a</sup>

Lipid class	Medium	
	NBYE <sup>b</sup>	Minimal plus Hexadecane
	$\mu\text{mol/g}$ of cell dry weight	
Phospholipids	46.0	129.0
Triglyceride	1.8	2.5
Mono- and diglyceride	0.4	6.8
Free fatty acid	7.5	8.2
Free fatty alcohol	Trace	2.6
Wax ester	11.5	18.0
Hexadecane	Not detected	360.0

<sup>a</sup>Adapted from Makula et al., 1975<sup>b</sup>Nutrient broth-yeast extract medium. Composition of medium not stated by author.Table 1-5: Quantitation of *Acinetobacter* sp. HO1-N extracellular lipids.<sup>a</sup>

Lipid class	Medium	
	NBYE <sup>b</sup>	Minimal plus Hexadecane
	$\mu\text{mol/L}$	
Phospholipids	Not detected	Not detected
Triglyceride	2.4	25.6
Mono- and diglyceride	0	410.0
Free fatty acid	4.0	60.0
Free fatty alcohol	0	0.5
Wax ester	0	280.0
Hexadecane	0	Not determined

<sup>a</sup>Adapted from Makula et al., 1975<sup>b</sup>Nutrient broth-yeast extract medium. Composition of medium not stated by author.

bodies formed in *A. calcoaceticus* grown under low nitrogen conditions in the presence of hexadecane, it can be assumed that triacylglycerol is being accumulated together with wax esters, and other neutral lipids in the form of inclusion bodies.

Why do organisms synthesize wax esters? Wax esters are composed of carbon in its most reduced form, which yields the maximum amount of energy when oxidized. Additionally, wax esters are extremely hydrophobic and are completely insoluble in water. Therefore, when they are stored intracellularly as inclusion bodies, there is no effect on the osmotic balance of the cell. Together, these two properties make wax esters an excellent means of energy storage. A comparison can be made between the energy yields of glucose, triacylglycerol and wax esters based on the information presented by Mathews and van Holde (Mathews & van Holde, 1990). They calculated the energy yields for glucose and a fatty acyl-CoA (palmitoyl-CoA) in moles of ATP synthesized from ADP. Assuming that the energy yield from one mole of triacylglycerol is equal to the oxidation of three fatty acyl-CoA chains (palmitoyl-CoA), and the oxidation of a wax ester is essentially equivalent to the oxidation of two fatty acyl-CoA chains (i.e. palmitoyl-CoA), Table 1-6 can be derived. It is clear that triacylglycerol and wax esters yield more energy than the oxidation of glucose. This clearly illustrates that both of these compounds can serve as excellent means of energy storage.

Wax esters play many important biological roles other than providing a means of carbon storage. Waxes are critical in the plant kingdom where they provide protection from DNA damaging ultra-violet light, a line of defense against insects, fungus and bacterial pathogens, and probably most importantly, prevention of

Table 1-6: Energy yields in moles of ATP per mole of energy source.

Energy Source	Oxidative Yield (moles of ATP)	ATP Yield per Carbon Oxidized to CO <sub>2</sub> (moles of ATP)
Glucose	38	6.3
Wax Ester (32 carbons)	262	8.2
Triglyceride (ie. 3, 16 carbon fatty acids)	393	8.2

desiccation. The steps believed to take place in the biosynthesis of wax esters in plants is similar to the pathway illustrated in Figure 1-2 for *A. calcoaceticus*, with the exception that the starting substrate is a very long chain fatty acid that is derived by elongating stearyl-CoA (18C) to eicosanoyl-CoA (20C). These long chain fatty acids are believed to be reduced to their corresponding fatty aldehydes, which in turn are further reduced to fatty alcohols. There is biochemical evidence that each of these steps is carried out separately by a fatty acid reductase and a fatty aldehyde reductase, respectively. Demonstration of such enzymatic activities in crude extracts has been shown by Kolattukudy et. al. in *Brassica oleracea* (Kolattukudy, 1971). Wax esters are thought to be formed by linking the long chain fatty alcohols to the long chain fatty aldehydes by an acyl-CoA:fatty alcohol transferase, as has been observed in jojoba. Genetic evidence for the complexity of this pathway in plants can be found in *Arabidopsis thaliana* where at least 21 different loci are thought to be involved in wax biosynthesis based upon the identification of mutants (*cer* for *eceriferum*) (Lemieux et al., 1994). The *cer* mutants of *Arabidopsis* are easily identifiable based on their glossy phenotype. Typically, the stems of wild type plants are coated with waxes giving

them a muted green color. *Cer* mutants, on the other hand, are glossy green in color, presumably because the reduction in the amount of waxes covering the stem leads to a decrease in the amount of diffracted light that is reflected.

Plant waxes are actually composed of many different materials; wax esters are only one component. Besides wax esters, plants accumulate long chain aldehydes, fatty acids, primary alcohols, hydrocarbons, secondary aldehydes and ketones (Lemieux et al., 1994). Thus, with all of these components being synthesized and secreted, it is not surprising to find so many different mutants. The problem then, in dealing solely with wax ester biosynthesis, is to identify mutants affected in only wax esters and their intermediates. To characterize the *cer* mutants of *Arabidopsis*, Lemieux et. al. (Lemieux et al., 1994) measured relative changes in neutral lipid compounds that make up the epicuticular waxes. This allowed them to assign possible defects to 5 of the 21 mutants. Two of these mutants, *cer4* and *cer8* appear to be blocked in steps directly related to the synthesis of wax esters. The data for these 2 mutants is summarized in Table 1-7 (Lemieux et al., 1994).

Table 1-7: Relative changes in the amounts of aliphatic compounds comprising the epicuticular waxes of 20 *eceriferum* (*cer*) mutants compared to wild type levels.<sup>a,b</sup>

Line	Fatty acids	Primary alcohols	Aldehydes	Alkanes	Secondary alcohols	Ketones
<i>cer4</i>	70.4	4.5	127	112	177	107
<i>cer8</i>	434	63.5	4.3	31.0	8.1	8.2

<sup>a</sup>Amounts expressed as percent of wild type levels.

<sup>b</sup>From Lemieux et al., 1994.

Because of the reduction of primary alcohols observed in *cer4*, this mutant is thought to have a lesion in its ability to convert fatty aldehydes to fatty alcohols. The other locus, *cer8*, is thought to regulate the reduction of fatty acids to fatty aldehydes, because of the dramatic accumulation of fatty acids and reduction in aldehyde content (Lemieux et al., 1994). Thus, based on genetic and biochemical evidence it would appear that wax ester biosynthesis in *Arabidopsis* is carried out in a similar manner to what is hypothesized to occur in *Acinetobacter*.

As stated previously, very little is known about the enzymes involved in wax ester biosynthesis in *A. calcoaceticus* species. By understanding the biosynthesis of wax esters, we can gain an insight into an alternative means of energy storage, which, on the surface, seems as energy rich as triacylglycerol (in terms of ATP yield per carbon atom). Additionally, an understanding of wax ester biosynthesis in *Acinetobacter* could lead to insights about similar pathways in other organisms, such as *Arabidopsis*.

Because of its ability to synthesize wax esters and triacylglycerol, *A. calcoaceticus* seemed like an excellent organism to use for the study of wax ester biosynthesis. Although there is direct biochemical evidence of enzymes involved in wax biosynthesis in plants, and genetic support of the proposed pathway in the form of the *cer* mutants of *Arabidopsis*, there were many advantages to using *A. calcoaceticus* instead of *Arabidopsis* for such a study. Both facile genetics and fast growth rate make *A. calcoaceticus* a more attractive model organism for wax ester biosynthesis than *Arabidopsis*. As previously mentioned wax ester and triacylglycerol accumulation are both induced under nitrogen limited conditions in *A. calcoaceticus*. This makes an

excellent premise for a genetic screen. Both of these compounds are presumably not necessary for the vitality of the organism under laboratory conditions. Thus, mutations in either pathway could be suffered by the organism with very little or no adverse affects. This is in contrast to some of the *cer* mutants of *Arabidopsis* which are male-sterile, or must be grown under very humid conditions to avoid death by desiccation (Lemieux et al., 1994). Waxes and triacylglycerol are both neutral lipids and can be readily separated and observed by thin layer chromatography (Kates, 1986). This presents an easy, although somewhat tedious, way of screening for mutants in either one of these pathways at the same time. The ability of *A. calcoaceticus* to be grown on hydrocarbons, fatty aldehydes (this work) and fatty alcohols as sole carbon sources presents a unique and simple means of characterizing mutants involved in wax ester biosynthesis. Presumably mutations in the wax ester pathway can be bypassed simply by adding a precursor of wax ester metabolism such as hexadecane, or intermediates such as hexadecanal or hexadecanol. The ability of these compounds to complement the mutants might signal where in the pathway a mutant has been effected.

Finally, an important characteristic of certain *A. calcoaceticus* species is that certain strains of *A. calcoaceticus* are naturally competent for DNA transformation (Juni & Janik, 1969; Palmen et al., 1993). It has been observed as early as 1969, that when actively growing cultures of *A. calcoaceticus* were presented with DNA they are able to up take the molecule and alter their genotype by utilizing genes from the exogenously acquired DNA. This property could be used to facilitate genetic complementation of mutants.

In this work I present experiments in which I have taken a genetic approach to

understanding wax ester biosynthesis in *A. calcoaceticus*. Chapter 2 details the conditions used to mutagenize and screen for mutants affected in wax ester and triacylglycerol accumulation. Also, the isolated mutants were characterized by nutritional supplementation experiments involving wax ester intermediates. Chapter 3 describes the genetic complementation of a mutant affected in wax ester biosynthesis. The cloning of the gene *acr1* is described along with *in vitro* enzyme assays demonstrating the function of the cloned gene. Chapter 4 deals with new mutants that were isolated by transposon mutagenesis using mini-Tn10PttKm. Flanking sequence surrounding the transposon in one of the triacylglycerol mutants is subcloned, sequenced and described. Finally, Chapter 5 summarizes the knowledge gained from the previous chapters and the three appendixes at the end of this text. Recommended directions of research are presented in context to the tools and discoveries highlighted in the previous chapters.

## REFERENCES

- Dewitt, S., Ervin, J. L., Howes-Orchison, D., Dalietos, D., and Neidleman, S. L.. 1982. Saturated and Unsaturated Wax Esters Produced by *Acinetobacter* sp. H01-N Grown on C<sub>16</sub>-C<sub>20</sub> *n*-Alkanes. *JAOCs* 59(2): 69-74.
- Ervin, J. L., Geigert, J., Neidleman, S. L., and Wadsworth, J.. Substrate-Dependent and Growth Temperature-Dependent Changes in the Wax Ester Compositions Produced by *Acinetobacter* sp. H01-N. In Biotechnology for the Oils and Fats Industry, American Oil Chemists Society, 1984. Eds. Ratledge, C., Dawson, P. and Rattray, L..
- Finnerty, W. R., Hawtrey, E. and Kallio, R. E.. 1962. Alkane-Oxidizing Micrococci. *Zeitschrift für Allg. Mikrobiologie* 2(3): 169-177.
- Fixter, L. M., Nagi, M. N., McCormack, J. G. and Fewson, C. A.. 1986. Structure, Distribution and Function of Wax Esters in *Acinetobacter calcoaceticus*. *J. Gen. Micro.* 132: 3147-3157.

- Fixter, L. M. and Sherwani, M. K.. Energy Reserves in *Acinetobacter*. In The Biology of *Acinetobacter*: Taxonomy, Clinical Importance, Molecular Biology, Physiology, Industrial Relevance. Plenum Press, New York, New York. 1991. Eds. Towner, K. J., Bergogne-Bérézin, E., and C. A. Fewson.
- Fox, M. G. A., Dickinson, M. and Ratledge, C.. 1992. Long-Chain Alcohol and Aldehyde Dehydrogenase Activities in *Acinetobacter calcoaceticus* strain H01-N. *J. Gen. Micro.* 138:1963-1972.
- Gallagher, I. H. C.. 1971. Occurrence of Waxes in *Acinetobacter*. *J. Gen. Micro.* 68:245-247.
- Geigert, J, Neidleman, S. L. and DeWitt, S. K.. 1984. Further Aspects of Wax Ester Biosynthesis by *Acinetobacter* sp. H01-N. *JAOCS*, 61(11): 1747-1750.
- Juni, E. and Janik, A.. 1969. Transformation of *Acinetobacter calco-aceticus* (*Bacterium anitratum*). *J. Bact.* 98(1): 281-288.
- Kates, M.. 1986. Techniques of Lipidology: Isolation, Analysis and Identification of Lipids. Elsevier Science Pub. Co., New York, New York.
- Kolattukudy, P. E.. 1971. Enzymatic Synthesis of Fatty Alcohols in *Brassica oleracea*. *Arch. Biochem. Biophys.* 142: 701-709.
- Lemieux, B., Koornneef, M. and Feldmann, K. A.. Epicuticular Wax and *eceriferum* Mutants. In *Arabidopsis*. Cold Spring Harbor Laboratory Press, New York, New York. 1994. Eds. Meyerowitz, E. M. and Somerville, C. R..
- Makula, R. A., Lockwood, P. J. and Finnerty, W. R.. 1975. Comparative Analysis of Lipids of *Acinetobacter* Species Grown on Hexadecane. *J. Bact.* 121(1): 250-258.
- Mathews, C. K. and van Holde, K. E.. 1990. Biochemistry. Benjamin/Cummings Pub. Co., Redwood City, California.
- Melville, H. 1851. Moby Dick.
- Metz, J. G., Lardizabal, K. D., and Lassner, M. W.. 1995. Calgene Inc.. United States Patent #5,445,947. Jojoba Wax Biosynthesis Gene. Filed May 20, 1993, awarded Aug. 29, 1995.
- Ohlrogge, J. B., Pollard, M. R. and Stumpf, P. K.. 1978. Studies on Biosynthesis of Waxes by Developing Jojoba Seed Tissue. *Lipids* 13(3): 203-210.
- Palmen, R., Vosman, B., Buijsman, P., Breek, C. K. D., and K. J. Hellingwerf. 1993. Physiological Characterization of Natural Transformation in *Acinetobacter*



*calcoaceticus*. *J. Gen. Micro.* 139:295-305.

Pollard, M. R. and Metz, J. G.. 1995. Calgene, Inc.. United States Patent #5,411,879. Fatty Acyl Reductases. Filed Nov. 8, 1993, awarded May 2, 1995.

Rock, C. O. and Cronan, J. E.. 1985. Lipid Metabolism in Prokaryotes. In Biochemistry of Lipids and Membranes. Eds. Vance, D. E. and Vance, J. E.. Benjamin/Cummings, Menlo Park, California.

Scott, C. C. L. and Finnerty, W. R.. 1976. Characterization of Intracytoplasmic Hydrocarbon Inclusions from the Hydrocarbon-Oxidizing *Acinetobacter* Species H01-N. *J. Bact.* 127(1): 481-489.

Singer, M. E., Tyler, S. M. and Finnerty, W. R.. 1985a. Growth of *Acinetobacter* sp. Strain H01-N on *n*-Hexadecanol: Physiological and Ultrastructural Characteristics. *Mol. Gen. Genetics* 162: 162-169.

Singer, M. E. and Finnerty, W. R.. 1985b. Alcohol Dehydrogenases in *Acinetobacter* sp. Strain H01-N: Role in Hexadecane and Hexadecanol Metabolism. *J. Bact.* 164(3): 1017-1024.

Singer, M. E. and Finnerty, W. R.. 1985c. Fatty Aldehyde Dehydrogenases in *Acinetobacter* sp. Strain H01-N: Role in Hexadecane and Hexadecanol Metabolism. *J. Bact.* 164(3): 1011-1016.

## CHAPTER 2

### *A. CALCOACETICUS* STRAIN BD413 AS A MODEL ORGANISM FOR THE BIOSYNTHESIS OF WAX ESTERS AND TRIACYLGLYCEROL

#### ABSTRACT

Mutants of *A. calcoaceticus* that are deficient in wax ester and triacylglycerol accumulation were induced using nitrosoguanidine. Colonies with reduced wax or triacylglycerol content were identified using the lipophilic dye Sudan Black B to stain replicas of colonies. Lighter stained colonies were selected and subsequently analyzed by TLC for wax and triacylglycerol content. In this manner over 6400 colonies were examined. A total of 25 mutants of three different phenotypic classes were isolated. Class I mutants are affected in wax ester accumulation, but have normal levels of triacylglycerol. Class II mutants have decreased levels of triacylglycerol, but normal amounts of wax esters, and class III mutants are affected in both wax ester and triacylglycerol accumulation.

Characterization of the mutants was carried out using chemical complementation experiments involving growing the cultures in the presence of 0.3% hexadecane or 0.3% hexadecanol under low nitrogen conditions. None of the mutants had any phenotypic change when cultured in the presence of hexadecane. However, all of the class I mutants were able to synthesize wax esters when incubated in the presence of hexadecanol. Hexadecanol had no affect on any of the class II or class III

mutants.

Characterization of the *Wow15* mutant (wax<sup>-</sup>) was further conducted with additional nutritional supplementation experiments using 0.3% Tween-40 or 0.3% *cis*-11-hexadecenal. Incubation of this mutant in the presence of Tween-40 had no effect on the mutant phenotype, while growth on *cis*-11-hexadecenal as a carbon source restored the ability of the mutant to produce wax esters. This result indicates that the *Wow15* mutant has been affected in its ability to convert acyl-CoA (or acyl-ACP) to the corresponding aldehyde.

## INTRODUCTION

*Acinetobacter* are known to accumulate both wax esters and triacylglycerol as intracellular inclusions under nutrient starvation conditions (Makula et al., 1975; Scott & Finnerty, 1976). It has been reported that the inclusions are synthesized under low nitrogen or low phosphorous conditions, presumably as a means of carbon storage (Fixter et al., 1991). The inclusions are primarily composed of wax esters which are predominantly 32 carbons in length (Fixter et al., 1986). Waxes are composed of an alkoxy segment donated by hexadecanol, a 16 carbon fatty alcohol, and a 16 carbon fatty acid segment presumably originating from either palmitoyl-CoA or palmitoyl-ACP. Wax esters composed of 34 carbon atoms are also common and are derived from 16 carbon alcohols and 18 carbon fatty acids (Fixter et al., 1986). Smaller amounts of different chain length wax esters are also observed, being derived from different chain length substrates (ie. 30, 31, 33, 35 and 36 carbon wax esters). It has been reported that temperature plays a key role in the saturation of the wax ester

compounds (Ervin et al., 1984). Mono and disaturated compounds become more prevalent as incubation temperatures decrease. No characterization of the triacylglycerol found in these inclusions has taken place, other than to note its presence (Makula et al., 1975; Scott & Finnerty, 1976; Singer et al., 1985).

Wax composition can also be altered by varying the carbon source in the medium (Dewitt & Ervin, 1982). *A. calcoaceticus* is able to metabolize fatty alcohols and alkanes. Different wax ester products can be predicted when the cells are cultured in their presence. For example, addition of an 18 carbon alcohol to the medium results in wax ester inclusions that are predominantly 34 carbons in length. This is the result of the 18 carbon alcohol being linked to palmitoyl-CoA. Thus, by growing *A. calcoaceticus* in the presence of fatty alcohols or alkanes, it is possible to directly provide both an intermediate or a precursor, respectively, to wax ester biosynthesis. This allows the formulation of experiments that would allow the biochemical analysis of wax ester production through the addition of these intermediates to the medium.

*A. calcoaceticus* can be transformed by incubating the bacteria in the presence of DNA (Juni & Janik, 1969; Palmen et al., 1993). This facilitates the application of recombinant DNA techniques where such a property makes working with *A. calcoaceticus* amenable to such methods as targeted gene replacement and complementation by introduction of exogenous DNA. As an interesting side note, *A. calcoaceticus* is so competent that it has become an increasing problem in hospitals where immune compromised patients fall prey to nosocomial (infections obtained when visiting a hospital, usually in an immune compromised state) infections from *A. calcoaceticus*. Although normally not a problem, recently *A. calcoaceticus* strains

have been identified as harboring antibiotic resistance genes which they have acquired from other organisms. It is thought that microbes like *A. calcoaceticus* may be sharing their genetic information with other more lethal pathogens, thus attributing to the increase in deaths in this country by contagious disease (Bergogne-Bérézin & Joly-Guillou, 1991).

In this chapter several different strains of *A. calcoaceticus* are compared in terms of wax ester and triacylglycerol accumulation. A particular strain, BD413, was selected for further study. Mutagenesis of this strain was carried out using nitrosoguanidine to generate mutants affected in wax ester and triacylglycerol biosynthesis. In order to characterize the mutants, I took advantage of the fact that *A. calcoaceticus* is able to utilize exogenous fatty alcohols and alkanes. By growing the mutants in the presence of these substrates, it was possible to get some understanding of the biochemical nature of the lesions in some of the mutants.

## **MATERIALS AND METHODS**

**Bacterial stains and plasmids.** The bacterial strains used in the experiments described in this chapter are shown in Table 2-1.

**Growth and culture conditions.** Low nitrogen minimal medium (per liter, 2.0 g  $\text{KH}_2\text{PO}_4$ , 1.18 g succinic acid, 0.1 g  $\text{NH}_4\text{SO}_4$ , pH adjusted to 7.0 with solid KOH; after autoclaving add 20 ml of sterilized 2%  $\text{MgSO}_4$ ) was used in experiments with *Acinetobacter calcoaceticus* strain BD413 to induce wax ester formation. High nitrogen minimal medium, which was the same as the above except for the addition of

Table 2-1: Bacterial strains from Chapter 2.

Bacterial Strains	Relevant Characteristics	Source or Reference
<i>A. calcoaceticus</i>		
ACB #14987	wild type	ATCC stock center
ATCC #23055	wild type	ATCC stock center
ATCC #19606	wild type	ATCC stock center
ATCC #33305, strain BD413	wild type used during these studies, unencapsulated mutant of <i>A. calcoaceticus</i> strain BD4	ATCC stock center
<i>Wow1</i>	wax <sup>-</sup> null mutant of BD413	This study, Chapter 2
<i>Wow2</i>	wax <sup>-</sup> null mutant of BD413	This study, Chapter 2
<i>Wow3</i>	wax <sup>-</sup> tag <sup>-</sup> null mutant of BD413	This study, Chapter 2
<i>Wow4</i>	wax <sup>-</sup> tag <sup>-</sup> leaky mutant of BD413	This study, Chapter 2
<i>Wow5</i>	wax <sup>-</sup> tag <sup>-</sup> leaky mutant of BD413	This study, Chapter 2
<i>Wow6</i>	tag <sup>-</sup> leaky mutant of BD413	This study, Chapter 2
<i>Wow7</i>	tag <sup>-</sup> null mutant of BD413	This study, Chapter 2
<i>Wow9</i>	wax <sup>-</sup> tag <sup>-</sup> leaky mutant of BD413	This study, Chapter 2
<i>Wow10</i>	wax <sup>-</sup> tag <sup>-</sup> leaky mutant of BD413	This study, Chapter 2
<i>Wow11</i>	tag <sup>-</sup> leaky mutant of BD413	This study, Chapter 2
<i>Wow12</i>	wax <sup>-</sup> tag <sup>-</sup> leaky mutant of BD413	This study, Chapter 2

Table 2-1 (cont'd)

<i>Wow13</i>	wax <sup>-</sup> null mutant of BD413	This study, Chapter 2
<i>Wow14</i>	wax <sup>-</sup> null mutant of BD413	This study, Chapter 2
<i>Wow15</i>	wax <sup>-</sup> null mutant of BD413	This study, Chapter 2
<i>Wow16</i>	wax <sup>-</sup> tag <sup>-</sup> leaky mutant of BD413	This study, Chapter 2
<i>Wow17</i>	tag <sup>-</sup> leaky mutant of BD413	This study, Chapter 2
<i>Wow18</i>	tag <sup>-</sup> null mutant of BD413	This study, Chapter 2
<i>Wow20</i>	tag <sup>-</sup> leaky mutant of BD413	This study, Chapter 2
<i>Wow22</i>	tag <sup>-</sup> leaky mutant of BD413	This study, Chapter 2
<i>Wow23</i>	wax <sup>-</sup> tag <sup>-</sup> leaky mutant of BD413	This study, Chapter 2
<i>Wow24</i>	tag <sup>-</sup> leaky mutant of BD413	This study, Chapter 2
<i>Wow25</i>	wax <sup>-</sup> tag <sup>-</sup> leaky mutant of BD413	This study, Chapter 2
<i>Wow26</i>	wax <sup>-</sup> tag <sup>-</sup> leaky mutant of BD413	This study, Chapter 2
<i>Wow27</i>	wax <sup>-</sup> tag <sup>-</sup> leaky mutant of BD413	This study, Chapter 2
<i>Wow28</i>	wax <sup>-</sup> null mutant of BD413	This study, Chapter 2

---

1.0 g  $\text{NH}_4\text{SO}_4$  per liter. For other purposes such as DNA isolation, *A. calcoaceticus* was grown and maintained on LB medium (10 g Bacto tryptone, 5 g Bacto yeast extract and 10 g NaCl per liter, pH 7.0). For chemical complementation experiments, the above minimal medium were used with the addition of 0.3% of the substrate (hexadecane, hexadecanol, Tween-40 (polyoxyethylenesorbitan monopalmitate) or *cis*-11-hexadecenal). Hexadecane and hexadecanol were sonicated for approximately 2 minutes in the medium to generate a suspension. *A. calcoaceticus* cultures were typically grown overnight with shaking at 30°C. For the growth of larger volume cultures (i.e. 50 mls and larger), 3 ml overnight cultures were collected by centrifugation, the cell pellet was washed in the new medium, recentrifuged and then added to the fresh medium, before being incubated at 30°C overnight. Maintenance and growth of *Escherichia coli* strains was on LB with appropriate antibiotics. Antibiotics were used in the following concentrations: ampicillin 100 µg/ml, chloramphenicol 50 µg/ml, kanamycin 25 µg/ml, rifampicin 50 µg/ml and tetracycline 15 µg/ml.

**Chemical mutagenesis.** A 25 ml culture of *Acinetobacter calcoaceticus* strain BD413 was inoculated with a 0.5 ml sample of overnight culture. Incubation continued at 30°C for 45 minutes until the observed optical density at 600 nm was approximately 0.6. Three milliliters was removed for determination of the number of viable cells at the beginning of the experiment. At this point, 2.3 mg of nitrosoguanidine (NTG) (0.1 mg/ml final concentration) was added and the culture was allowed to incubate for an additional 50 minutes at room temperature (in a chemical safety hood) with shaking. Every 10 minutes (time=0, 10, 20, 30, 40 and 50 minutes)



a 3 ml sample was removed and placed on ice. In between the collection of every sample, the previous sample was centrifuged to pellet the cells and the supernatant was removed and replaced with fresh LB broth without NTG. Each sample was diluted (a thousand fold, one hundred thousand fold and ten million fold) and plated onto LB plates to determine the number of viable colonies. The remainder of the samples was spun again to collect the cells, the medium containing NTG was removed, and another 3 mls of fresh LB medium added. These 3 ml cultures were incubated at 30°C overnight. The next day, 1 ml of each culture was frozen in 7% DMSO and stored at -80°C as a stock. Another 1 ml from each time point was collected and plated onto LB plates containing 100 µg/ml rifampicin to determine the spontaneous, and induced rates of resistance, thus giving some indication of the mutagenic effect of NTG on *A. calcoaceticus*. Samples from 30 and 50 minutes were then spread onto LB plates and the resulting colonies were transferred onto LB master plates in arrays of 100 colonies per 100 mm petri plate.

**Mutant screening using the lipophilic dye Sudan black B.** The master plates were replica plated onto low nitrogen minimal medium and the replicas were incubated overnight at 30°C to induce wax formation. The induced colonies were then stained by irrigating the plates with sudan black B (0.02% in 50:45:5 DMSO:ethanol:water) and gently shaking for approximately 20 minutes. The stain was aspirated away and the plates were carefully washed with 70% ethanol and gently shaking them for approximately 2 minutes. Lighter staining colonies were identified from the stained plates and the corresponding colony from the master plate was subsequently analyzed by thin layer chromatography.

**Thin layer chromatography (TLC).** For mutant screening, *A. calcoaceticus* samples to be analyzed by TLC were typically grown in 3 ml cultures in low nitrogen minimal medium. Fifty milliliter cultures were used at other times. Samples were collected by centrifugation (5 minutes at 3000 x g) and the medium removed. Pellets were washed in additional medium, centrifuged, and the supernatant removed. Neutral lipids were isolated from 50 ml cultures by extracting the cells with 3 ml (75  $\mu$ l for 3 ml cultures) chloroform:methanol (50:50) followed by phase separation using 1 ml (25  $\mu$ l for 3 ml cultures) 1 M potassium chloride in 0.2 M phosphoric acid. Samples were centrifuged at 2000 x g in a clinical centrifuge at room temperature for 2 minutes. The chloroform phase was then transferred to a new glass tube and dried under nitrogen, or in the case of the 3 ml cultures used during screening, the chloroform phase was directly spotted onto a TLC plate. Samples were subsequently resuspended in amounts of chloroform proportional to their cellular wet weights (typically 0.5 ml for a 50 ml culture). Twenty microliters of these samples were spotted onto 19-channel Si-250 TLC plates containing preadsorbant layers (Baker) that had been charged by incubating at 120°C for 10 minutes. Ten microliters of 2 mg/ml standards of known lipid species were also loaded for comparison during subsequent analysis. Lipids were resolved by running the plates in hexane:ethyl ether:acetic acid (90:10:1). Samples were visualized by spraying the plates with 50% sulfuric acid and charring at 160° for approximately 5 minutes, or by iodine staining by immersing the plate in iodine vapor until visualization of the lipids was possible.

## RESULTS AND DISCUSSION

### Comparison of neutral lipid accumulation in various strains of *A.*

*calcoaceticus*. To determine which strain of *A. calcoaceticus* to work with, four different strains (ACB #14987, ATCC #23055, ATCC #19606 and ATCC #33305) were examined to determine their degree of wax ester accumulation under low nitrogen conditions. The four strains were selected based on their use by other researchers working with *Acinetobacter*. Neutral lipids from 50 ml cultures, grown under noninducing (high nitrogen) and inducing (low nitrogen) conditions, were isolated by chloroform:methanol extraction. The lipids were spotted proportionately based on cellular wet weight onto a TLC plate, separated, and visualized by charring (Figure 2-1). Two of the four strains exhibited a strong, inducible accumulation of wax esters under low nitrogen conditions. Additionally, one of these strains, ATCC #33305 commonly referred to as *A. calcoaceticus* strain BD413, also showed the accumulation of another neutral lipid under low nitrogen conditions. This lipid species comigrates with a known triacylglycerol standard. The identity of this lipid as triacylglycerol is consistent with several previous reports of the kinds of lipids that accumulate in *A. calcoaceticus* under low nitrogen conditions (Makula et al., 1975; Scott & Finnerty, 1976; Singer et al., 1985). These findings together with a report that strain BD413 is naturally competent for genetic transformation (Juni & Janik, 1969; Juni, 1972; Palmen et al., 1993), suggested to me that *A. calcoaceticus* strain BD413 was the best available strain for the genetic analysis of wax ester biosynthesis in *A. calcoaceticus*.

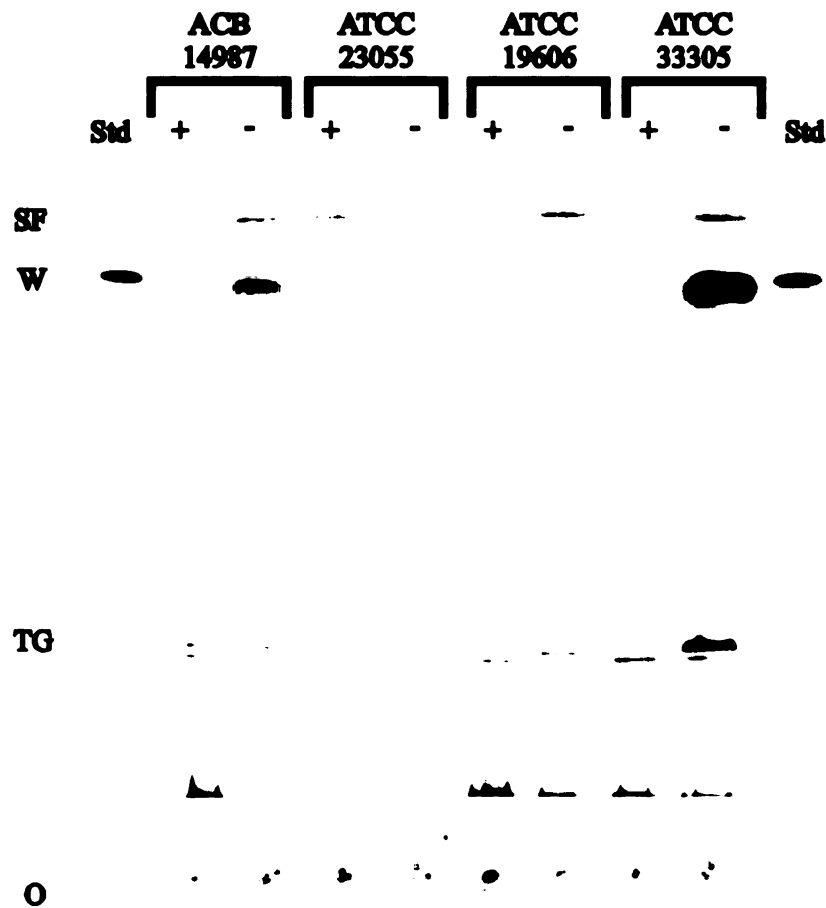
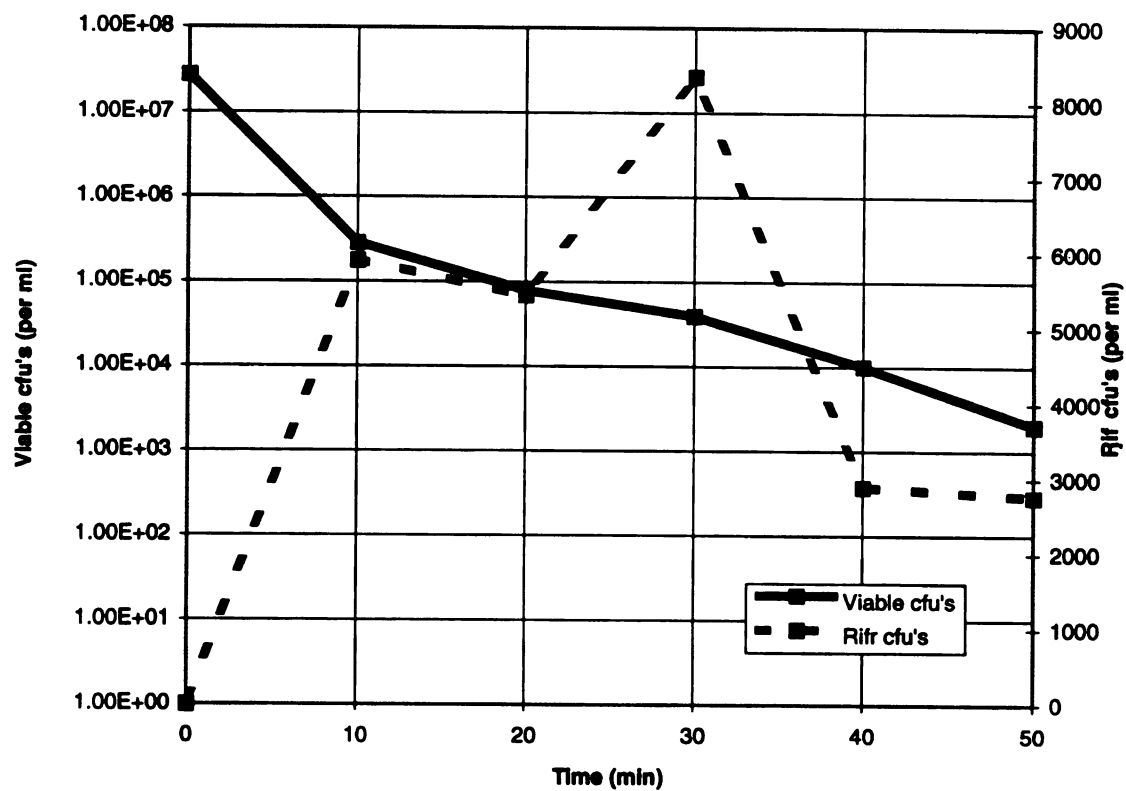


Figure 2-1: A comparison of wax ester accumulation from four strains of *A. calcoaceticus*. High nitrogen, non-inducing (+) and low nitrogen, inducing (-) conditions. Std, 0.2 mg of oleic acid stearyl ester; SF, solvent front; W, wax esters; TG, triacylglycerol; O, origin.

**Conditions for mutagenesis.** In order to determine the optimum level of mutagenesis, the effect of the duration of NTG treatment for a given amount of NTG was measured in a manner similar to Benning (Benning, 1991). Mutagenesis was evaluated by plotting the number of viable colonies versus time on a graph. This graph was then overlaid with a plot showing the number of colonies that were observed to be resistant to rifampicin, following the mutagenic treatment for each time point (Figure 2-2). Based on these data we selected the samples that were removed at 30 and 50 minutes time points for the mutant screening. The 30 minute time point was selected because it represented a time point in which an acceptable proportion of the culture was surviving the chemical treatment, yet at the same time had a high degree of mutation, as witnessed by the amount of Rif<sup>r</sup> colonies. The 50 minute time point represented the maximum amount of mutagenesis. This is important because of the method with which I have chosen to screen for mutants. TLC analysis of individual colonies is a tedious process and therefore it was important to maximize the number of mutations per colony. Therefore, the 50 minute time point which represents a high kill rate, and is presumably equivalent to a high mutation rate, was also used.

**Mutant screening.** I developed a quick method for screening for mutants affected in lipid accumulation. Mutagenized colonies were first plated onto a LB plate, thus creating a master plate. Next, this master plate was replica plated onto a minimal medium plate with low nitrogen to induce wax ester and triacylglycerol accumulation. Replica plating onto the minimal medium not only served to induce wax ester and triacylglycerol biosynthesis, but it also eliminated auxotrophic mutants generated by the mutagenesis. Next, these low nitrogen plates were flooded with a



**Figure 2-2: Effect of duration of NTG treatment on cell viability over time following NTG mutagenesis and induced number of Rif<sup>r</sup> colonies.**

solution containing Sudan black B, a nonspecific lipophilic dye. Because wax esters and triacylglycerol are very nonpolar, colonies containing these compounds are darker in color, after being stained with Sudan black B, than colonies lacking neutral lipid accumulation. The results from such a staining procedure are shown in Figure 2-3. Following such a procedure approximately 10% of the mutagenized colonies were selected as "lighter staining". To determine if these colonies were truly affected in wax ester or triacylglycerol accumulation, the colonies from the master plate were restreaked and then cultured in low nitrogen medium for analysis by TLC.

**Mutant phenotypes.** A total of more than 6400 chemically mutagenized colonies were screened using the lipophilic dye Sudan black B in combination with TLC analysis. A total of 25 mutants were recovered (Table 2-1). These 25 mutants can be divided into 3 phenotypic classes (Figure 2-4). Class I mutants are (wax<sup>+</sup>tag<sup>+</sup>), class II mutants are (wax<sup>+</sup>tag<sup>-</sup>) and class III mutants (wax<sup>-</sup>tag<sup>-</sup>). Chemical mutagenesis produced a wide variety of phenotypes within the three classes. The amounts of neutral lipids in the 25 mutants are illustrated in Figure 2-5. The first mutant that was isolated was a class I mutant. Because of its inability to accumulate wax esters the mutant was given the name *Wow1*, for without wax. Subsequent mutants were isolated, not all of which were solely deficient in wax ester accumulation. However for the sake of simplicity in dealing with the large number of mutants that were generated, the *wow* designation was adopted and a number was assigned to each subsequent mutant that was isolated, despite its phenotype.

**Chemical complementation as a basis for characterization.** Based on previous observations by other researchers it was known that *A. calcoaceticus* could be

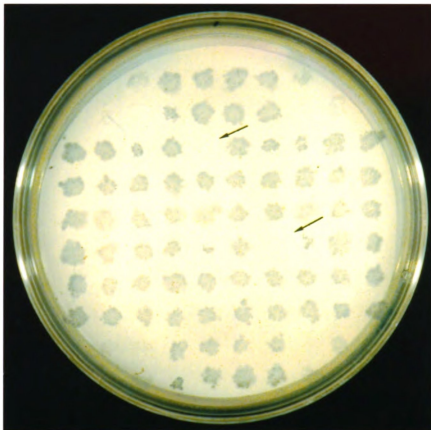
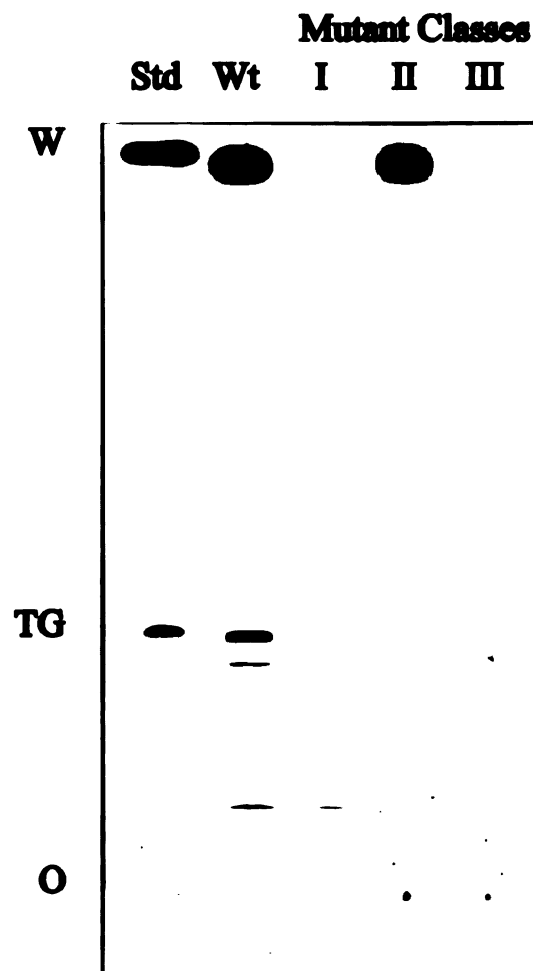


Figure 2-3: Example of staining for mutants affected in neutral lipid accumulation using the lipophilic dye Sudan black B. Arrows indicate lighter staining colonies that would have been selected for further study. In this example, the known wax<sup>-</sup> mutant, *Wow1* was placed in the corners of the plate for comparison.





**Figure 2-4: TLC plate illustrating the three general classes of mutants. Class I mutants fail to accumulate wax esters under nitrogen (wax inducing) limited conditions. Class II mutants fail to accumulate triacylglycerol and class III mutants accumulate neither waxes or triacylglycerol under nitrogen limited conditions. Lipids were visualized by spraying the TLC plate with 50% sulfuric acid and charring at 160°C. Wax ester and triacylglycerol standards, 0.2 mg each (Std), *A. calcoaceticus* strain BD413 (Wt), wax esters (W), triacylglycerol (TG) and the origin (O).**

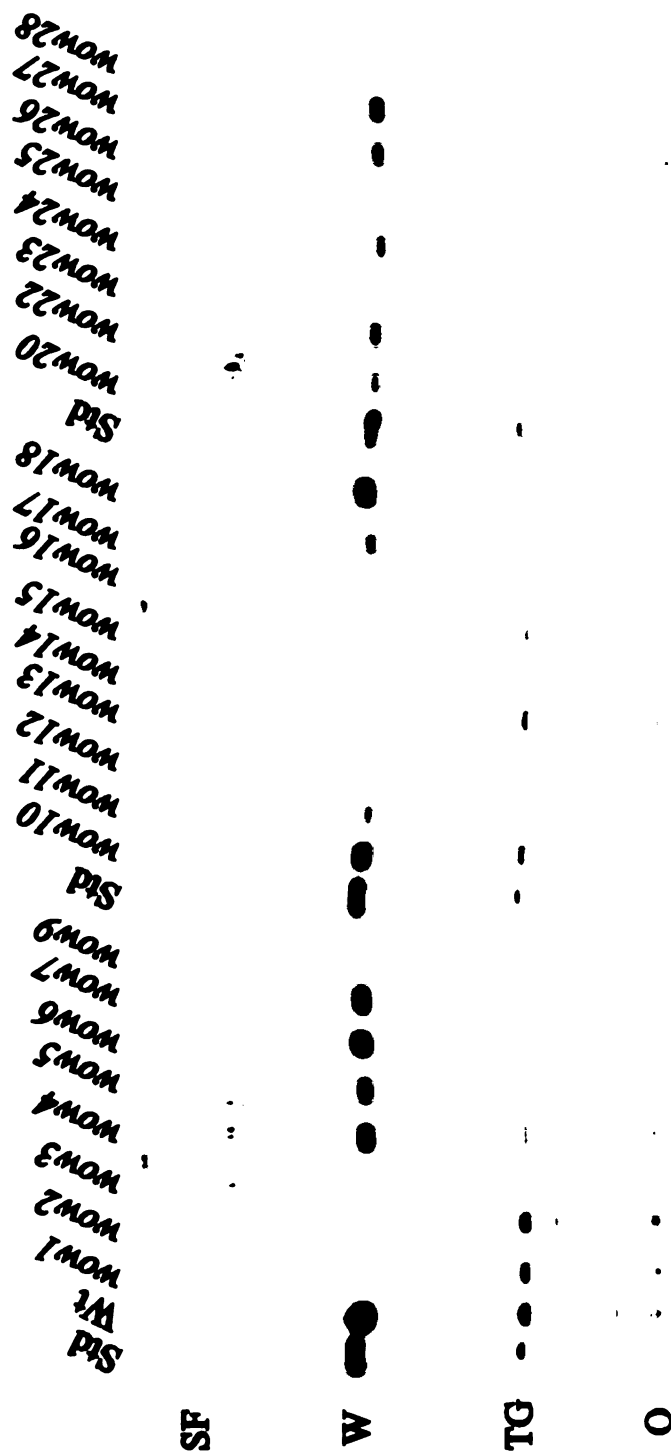


Figure 2-5: Qualitative TLC analysis of the mutants isolated following NTG mutagenesis. Samples were loaded proportionately based on cellular fresh weight. Samples were grown under low nitrogen (wax inducing) conditions. Lipids have been visualized by spraying the TLC plates with 50% sulfuric acid and charring the plate at 160°C. Wax ester and triacylglycerol standards 0.2 mg each (Std), *A. calcoaceticus* strain BD413 (Wt), solvent front (SF), wax esters (W), triacylglycerol (TG) and the origin (O).

cultured in the presence of alkanes and fatty alcohols as a carbon source (Makula et al., 1975; Dewitt & Ervin, 1982; Singer et al., 1985). These previous studies also showed that when *A. calcoaceticus* is incubated in the presence of these substrates they are directly utilized in wax ester accumulation. I conducted similar types of experiments on the mutants that had been isolated in order to characterize the sites of the biochemical lesions in the various mutants. The rationale for these experiments is based upon the proposed pathway for wax ester biosynthesis (Figure 2-6). An experiment in which the mutants were fed hexadecanol and subsequently there was an accumulation of wax esters would be indicative of a lesion in the pathway at either of the two reductase steps. If waxes were not formed then it might be concluded that the mutation had affected the acyl-CoA fatty alcohol transferase. By growing the mutants in the presence of hexadecane, it was hoped to reveal if the mutant phenotype was the result of a lesion upstream of the outlined wax ester pathway that blocked the pathway from getting the necessary substrate.

Culturing the mutants in the presence of hexadecanol (a 16 carbon alcohol) as a substrate showed that all of the class I mutants were able to synthesize wax esters (Figure 2-7). However, when the class I mutants were grown in the presence of hexadecane no evidence for complementation of the phenotypes was apparent (data not shown). Growth of the class II and class III mutants in medium containing hexadecanol and hexadecane had no affect on the mutant phenotypes (data not shown). These data are summarized in Table 2-2. Unfortunately, at the time of these experiments a commercial source of fatty aldehydes was not available. However, recently this has changed and further experiments will be carried out with

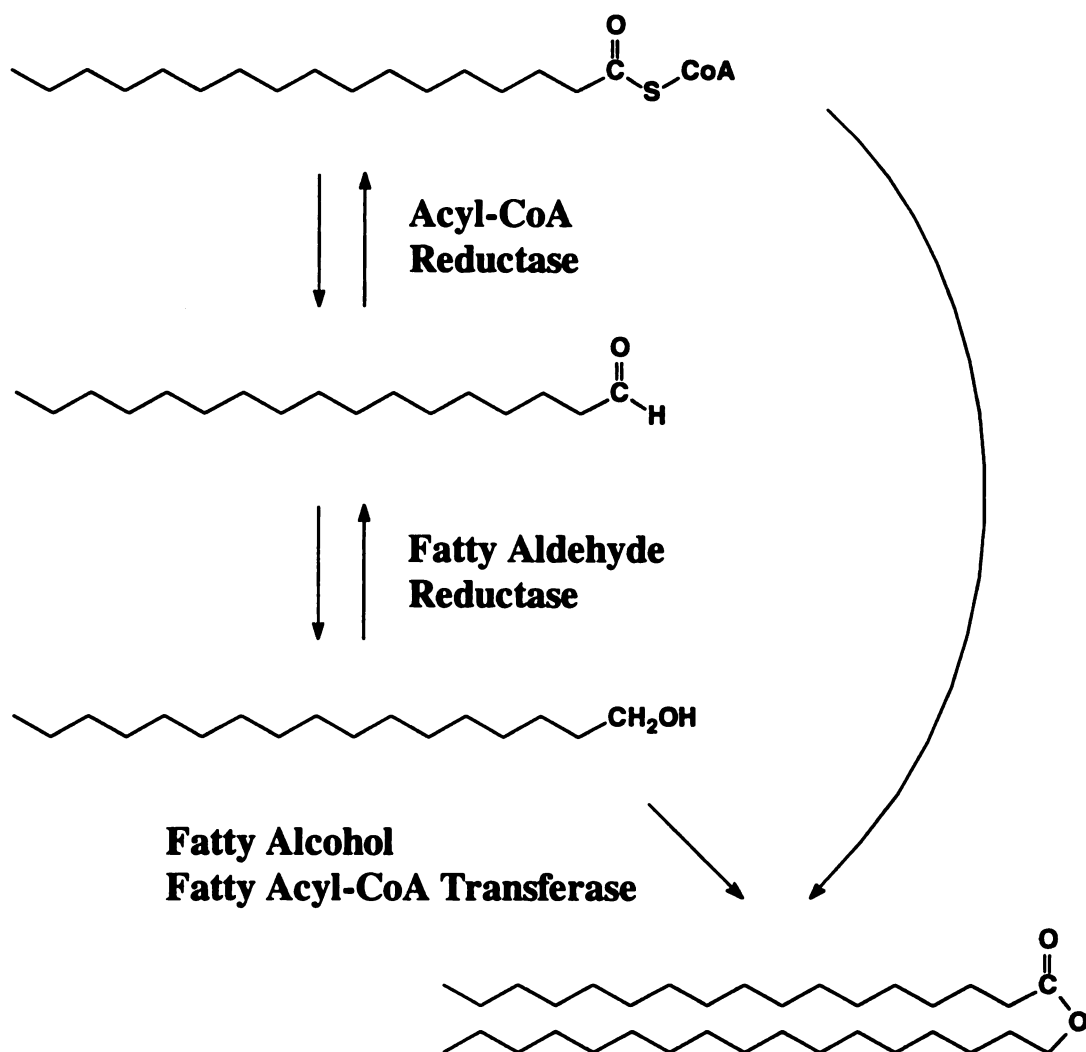


Figure 2-6: Proposed pathway for wax ester biosynthesis in *Acinetobacter calcoaceticus* strain BD413.

W

TG

H

O

**Figure 2-7: Chemical complementation of class I and class III mutants grown under nitrogen starvation (wax inducing) conditions in the presence of 0.3% hexadecanol. Samples were loaded proportionately based on cell pellet fresh weight. *A. calcoaceticus* strain BD413 (Wt), wax ester, triacylglycerol and hexadecanol standards 0.2 mg each (Std), solvent front (SF), wax ester (W), triacylglycerol (TG), hexadecanol (H) and the origin (O). Lipids were visualized by spraying the TLC plates with 50% sulfuric acid and charring at 160°C.**

Table 2-2: Effect of inclusion of hexadecane (0.3% w/v) and hexadecanol (0.3% w/v) on neutral lipid composition of various mutants.

Strains	Phenotype Unsupplemented	Phenotype on Hexadecane	Phenotype on Hexadecanol
Wild type strain BD413	wax <sup>+</sup> tag <sup>+</sup>	wax <sup>+</sup> tag <sup>+</sup>	wax <sup>+</sup> tag <sup>+</sup>
<i>Wow1</i>	wax <sup>-</sup> tag <sup>+</sup>	wax <sup>-</sup> tag <sup>+</sup>	<b>wax<sup>+</sup>tag<sup>+</sup></b>
<i>Wow2</i>	wax <sup>-</sup> tag <sup>+</sup>	wax <sup>-</sup> tag <sup>+</sup>	<b>wax<sup>+</sup>tag<sup>+</sup></b>
<i>Wow3</i>	wax <sup>-</sup> tag <sup>-</sup>	wax <sup>-</sup> tag <sup>-</sup>	wax <sup>-</sup> tag <sup>-</sup>
<i>Wow4</i>	wax <sup>-</sup> tag <sup>-</sup>	wax <sup>-</sup> tag <sup>-</sup>	wax <sup>-</sup> tag <sup>-</sup>
<i>Wow5</i>	wax <sup>-</sup> tag <sup>-</sup>	wax <sup>-</sup> tag <sup>-</sup>	wax <sup>-</sup> tag <sup>-</sup>
<i>Wow6</i>	wax <sup>+</sup> tag <sup>-</sup>	wax <sup>+</sup> tag <sup>-</sup>	wax <sup>+</sup> tag <sup>-</sup>
<i>Wow7</i>	wax <sup>+</sup> tag <sup>-</sup>	wax <sup>+</sup> tag <sup>-</sup>	wax <sup>+</sup> tag <sup>-</sup>
<i>Wow9</i>	wax <sup>-</sup> tag <sup>-</sup>	wax <sup>-</sup> tag <sup>-</sup>	wax <sup>-</sup> tag <sup>-</sup>
<i>Wow10</i>	wax <sup>-</sup> tag <sup>-</sup>	wax <sup>-</sup> tag <sup>-</sup>	wax <sup>-</sup> tag <sup>-</sup>
<i>Wow11</i>	wax <sup>+</sup> tag <sup>-</sup>	wax <sup>+</sup> tag <sup>-</sup>	wax <sup>+</sup> tag <sup>-</sup>
<i>Wow12</i>	wax <sup>-</sup> tag <sup>-</sup>	wax <sup>-</sup> tag <sup>-</sup>	wax <sup>-</sup> tag <sup>-</sup>
<i>Wow13</i>	wax <sup>-</sup> tag <sup>+</sup>	wax <sup>-</sup> tag <sup>+</sup>	<b>wax<sup>+</sup>tag<sup>+</sup></b>
<i>Wow14</i>	wax <sup>-</sup> tag <sup>+</sup>	wax <sup>-</sup> tag <sup>+</sup>	<b>wax<sup>+</sup>tag<sup>+</sup></b>
<i>Wow15</i>	wax <sup>-</sup> tag <sup>+</sup>	wax <sup>-</sup> tag <sup>+</sup>	<b>wax<sup>+</sup>tag<sup>+</sup></b>
<i>Wow16</i>	wax <sup>-</sup> tag <sup>-</sup>	wax <sup>-</sup> tag <sup>-</sup>	wax <sup>-</sup> tag <sup>-</sup>
<i>Wow17</i>	wax <sup>+</sup> tag <sup>-</sup>	wax <sup>+</sup> tag <sup>-</sup>	wax <sup>+</sup> tag <sup>-</sup>
<i>Wow18</i>	wax <sup>+</sup> tag <sup>-</sup>	wax <sup>+</sup> tag <sup>-</sup>	wax <sup>+</sup> tag <sup>-</sup>
<i>Wow20</i>	wax <sup>+</sup> tag <sup>-</sup>	wax <sup>+</sup> tag <sup>-</sup>	wax <sup>+</sup> tag <sup>-</sup>
<i>Wow22</i>	wax <sup>+</sup> tag <sup>-</sup>	wax <sup>+</sup> tag <sup>-</sup>	wax <sup>+</sup> tag <sup>-</sup>
<i>Wow23</i>	wax <sup>-</sup> tag <sup>-</sup>	wax <sup>-</sup> tag <sup>-</sup>	wax <sup>-</sup> tag <sup>-</sup>
<i>Wow24</i>	wax <sup>+</sup> tag <sup>-</sup>	wax <sup>+</sup> tag <sup>-</sup>	wax <sup>+</sup> tag <sup>-</sup>
<i>Wow25</i>	wax <sup>-</sup> tag <sup>-</sup>	wax <sup>-</sup> tag <sup>-</sup>	wax <sup>-</sup> tag <sup>-</sup>
<i>Wow26</i>	wax <sup>-</sup> tag <sup>-</sup>	wax <sup>-</sup> tag <sup>-</sup>	wax <sup>-</sup> tag <sup>-</sup>
<i>Wow27</i>	wax <sup>-</sup> tag <sup>-</sup>	wax <sup>-</sup> tag <sup>-</sup>	wax <sup>-</sup> tag <sup>-</sup>

Table 2-2 (cont'd)

<i>Wow28</i>	wax <sup>-</sup> tag <sup>+</sup>	wax <sup>-</sup> tag <sup>+</sup>	wax <sup>+</sup> tag <sup>+</sup>
--------------	-----------------------------------	-----------------------------------	-----------------------------------

---

*cis*-11-hexadecenal to further characterize the mutant phenotypes.

**Further chemical complementation experiments on *Wow15*.** In order to determine if the *Wow15* mutant was able to convert a fatty aldehyde to a fatty alcohol additional chemical complementation experiments were carried out on *Wow15*. Previously described experiments illustrated the ability of hexadecanol to complement the mutant phenotype, while incubation in the presence of hexadecane had no effect. Chemical complementation studies specific to *Wow15* were carried out using two more substrates involved in wax ester biosynthesis.

Incubation of the mutant in the presence of *cis*-11-hexadecenal (a 16 carbon, monounsaturated aldehyde) restored wax ester production (Figure 2-8). This indicates that the *wow15* mutation inactivates an enzyme that converts either acyl-CoA, or acyl-ACP to the corresponding aldehyde.

Tween-40, a sucrose polyester of palmitic acid, is a metabolically active and transportable form of palmitic acid for many organisms (Shintani & Ohlrogge, 1995). It would be predicted to act as a source of hexadecanoic acid in chemical complementation experiments of *Wow15*. As would be predicted based on chemical complementation experiments with hexadecane, when the mutant was grown in the presence of Tween-40, it failed to accumulate wax esters (Figure 2-8). This lends further evidence that a mutation has occurred in the step involving the reduction of the acyl-CoA, or acyl-ACP, to its corresponding aldehyde or alcohol.

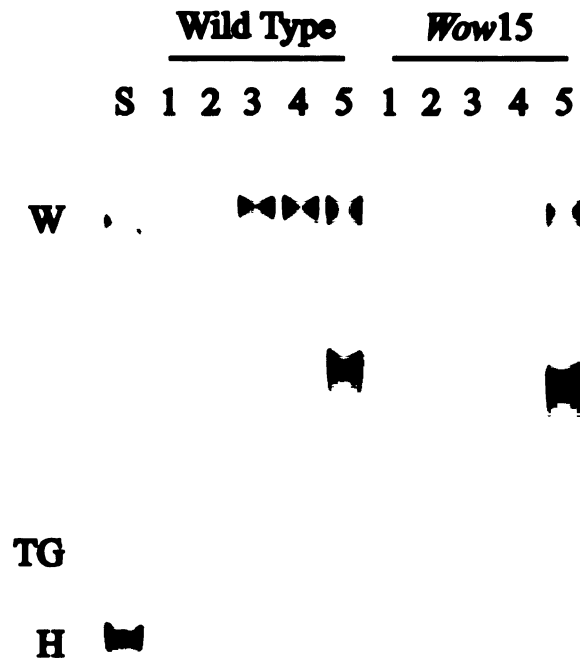


**Figure 2-8: Chemical complementation of the *Wow15* mutant.** Cell cultures from *A. calcoaceticus* strain BD413 (wild type) and the mutant *Wow15* were grown in various media. The neutral lipids were extracted with chloroform:methanol, spotted proportionately based on cellular wet weight onto the TLC plate, separated and visualized by spraying the plate with 50% sulfuric acid and charring at 160°C. Samples were grown in LB (lane 1), LB + 0.3% Tween-40 (lane 2), low nitrogen minimal media (lane 3), low nitrogen minimal media + 0.3% Tween-40 (lane 4) and low nitrogen minimal media + 0.3% *cis*-11-hexadecanol (lane 5). Wax ester (W) standards, triacylglycerol (TG) and hexadecanol (H) standards (lane S) were loaded at 0.2 mg each.



## CONCLUSION

The neutral lipids of four different strains of *A. calcoaceticus* were analyzed by TLC. One of these strains, BD413, accumulated the greatest amount of wax esters when induced under nitrogen starvation conditions. There was no accumulation of wax esters evident by TLC analysis when the bacteria were grown in LB medium. This observation reaffirms findings that wax ester accumulation in *A. calcoaceticus* is induced under nutrient starvation conditions. It was also observed that when strain BD413 is grown under nitrogen limited conditions, it accumulates a substantial amount of another neutral lipid that comigrates with triacylglycerol. This finding is consistent with reports describing the accumulation of triacylglycerol in *A. calcoaceticus* under similar growth conditions (Makula et al., 1975; Scott & Finnerty, 1976; Singer et al., 1985). These two findings, together with the fact that *A. calcoaceticus* strain BD413 is naturally competent for genetic transformation, led me to select it for further study (Juni & Janik, 1969; Palmen et al., 1993). It was my hope that by mutagenizing strain BD413 I might identify mutants not only in wax ester biosynthesis, but also in triacylglycerol accumulation.

Chemical mutagenesis using the guanidine analog, nitrosoguanidine, was carried out on *A. calcoaceticus* strain BD413 to generate mutants affected in wax ester and triacylglycerol production. A total of 25 mutants were recovered. The mutants could be separated into three distinct classes based on their neutral lipid composition. Class I mutants fail to accumulate wax esters under nitrogen limited conditions. Class II mutants fail to accumulate triacylglycerol, and class III mutants are affected in their ability to accumulate both wax esters and triacylglycerol under nitrogen starvation

conditions. As seen in Figure 2-5, several of the mutant phenotypes are leaky. Leakiness in a mutant phenotype is a very common occurrence, especially when using a mutagen that generates point mutations. There could be several different explanations for the observation. These could include mutations in the promoter elements of genes involved in wax ester biosynthesis, such that these genes are not being transcribed as efficiently as in the wild type. Another likely scenario is that a missense mutation has occurred that reduces the activity of the enzyme or causes destabilization of the protein or mRNA. Finally, another possibility is that the mutation has not occurred in a wax ester or triacylglycerol structural gene. Instead the mutation has affected another gene upstream of this pathway, in nitrogen sensing and regulation, for example. These upstream mutations may cause a decrease in wax and triacylglycerol accumulation, because the bacteria do not respond to the environmental conditions.

A limited characterization of the mutant phenotypes was carried out using chemical complementation experiments. Hexadecane is known to be taken up by *A. calcoaceticus* and directly incorporated into wax esters (Makula et al., 1975). Thus, it might be expected that culturing the class I (wax<sup>-</sup>) mutants in the presence of hexadecane might give some indication of whether or not the mutations were due to mutations in structural genes involved in wax ester biosynthesis or in genes involving pathways prior to wax ester biosynthesis, like nitrogen regulation. When the mutants were grown in medium supplemented with hexadecane it was observed that none of the mutants (class I, II and III mutants) exhibited a wild type phenotype. Although these results are difficult to interpret by themselves, they become more meaningful in

conjunction with results from the experiment outlined below.

Incubation of the class I (wax<sup>-</sup>) mutants with hexadecanol resulted in normal levels of wax accumulation in all cases. This implies that since wax biosynthesis from hexadecanol is still possible in these mutants the acyl-CoA (or acyl-ACP) fatty alcohol transferase has not been affected. Thus, the fact that the mutants did not accumulate wax when grown on hexadecane suggests that the class I (wax<sup>-</sup>) mutants may be deficient in either of the first two reductase steps (Figure 2-6). Another interpretation is that the mutants have been affected in their ability to take up and utilize hydrocarbons. Since it is believed that wax ester biosynthesis starts with either an acyl-CoA or acyl-ACP substrate, it is hard to imagine that a mutation in the synthesis of either one of these compounds would be compatible with cell viability. Therefore, it seems likely that the 8 class I mutants were the results of mutations in one of the two reductase steps.

*Wow15* was further characterized by additional chemical complementation experiments involving 0.3% Tween-40 or 0.3% hexadecenal. These experiments were carried out at a much later date than previously described experiments involving hexadecane and hexadecanol, but were included here for the sake of consistency. Growth of this mutant on both hexadecane and Tween-40 (a sucrose polyester of palmitic acid) resulted in no production of wax esters. However, incubation of this mutant in the presence of hexadecanol resulted in the production of wax esters. This indicates that either the reductase involved in converting acyl-CoA (or acyl-ACP) to aldehyde, or the second reductase which catalyzes the conversion of aldehydes to alcohols, had been mutagenized. Growth of the *Wow15* mutant on *cis*-11-hexadecenal

(a commercial source of fatty aldehyde was not available until after the chemical complementation experiments were completed) restored the ability of this mutant to synthesize wax esters. This shows that the genetic lesion in this mutant is an inability to catalyze the conversion of acyl-CoA (or acyl-ACP) to the corresponding fatty aldehyde.

Triacylglycerol levels in the class II mutants (tag<sup>-</sup>) did not respond to the addition of either alkanes or hexadecanol to the growth medium. This was predicted since it is assumed that the mutations that are being observed in the class II mutants are the result of a mutation in a gene involved in triacylglycerol biosynthesis or the regulation of triacylglycerol biosynthesis. The possibility that these mutations are the result of a defect in nitrogen sensing and response seems remote since they accumulate significant amounts of wax esters, indicating that the nitrogen response systems are intact. Incubation of wild type strain BD413 in the presence of either compound results in a greater accumulation of both wax esters and triacylglycerol implying that substrate availability may be a limiting factor in wax ester accumulation.

Chemical complementation studies of the class III mutants with both hexadecane and hexadecanol indicated that wax and triacylglycerol accumulation in these mutants is not restored by nutritional supplementation. I interpreted this to mean that these mutants may be the result of mutations in genes that permit the organism to sense and respond to nitrogen levels in the medium. The possibility that the class III mutants are defective in an enzyme involved in wax or triacylglycerol biosynthesis is unlikely because there is no known enzyme involved in both pathways after the steps involved in acyl-ACP biosynthesis and no such enzyme can be readily envisioned.

Thus, the class III mutants are either due to two mutations in structural genes for pathway specific biosynthetic enzymes, or in regulatory genes that participate in regulation of both pathways.

## REFERENCES

Benning, C.. 1991. Genetic Analysis of the Pathway for the Biosynthesis of the Plant Sulfolipid in the Purple Bacterium *Rhodobacter sphaeroides*. Ph.D. Dissertation, Michigan State University.

Bergogne-Bérézin and Joly-Guillou, M. L.. Antibiotic Resistance Mechanisms in *Acinetobacter*. In The Biology of *Acinetobacter*: Taxonomy, Clinical Importance, Molecular Biology, Physiology, Industrial Relevance. Plenum Press, New York, New York. 1991. Eds. Towner, K. J., Bergogne-Bérézin, E., and C. A. Fewson.

Dewitt, S., Ervin, J. L., Howes-Orchison, D., Dalietos, D., and Neidleman, S. L.. 1982. Saturated and Unsaturated Wax Esters Produced by *Acinetobacter* sp. H01-N Grown on C<sub>16</sub>-C<sub>20</sub> *n*-Alkanes. *JAOC* 59(2): 69-74.

Ervin, J. L., Geigert, J., Neidleman, S. L., and Wadsworth, J.. Substrate-Dependent and Growth Temperature-Dependent Changes in the Wax Ester Compositions Produced by *Acinetobacter* sp. H01-N. In Biotechnology for the Oils and Fats Industry, American Oil Chemists Society, 1984. Eds. Ratledge, C., Dawson, P. and Rattray, L..

Fixter, L. M., Nagi, M. N., McCormack, J. G. and Fewson, C. A.. 1986. Structure, Distribution and Function of Wax Esters in *Acinetobacter calcoaceticus*. *J. Gen. Micro.* 132: 3147-3157.

Fixter, L. M. and Sherwani, M. K.. Energy Reserves in *Acinetobacter*. In The Biology of *Acinetobacter*: Taxonomy, Clinical Importance, Molecular Biology, Physiology, Industrial Relevance. Plenum Press, New York, New York. 1991. Eds. Towner, K. J., Bergogne-Bérézin, E., and C. A. Fewson.

Juni, E. and Janik, A.. 1969. Transformation of *Acinetobacter calco-aceticus* (*Bacterium anitratum*). *J. Bact.* 98(1): 281-288.

Juni, E. 1972. Interspecies Transformation of *Acinetobacter*: Genetic Evidence for a Ubiquitous Genus. *J. Bact.* 112:917-931.

Kates, M.. 1986. Techniques of Lipidology: Isolation, Analysis and Identification of Lipids. Elsevier Science Pub. Co., New York, New York.

Makula, R. A., Lockwood, P. J. and Finnerty, W. R.. 1975. Comparative Analysis of Lipids of *Acinetobacter* Species Grown on Hexadecane. *J. Bact.* 121(1): 250-258.

Palmen, R., Vosman, B., Buijsman, P., Breek, C. K. D., and K. J. Hellingwerf. 1993. Physiological Characterization of Natural Transformation in *Acinetobacter calcoaceticus*. *J. Gen. Micro.* 139:295-305.

Scott, C. C. L. and Finnerty, W. R.. 1976. Characterization of Intracytoplasmic Hydrocarbon Inclusions from the Hydrocarbon-Oxidizing *Acinetobacter* Species H01-N. *J. Bact.* 127(1): 481-489.

Shintani, D. K. and Ohlrogge, J. B.. 1995. Feedback Inhibition of Fatty Acid Synthesis in Tobacco Suspension Cells. *The Plant Journal* 7(4): 577-587.

Singer, M. E., Tyler, S. M. and Finnerty, W. R.. 1985. Growth of *Acinetobacter* sp. Strain H01-N on *n*-Hexadecanol: Physiological and Ultrastructural Characteristics. *Mol. Gen. Genetics* 162: 162-169.

## CHAPTER 3

### ISOLATION AND CHARACTERIZATION OF A CLONE COMPLEMENTING THE WAX ESTER MUTANT *WOW1* OF *A. CALCOACETICUS*

#### ABSTRACT

Wax esters are present in a variety of different organisms. They perform many different functions such as providing desiccation tolerance in the form of epicuticular waxes on the surfaces of plants, or serving as a means of carbon storage in microbes. *Acinetobacter calcoaceticus* strain BD413 is an example of a microorganism that accumulates wax esters as a means of carbon storage when it undergoes nutrient starvation in the presence of excess carbon, particularly nitrogen starvation. Mutants that failed to accumulate wax esters under nitrogen limited conditions have been described previously. In this chapter it was discovered that by providing *cis*-11-hexadecenal (a monounsaturated 16 carbon fatty aldehyde) in the growth medium of one of these mutants, *Wow15*, it was possible to restore wax accumulation in the mutant. This suggests that the mutant is defective in the synthesis of fatty aldehyde from acyl-CoA (or acyl-ACP). Two of the mutants, *Wow1* and *Wow15*, were complemented with a cosmid genomic library. The ability of the cosmid to complement the phenotype was localized to a single gene (*acr1*) encoding a protein that is 44% identical (over 264 amino acids) to an open reading frame identified in *Mycobacterium tuberculosis* that is thought to encode an enzyme involved in mycolic

acid

prod

thioe

The

uniqu

liter

step

enzy

INT

ester

a ge

libra

mati

samp

TLC

had

trans

cosm

inabi



acid metabolism. Expression of the *acr1* gene in *Escherichia coli* resulted in production of a functional enzyme that catalyzes the reduction of an acyl-CoA thioester directly to its corresponding long chain alcohol via an aldehyde intermediate. The reduction of acyl-CoA to its corresponding fatty alcohol by a single enzyme is a unique enzymatic function and has not previously been detailed in the scientific literature. Observation of this activity dispels the notion that three separate enzymatic steps would be directly involved in wax biosynthesis, thus reducing the number of enzymes needed to two.

## INTRODUCTION

In the previous chapter, the isolation and characterization of mutants in wax ester and triacylglycerol accumulation were described. Here I describe the isolation of a gene that complements the *wow15* phenotype.

To complement the mutated genes from *wow1* and *wow15*, a cosmid genomic library was constructed. This library was used to transform the mutants by triparental mating. The resulting exconjugates were screened for complementation by staining the samples with Sudan black B followed by examination of the neutral lipid profiles by TLC. The ability of the mutants to synthesize wax esters indicated that the mutation had been complemented by genes localized on the cosmids.

The cosmids containing the complementary genes were mutagenized with the transposon mini-Tn10Cm to delineate the regions of interest. The mutagenized cosmids were then used to transform the mutants, *wow1* and *wow15*, respectively. The inability of a mutagenized cosmid to complement the mutant phenotype was evidence

the

res

wa

con

we

du

con

fra

exp

an

MA

desc

this

g KI

after

Acin

nitro

1.0 g

was g

that the transposon had inserted into a region containing a complementary gene. The restriction pattern of 4A-55, the cosmid which complements the *wow15* phenotype, was compared to the restriction patterns of 4A-55 cosmids which were unable to complement the mutant phenotype because of the transposon insertions. Fragments were identified in mutagenized cosmids that showed an increase in molecular weight due to the presence of the transposon. The corresponding fragment from the complementary cosmid was subcloned and sequenced.

DNA sequencing of the fragment allowed the identification of an open reading frame of interest. The open reading frame was subcloned and the encoded protein was expressed in *E. coli*. Expression of the protein in *E. coli* allowed the development of an *in vitro* assay which demonstrated the protein's function.

## MATERIALS AND METHODS

**Bacterial stains and plasmids.** The bacterial strains used in the experiments described in this chapter are shown in Table 3-1. The source of the plasmids used in this chapter, or in the construction of novel plasmids is presented in Table 3-2.

**Growth and culture conditions.** Low nitrogen minimal medium (per liter, 2.0 g  $\text{KH}_2\text{PO}_4$ , 1.18 g succinic acid, 0.1 g  $\text{NH}_4\text{SO}_4$ , pH adjusted to 7.0 with solid KOH; after autoclaving add 20 ml of sterilized 2%  $\text{MgSO}_4$ ) was used in experiments with *Acinetobacter calcoaceticus* strain BD413 to induce wax ester formation. High nitrogen minimal medium, which was the same as the above except for the addition of 1.0 g  $\text{NH}_4\text{SO}_4$  per liter. For other purposes such as DNA isolation, *A. calcoaceticus* was grown and maintained on LB medium (10 g Bacto tryptone, 5 g Bacto yeast

Table 3-1: Bacterial strains used in Chapter 3.

Bacterial Strains	Relevant Characteristics	Source or Reference
<b><i>A. calcoaceticus</i></b>		
ATCC #33305, strain BD413	wild type used during these studies, unencapsulated mutant of <i>A. calcoaceticus</i> strain BD4	ATCC stock center
Ac412	TrpE <sup>-</sup> mutant of strain BD413	A gift from Dr. Elliot Juni (Juni, 1972)
Wow1	wax <sup>-</sup> null mutant of BD413	This study, chapter 2
Wow1:Rif <sup>r</sup>	spontaneous Rif <sup>r</sup> mutant of wow1	This study, Chapter 3
Wow2	wax <sup>-</sup> null mutant of BD413	This study, Chapter 2
Wow13	wax <sup>-</sup> null mutant of BD413	This study, Chapter 2
Wow14	wax <sup>-</sup> null mutant of BD413	This study, Chapter 2
Wow15	wax <sup>-</sup> null mutant of BD413	This study, Chapter 2
Wow15:Rif <sup>r</sup>	spontaneous Rif <sup>r</sup> mutant of wow15	This study, Chapter 3
Wow28	wax <sup>-</sup> null mutant of BD413	This study, Chapter 2
<b><i>E. coli</i></b>		
HB101	F <sup>-</sup> proA2 recA13 mcrB	(Maniatis et al., 1982)
DH5 $\alpha$	F <sup>+</sup> /endA1 recA1 $\Delta$ (lacZYA-argF) U169 ( $\phi$ 80dlac $\Delta$ (lacZM15))	(Raleigh et al., 1989)
MM294	F <sup>-</sup> endA1 hsdR17 thi-1	(Bachmann, 1987)
BD21(DE3)	F <sup>-</sup> ompT hsdS <sub>B</sub> (r <sub>B</sub> <sup>-</sup> m <sub>B</sub> <sup>-</sup> ) gal dcm(DE3)	Novagen

Tat

MC

Ph

AN

Table 3-1 (cont'd)

MG1655	wild type, for carrying out Tn mutagenesis	A gift from Dr. Nancy Kleckner
<b>Phage</b>		
$\lambda$ NK1324	mini-Tn10Cm	(Kleckner et al., 1991)

---

Tabl

---

Pla

---

pB

pR

pL

pE

pSE

pSF

pSF

pSF

pSE

Table 3-2: Plasmid sources and derivations for Chapter 3.

Plasmid	Description or Construction	Source or Reference
pBS-KS <sup>+</sup> , pBS-KS <sup>-</sup>	Bluescript Vector	Stratagene
pRK2013	Km <sup>r</sup> self-transmissible RK2 derivative containing ColE1 replicon and transfer functions to mobilize RK2 derivatives	(Figurski & Helinski, 1979)
pLA2917	Cosmid Vector (Tet <sup>r</sup> ) derived from RK2	(Allen & Hanson, 1985)
pET21	Transcriptional expression vector for use in <i>E. coli</i> .	Novagen
pSER2	<i>A. calcoaceticus</i> / <i>E. coli</i> shuttle vector (Tet <sup>r</sup> Km <sup>r</sup> )	Figure B-1, Appendix B, this study
pSR1	Bluescript with EcoRV fragment from 4A-55	this study
pSR2	Bluescript with EcoRV fragment from 4A-55. Gave rise to sequence ID#4-9	this study, chapter 3 for construction and appendix A for sequence information
pSR6	Bluescript with EcoRV fragment from 4A-55. Gave rise to sequence ID#1-3	this study, chapter 3 for construction and appendix A for sequence information
pSER2: <i>acr1</i>	pSER2 derivative containing PCR fragment amplified using primers P5 and P6 (Figure 3-8)	this study



Ta

pE

1A

4A

2A

SEI

SEI

SEI

SER

Table 3-2 (cont'd)

pET21: <i>acr1</i>	pET21 derivative for protein expression of <i>acr1</i> in <i>E. coli</i> strain BL21(DE3). Contains PCR fragment amplified using primers P7 and P8 (Figure 3-8)	this study
1A-3F	pLA2917 derived cosmid clone complementing the <i>Wow1</i> mutant	Figure 3-4, this study
4A-55	pLA2917 derived cosmid clone complementing the <i>Wow15</i> mutant	Figure 3-3, this study
2A-87	pLA2917 derived cosmid clone complementing the <i>Wow15</i> mutant	this study
SER101	mini-Tn10Cm <sup>r</sup> containing derivative of 4A-55 that is no longer able to complement the <i>Wow15</i> mutant	this study
SER102	mini-Tn10Cm <sup>r</sup> containing derivative of 4A-55 that is no longer able to complement the <i>Wow15</i> mutant	this study
SER103	mini-Tn10Cm <sup>r</sup> containing derivative of 4A-55 that is no longer able to complement the <i>Wow15</i> mutant	this study
SER104	mini-Tn10Cm <sup>r</sup> containing derivative of 4A-55 that is no longer able to complement the <i>Wow15</i> mutant	this study

Table 3-2 (cont'd)

SER105	mini-Tn10Cm <sup>r</sup> containing derivative of 4A-55 that is no longer able to complement the <i>Wow15</i> mutant	this study
SER106	mini-Tn10Cm <sup>r</sup> containing derivative of 4A-55 that is no longer able to complement the <i>Wow15</i> mutant	this study
SER107	mini-Tn10Cm <sup>r</sup> containing derivative of 4A-55 that is no longer able to complement the <i>Wow15</i> mutant. Sample contains rearrangement or deletion as observed by restriction analysis.	this study
SER108	mini-Tn10Cm <sup>r</sup> containing derivative of 4A-55 that is no longer able to complement the <i>Wow15</i> mutant	this study
SER109	mini-Tn10Cm <sup>r</sup> containing derivative of 4A-55 that is no longer able to complement the <i>Wow15</i> mutant. Sample contains rearrangement or deletion as observed by restriction analysis.	this study
SER110	mini-Tn10Cm <sup>r</sup> containing derivative of 4A-55 that is no longer able to complement the <i>Wow15</i> mutant	this study

---

extract and 10 g NaCl per liter, pH 7.0). *A. calcoaceticus* cultures were typically grown overnight at 30°C. In the case of larger volume cultures (i.e. 50 mls and larger), 3 ml overnight cultures were collected by centrifugation, the cell pellet was washed in the new medium, recentrifuged and then added to the fresh medium, before being incubated at 30°C overnight. Maintenance and growth of *Escherichia coli* strains was on LB with appropriate antibiotics. *Escherichia coli* strain BD21(DE3) for expression studies was grown in LB medium with ampicillin (100 µg/ml). Three milliliter overnight cultures were collected, washed and used to inoculate larger 50 ml cultures. When the cultures reached an optical density of 0.6 at 600 nm, they were induced to synthesize the protein of interest by adding IPTG to a final concentration of 0.1 mM. Antibiotics were commonly used in the following concentrations: ampicillin 100 µg/ml, chloramphenicol 50 µg/ml, kanamycin 25 µg/ml, rifampicin 50 µg/ml and tetracycline 15 µg/ml.

**Complementation Screening Using the Lipophilic Dye Sudan Black B.** The master plates were replica plated onto low nitrogen minimal medium and were incubated overnight at 30°C to induce wax formation. The induced colonies were then stained by irrigating the plates with sudan black B (0.02% in 50:45:5 DMSO:ethanol:water) and gently shaking for approximately 20 minutes. The stain was aspirated away and the plates were carefully washed with 70% ethanol and gently shaking them for approximately 2 minutes. Lighter staining colonies were identified from the stained plates and the corresponding colony from the master plate was subsequently analyzed by thin layer chromatography.

**Thin layer chromatography (TLC).** TLC was carried out in the same manner

as described in Chapter 2.

**Library Construction.** *A. calcoaceticus* genomic DNA for the construction of the cosmid library was prepared in the following manner. A 200 ml culture of *A. calcoaceticus* strain BD413 was grown overnight. Cells were collected by centrifugation and resuspended in 16 mls of buffer (8% sucrose, 50 mM Tris pH 8.0, 50 mM EDTA pH 8.0). Lysozyme (Sigma) was added to a final concentration 2 mg/ml. Cells were incubated at 30°C for 30 minutes to make spheroplasts. Twenty four milliliters of lysis buffer (3% SDS, 0.5 M Tris-HCl pH 8.0, 0.2 M EDTA pH 8.0) was added and the sample was incubated at 65°C for 30 minutes. The sample was then cooled on ice. A sucrose step gradient was prepared for centrifugation in the following manner. Five milliliters of 50% sucrose on the bottom, 10 mls of 20% sucrose in the middle, and 10 mls of 15% sucrose on top in the lysis buffer described above. Ten milliliters of the sample was then layered on top of the sucrose solutions and the gradient was centrifuged in an SW222 (Beckman) swing out rotor at 27,000 rpm for 3 hours at 15°C. The DNA was recovered as a pellet above the 50% sucrose step, from where it was removed to a dialysis bag. The DNA was dialyzed in 1.5 L of 1x TE overnight, with change of the solution. The DNA was then gently extracted with 1 volume of phenol then extracted with 1 volume of chloroform/isoamyl alcohol. The DNA was dialyzed in 4 L of TE for 2 days then was partially digested with *Sau*III A to a mean size of approximately 25 kb. Fragments of approximately 25 kb and larger were size selected by running the partially digested DNA on a 0.6% agarose gel, cutting the band containing the fragments of interest from the gel, and isolating the DNA by electroelution (Maniatis et al., 1982). The fragments were ligated directly

to BglII-digested cosmid, pLA2917, and packaged using Gigapack Gold packaging extracts (Stratagene). Approximately 1300 *E. coli* HB101 primary transfectants were selected and transferred to 96 well plates. Examination of 19 randomly chosen cosmids from the library by restriction analysis indicated that 68% of the transfectants contained inserts.

**Triparental filter matings.** Identification of a complementary cosmid was carried out by triparental filter matings of the cosmid genomic library to *Wow1* and *Wow15* in the presence of MM294, a helper strain. Matings were carried out for all the mutants in the manner described for *Wow15* below. The cosmid library was contained in *E. coli* strain HB101 which was Tet<sup>r</sup> due to the presence of the cosmid. MM294 is a strain containing pRK2013, a helper plasmid that enables triparental mating through its *mob* genes. The pRK2013 plasmid imparts Km<sup>r</sup>. Finally, the mutant strain *Wow15*:Rif<sup>r</sup> was the target of the mating and was a Rif<sup>r</sup> derivative of *Wow15*. It was obtained by plating *Wow15* on rifampicin plates and selecting for the presence of spontaneous Rif<sup>r</sup> colonies. The neutral lipid profiles of these Rif<sup>r</sup> strains were examined to make sure they matched those of the original *Wow15* mutant. At the end of the mating, *Wow15*:Rif<sup>r</sup> mutants containing the cosmids were selected by plating the product of the cross onto LB medium containing rifampicin, to select for *Wow15*:Rif<sup>r</sup>, and tetracycline to select for the presence of the cosmid. MM294 and the HB101 donor failed to grow under these conditions.

The *Wow15* strain and MM294 were grown overnight as 3 ml cultures, and the library was grown in 96-well plates as replicates of the original. The day of the mating, 0.5 ml of MM294 was used to inoculate a 50 ml of culture, and 3 ml of

*Wow15* was used to inoculate a 50 ml culture. Cultures were collected at an  $OD_{600}=0.6$ , washed and then resuspended in 50 ml of LB. Twenty five milliliters of MM294 was combined with 50 ml of the *Wow15* culture. Ten milliliters of this mixture was drawn onto a sterilized 45 $\mu$  filter (85 mm in diameter) via a vacuum apparatus creating an even lawn of bacteria. The filter was then removed and placed on to an LB plate. Using sterilized set of prongs arranged to match 48 wells of the 96 well titer plates containing the library, the library was stamped onto the lawn of bacteria and matings were allowed to incubate at 30°C overnight. Filters were then transferred to selective medium containing rifampicin (100  $\mu$ g/ml) and tetracycline (15  $\mu$ g/ml) to select for *Wow15*:Rif<sup>r</sup> containing the cosmids. The resulting patches were then restreaked onto a master plate containing the selective medium, before being replica plated onto minimal, low nitrogen, wax-inducing medium for subsequent analysis by lipophilic staining and TLC.

**Transposon mutagenesis of the complementary cosmid.** Phage vehicle  $\lambda$ NK1324 was used to transfect *E. coli* strain MG1655 containing the cosmids that complemented the *Wow15* and *Wow1* phenotypes. Protocols for transfection, growth and maintenance of  $\lambda$ NK1324 have been published by Kleckner et. al. (Kleckner et al., 1991). Resulting colonies were selected on tetracycline (15  $\mu$ g/ml) for the presence of the cosmid and chloramphenicol (50  $\mu$ g/ml) for the presence of the transposon. To separate insertion events that were located in the genome versus the desired insertions in the cosmid, approximately 3000 transfectants were pooled and cosmid DNA was isolated. The resulting cosmids were used to transform *E. coli* strain DH5 $\alpha$ . Cosmids with transposon insertions were selected by plating the transformants on medium

containing tetracycline and chloramphenicol. One hundred and ninety six of the resulting transformants were transferred to 96-well plates and used for triparental matings with *Wow15* and *Wow1* as previously described. The resulting exconjugates were then screened by TLC looking for insertions that resulted in the loss of the ability of the cosmid to complement the mutant phenotypes.

**Extended PCR.** To delineate the region on cosmid 4A-55 that was responsible for complementation of the *wow15* phenotype, extended PCR was used in conjunction with transposon mutagenesis of the cosmid. To map the location of transposon insertions relative to the cosmid, primers were constructed on either end of the BglIII site of pLA2917 facing in toward the insert. Additionally, primers for both ends of the transposon element were constructed to face out, toward the edge of the insert DNA. Using one anchor on the cosmid in conjunction with the primers specific to the transposon (Table 3-3), it was possible to amplify the DNA in between the primers allowing us to assign a distance of the transposon relative to the anchoring (cosmid specific) primer (Figure 3-3). Transposon mapping of the cosmids was possible using Boehringer Mannheim's Expand Long Template PCR System. Reactions contained 350  $\mu$ M of dNTP's, 300 nM of each primer, 5  $\mu$ l of 10x buffer 1 (17.5 mM  $\text{MgCl}_2$ , 500 mM Tris-HCl, pH 9.2, 160 mM  $(\text{NH}_4)_2\text{SO}_4$ ), 0.15  $\mu$ g of template DNA and 0.75  $\mu$ l of the supplied enzyme mix in a total volume of 50  $\mu$ l. Cycling was carried out in the following manner:

Step 1: 94°C for 2 minutes

Step 2: 94°C for 10 seconds

Step 3: 65°C for 30 seconds



Table 3-3: List of synthetic oligonucleotides used in Chapter 3.

<b>Name of primer</b>	<b>Sequence (5'-3')</b>	<b>Description</b>
P1	CTTTCTTGCCGCCA AGGATCTGATG	Primer used in mapping the location of Tn insertions in 4A-55. Specific to 5' side of BglII site of pLA2917 in the Km cassette which originated from Tn-5. Faces toward BglII site
P2	GGCCGGAGAACCT GCGTGCAAT	Same as 5' Km Tn-5 but specific to the 3' side of the BglII site.
P3	GACGGGGTGGTGC GTAACGGC	Primer used in mapping the location of Tn insertions in 4A-55. Specific to 5' end of mini-Tn10Cm facing out.
P4	CAGGCTCTCCCCGT GGAGGTAAT	Same as 5' Cm Tn-10, but specific to 3' end of the transposon.
P5	GCAGGATCCTTGGG ATTGAACATATTG	Used with 3'End of Reductase to amplify PCR product to generate pSER2: <i>acr1</i> . Contains BamHI linker at 5' end.
P6	GCAGGATCCGGTGC GATTTATGATGTA	Used with 5'End of Reductase to amplify PCR product to generate pSER2: <i>acr1</i> . Contains BamHI linker at 5' end
P7	GCAGGATCCAAAA CATTTGGTAATTCA GATACT	Used with 3' Reductase +EcoRI to amplify PCR product to generate pET21: <i>acr1</i> . Contains BamHI linker at 5' end.

Table 3-3 (cont'd)

P8	GCAGAATTCGGTGC GATTTATGATGTA	Used with 5' Reductase +BamHI to amplify PCR product to generate pET21: <i>acr1</i> . Contains EcoRI linker at 5' end
----	---------------------------------	---

---

Step 4: 68°C for 7 minutes

Step 5: repeat from step 2 10 more times

Step 6: 94°C for 10 seconds

Step 7: 65°C for 30 seconds

Step 8: 68°C for 7 minutes + 20 seconds each cycle

Step 9: repeat from step 6 15 more times

Step 10: 68°C for 7 minutes

Step 11: Hold at 4°C

**Genomic DNA preparation.** Genomic DNA for Southern blot analysis was prepared by growing 3 ml cultures of the bacteria overnight in LB at 30°C. Half of the culture was collected by centrifugation in a microfuge at maximum speed for 5 minutes. The pellet was washed with 500 µl of 10 mM Tris-HCl (pH 7.6), 5 mM EDTA (pH 8.0). The sample was centrifuged, and resuspended in 350 µl of the above buffer. To this 50 µl of 10% SDS and 100 µl of 2.5 mg/ml stock of pronase (Sigma) was added. The samples were incubated at 37°C for 1 hour. Samples were then drawn through a 1 ml syringe with an 18 gauge needle attached to it 3 times to partially shear the DNA. Samples were extracted once in 1 volume of phenol, twice in 1 volume of phenol/chloroform (50:50) and once in 1 volume of chloroform. The

supernatant was removed and the DNA precipitated from solution by the addition of 2 volumes of 100% ethanol. DNA was recovered by spindling it out of solution with a capillary tube that had been sealed and bent using a bunsen burner. As much ethanol was removed as possible by gently touching the sample to the side of the eppendorf tube and letting the ethanol drain off. DNA was gently transferred to 100  $\mu$ l of the above buffer and allowed to enter solution by incubating the sample overnight at 4°C.

**Colony lifts for hybridization.** Ninety five millimeter nitrocellulose filters (Amersham) were placed on top of LB plates containing 15  $\mu$ g/ml of tetracycline. Replicas of the genomic library were stamped onto the filters using a sterile prong device that matched the 96 well array containing the library. The colonies on the filters were allowed to grow for approximately 6 hours at 37°C, or until colonies were just evident. Filters were removed and placed onto 3 mm Whatman paper saturated with 0.5 M NaOH for 5 minutes. The filters were then transferred to 3 mm Whatman paper saturated in 1 M Tris-HCL, pH 8.0 for 3 minutes. Next, the filters were neutralized on 3 mm Whatman paper soaked in 1 M Tris-HCL, pH 8.0 plus 1.5 M NaCl for 3 minutes. Filters were briefly washed in 2x SSC and then dried on 3 mm Whatman paper before being baked at 80°C for 30 minutes to fix the DNA to the filter.

**Restriction digestions and southern blot analysis.** Restriction digestions were carried out using Pharmacia's One-Phor-All buffer system and restriction enzymes. Southern blot analysis and detection was performed in keeping with Boehringer Mannheim's instructions for their Genius system with luminescent and nitro-blue-tetrazolium detection. In brief, probes were labelled by incorporation of digoxigenin-

11-UTP. In detecting the probe, the filter was washed twice in 2x SSC, 0.5% SDS at room temperature. Two high stringency washes were carried out at 65°C for 15 minutes in 0.5x SSC, 0.5% SDS. Finally, to detect the probe, the filter is incubated in the presence of anti-digoxigenin antibody conjugated to alkaline phosphatase. The conjugated antibody was then visualized by either Lumi-Phos 530 or nitro-blue-tetrazolium.

**Nested deletions and DNA sequencing.** To expedite the process of DNA sequencing, nested deletions were constructed using Promega's Erase-a-Base system. In brief, 1.0 µg of DNA was digested with EcoRV and KpnI to yield one blunt end which was susceptible to digestion with DNA exonuclease III. Samples were removed every 30 seconds, yielding a nested set of deletions varying by approximately 250 bp at each time point. The treated DNA was then recircularized and used to transform *E. coli* strain DH5α. The nested deletions were sequenced on a Perkin Elmer ABI310 automated sequenator using dye deoxyterminator reactions.

**Database analysis of DNA sequences.** To determine if identified DNA sequences shared any similarity to previously characterized proteins, DNA sequences were typically compared by BLASTX (Altschul et al., 1990) alignment to GenBank release 92.0 via an electronic mail server.

**Overexpression of *acr1* in *E. coli*, protein purification and separation.** The *acr1* gene was PCR amplified from the complementary cosmid using synthetic oligonucleotide primers, P7 and P8, containing BamHI and EcoRI linkers, respectively, for directional cloning (Table 3-3). The PCR product was gel purified, digested and subcloned into Novagen's pET21 transcriptional expression vector to produce plasmid

pET21:*acr1* which was used to transform *E. coli* strain BL21(DE3). *E. coli* strain BD21(DE3) for expression studies was grown in LB medium with ampicillin (100 µg/ml). Three milliliter overnight cultures were collected, washed and used to inoculate 50 ml cultures. When the cultures reached an optical density of 0.6 at 600 nm, they were induced to synthesize the protein of interest by adding IPTG to a final concentration of 1 mM. Cultures were grown for 2.5 hours before being collected and processed.

To isolate the protein from cells containing pET21:*acr1*, or just pET21 as a control, cells were harvested by centrifugation at 5000 x g for 10 minutes. Cells were resuspended in 500 mM sodium phosphate buffer (pH 7.4) and incubated 30°C for 15 minutes in the presence 100 µg/ml of lysozyme (Sigma). Cells were then sonicated for two 40 second bursts at maximum power. Soluble proteins were separated from cell walls and insoluble materials by centrifugation at 35,000 x g for 30 minutes at 4°C. The soluble fraction was collected as fraction I. The insoluble fraction was resuspended and resonicated as before. The sample was centrifuged at 35,000 x g for 30 minutes at 4°C and the aqueous layer was collected as fraction II. The resulting pellet was resuspended in a minimal amount of phosphate buffer to make a suspension as the insoluble fraction (fraction III). SDS-PAGE analysis of proteins was carried out using Pharmacia's Phast Gel system using 12.5% homogeneous gels as per the manufacturers instructions for SDS-PAGE gels and silver staining.

**Enzymatic assays for reductase activity.** To test for enzymatic activity of the expressed protein from transformed *E. coli*, an assay was developed using radiolabelled palmitoyl-1-<sup>14</sup>C-coenzyme A (44.4 mCi/mmol, 30 µM final concentration per reaction,

(Dupont). Reactions were run in 30  $\mu$ l volumes containing 167 mM sodium phosphate buffer (pH 7.4) in the presence of 100  $\mu$ M NADPH and 13.5  $\mu$ g of protein at 30°C for 15 minutes. Components were added in the following order: water, buffer, NADPH, palmitoyl-1-<sup>14</sup>C-coenzyme A and finally the protein. The assays were then extracted with 75  $\mu$ l of chloroform:methanol (50:50), vortexed for 10 seconds and then centrifuged for 20 seconds for phase separation at maximum speed in a microfuge. The chloroform phase was then removed and spotted onto a TLC plate where the lipids were separated using a hexane:ethyl ether:acetic acid (90:10:1) solvent system. The TLC plate was then removed and allowed to dry before being exposed to a phosphorimaging cassette.

**Synthesis of acyl-ACP.** In order to determine if acyl-ACP was used as a substrate by *acr1*, it was necessary to synthesize this substrate from 1-<sup>14</sup>C-palmitic acid and ACP using acyl-ACP synthase (a kind gift from Dr. Jan Jaworski). Thirteen and a half microcuries (77  $\mu$ l, 55.5 mCi/mmol,  $3.54 \times 10^4$  dpm/ $\mu$ l) of 1-<sup>14</sup>C-palmitic acid in hexane was dried under nitrogen gas and resuspended in 100  $\mu$ l of ethanol. Two drops of concentrated ammonia was added, the mixture was incubated at 65°C for 5 minutes and dried under nitrogen gas. The sample was then resuspended in 250  $\mu$ l (final concentration 600  $\mu$ M,  $1.1 \times 10^4$  dpm/ $\mu$ l) of 20% oxidant free Triton X-100 and heated to 65°C for 5 minutes.

Oxidant free Triton X-100 was prepared in the following manner. One hundred microliters of Triton X-100 was mixed into solution with 5 ml of 10 mM Tris-HCl, pH 8.0. Approximately 100 mg of NaBH<sub>4</sub> was added to the solution. The solution was sealed in a teflon lined screw capped tube, shaken vigorously and incubated at 37°C

for 30 minutes. Concentrated HCl was added dropwise with vortexing until the addition of acid did not produce anymore foaming. The solution was then extracted twice with 2 ml of chloroform. The chloroform phases were dried down under nitrogen at 55°C until there was no remaining smell of chloroform.

To synthesize the acyl-ACP, the following were combined in a screw cap microcentrifuge tube. Fifty microliters of 5x TML solution (0.5 M Tris-HCl (pH 8.0), 25 mM MgCl<sub>2</sub>, 2 M LiCl), 5 µl of 0.1 M DTT, 12.5 µl of 0.1 M ATP (pH 7.6), 25 µl 20% oxidant free Triton X-100 (described above), 25 µl of 600 µM 1-<sup>14</sup>C-palmitic acid (the ammonium salt, described above, total of 2.7x10<sup>5</sup> dpm), 25 µl of acyl-ACP synthetase (a gift from Dr. Jan Jaworski), and 8 µg of ACP protein (Sigma) resuspended in 22.3 µl of 10 mM Tris-HCl (pH 8.0). This reaction mixture was incubated at 37°C for 3 hours. At the end of the reaction the mixture was diluted 10x with H<sub>2</sub>O to reduce the LiCl concentration.

A gravity flow column was prepared with a 100 µl bed of DEAE cellulose in a 0.25" diameter, 3 ml column. The reaction was gently layered on top of the bed and allowed to gravity flow through the resin. The bed was then washed 4 times with 2 ml of wash solution (19.6 ml H<sub>2</sub>O, 80 ml isopropanol, 0.4 ml of 5 M NaCl, 0.2 ml of 1 M K<sub>2</sub>HPO<sub>4</sub> (pH 6.0)). The bed was then washed with 2 ml of 50 mM Tris-HCl (pH 7.6). The column was then centrifuged to dryness at 1000 rpm in a table top centrifuge for 2 minutes. The acyl-ACP was then eluted from the bed of the column by washing the cellulose four times, each time with 100 µl of 0.4 M LiCl in 50 mM Tris-HCl (pH 7.6). Between each application of the 100 µl of LiCl solution, the column was centrifuged for 2 minutes at 1000 rpm and the fraction collected. The

rac

sc

pe

th

s

fo

RI

ph

ca

se

un

nu

pre

25

th

ex

a

Wh



radioactivity present in ten microliter samples from each fraction was determined by scintillation counting. The first fraction was the most concentrated, at  $1.26 \times 10^4$  dpm per 10  $\mu$ l. The total counts for the entire volume collected measured  $2.66 \times 10^5$ , making the efficiency of the reaction about 97%. A total of  $1.0 \times 10^4$  dpm (approximately  $5.6 \times 10^{-4}$   $\mu$ mol of labelled acyl-ACP) of fraction 1 was used for each reaction testing for *acr1* activity from the *E. coli* protein extracts.

## RESULTS AND DISCUSSION

**Library construction and testing.** In order to complement the mutant phenotypes, a cosmid genomic library was prepared by partially digesting *A. calcoaceticus* genomic DNA with *Sau*III. Fragments greater than 25 kb were size selected from a gel, purified and ligated to pLA2917, a broad host range cosmid with a unique *Bgl*III site for the insertion of foreign DNA (Figure 3-1). To determine the number of cosmid clones that contained insertions, cosmid DNA from 19 clones was prepared. It was observed that 13 of 19 clones contained insert DNA of approximately 25-30 kb in size. Thus, only 68% of the colonies selected contained insertions. Using the following equation it is possible to predict the number of colonies (e.g. exconjugates following mating to the mutants) that would need to be screened to give a 99% coverage of the genome (Zilsel et al., 1992):

$$N = \frac{\ln(1-P)}{\ln(1-\frac{x}{y})} = \frac{\ln(1-0.99)}{\ln(1-\frac{25000}{4 \times 10^6})}$$

Where N is the number of colonies that need to be screened, p is the percentage

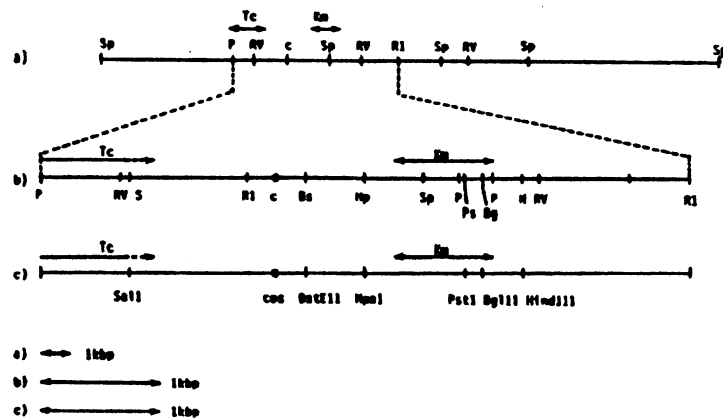


Figure 3-1: Detailed restriction map of pLA2917 (taken from Allen, 1985). The vector is shown linearized at one of the SphI sites. Abbreviations: Bg, BglII; Bs, BstEII; c, cos site; H, HindIII; Hp, HpaI; Km, kanamycin; Ps, PstI; P, PvuII; R1, EcoRI; RV, EcoRV; S, SalI; Sp, SphI; and Tc, tetracycline. (a) pLA2917; (b) expanded view of the region between the PvuI site in the tetracycline cassette and one of the EcoRI sites; (c) same as (b) showing antibiotic resistance determinants, cos site and unique restriction sites. SauIIIA partially digested Genomic DNA fragments from *A. calcoaceticus* were inserted into the BglII site located at the 5' end of the Km<sup>r</sup> cassette.

chance of covering the genome (99%),  $x$  is the insert size (25 kb) and  $y$  is the genome size (assume  $4 \times 10^6$  bp). This makes  $N=746$  colonies. I recovered approximately 1300 colonies, almost twice as many as calculated above, and arranged them in 96-well plates. In order to test the utility of the library, it was mated to Ac412, a known tryptophan auxotrophic mutant of *A. calcoaceticus* (Juni, 1972). Five  $\text{trp}^+$  exconjugates were recovered implying that the gene was adequately represented in the library. This indicated that the library was adequately representative of the genome.

**Complementation of *Wow1* and *Wow15*.** The library was then mated to *Wow1* and *Wow15* (both class I,  $\text{wax}^-$  mutants). The lipophilic dye Sudan black B was used to identify darker staining colonies, which might contain greater amounts of neutral lipids than the mutants. These darker staining colonies were then further investigated by TLC analysis to confirm whether or not they contained normal levels of wax esters. Following examination of 50 exconjugates by TLC, a cosmid clone, 1A-3F was found to complement the *wow1* phenotype (Figure 3-2). After searching through 350 exconjugates two cosmids, 2A-87 and 4A-55, were found to complement the *wow15* phenotype. Two of these original cosmids, 1A-3F and 4A-55, were used in all subsequent work.

In the case of 1A-3F, the end fragments from the insert region of the cosmid were used as probes to screen the genomic library by colony hybridization to identify other overlapping cosmids that also complemented the *wow1* phenotype. These are summarized in Table 3-4. Only the two original cosmids that were found to complement the *wow15* phenotype were isolated.

The cosmids were restriction mapped with a limited number of restriction

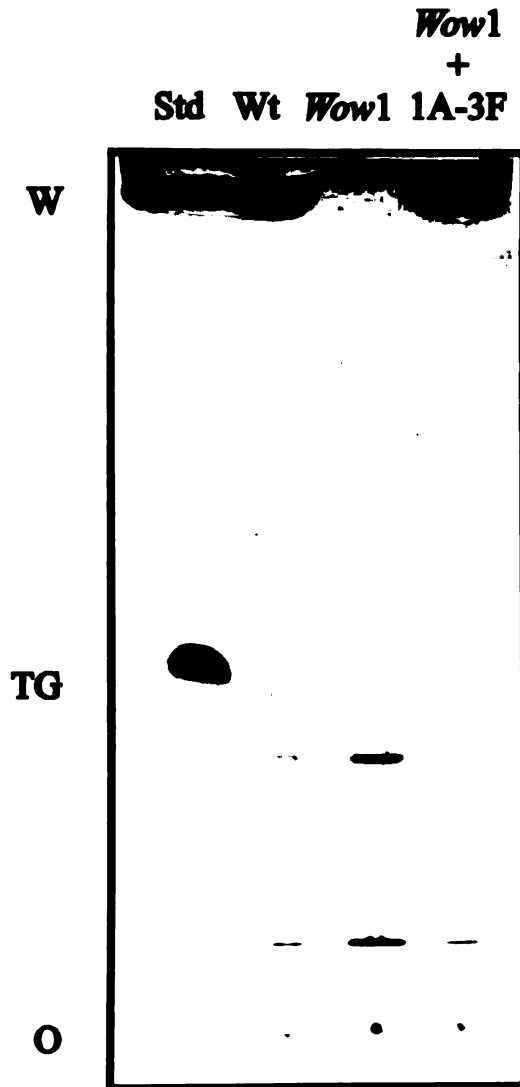


**Figure 3-2: Complementation of *Wow1*.** This TLC plate illustrates the ability of the cosmid, 1A-3F to complement the *wow1* phenotype. Samples were grown under nitrogen limited conditions. Lipids were visualized by spraying the TLC plate with 50% sulfuric acid and charring the plate at 160°C. Wax ester (W) and triacylglycerol (TG) standards, 0.2 mg each (Std), *A. calcoaceticus* strain BD413 (Wt) and the origin (O).



Table 3-4: Cosmids that share homology to 1A-3F.

Name of Cosmid	Phenotype of transformed <i>wow1</i>
1A-3F	<i>wax</i> <sup>+</sup>
2B-2A	<i>wax</i> <sup>+</sup>
3A-3C	<i>wax</i> <sup>+</sup>
3A-3D	<i>wax</i> <sup>+</sup>
3A-3F	<i>wax</i> <sup>+</sup>
3A-6F	<i>wax</i> <sup>+</sup>
4A-1D	<i>wax</i> <sup>-</sup>
5A-4E	<i>wax</i> <sup>-</sup>
5A-4H	<i>wax</i> <sup>-</sup>
6B-4D	<i>wax</i> <sup>-</sup>
7A-3C	<i>wax</i> <sup>-</sup>
7A-4B	<i>wax</i> <sup>+</sup>
7A-4D	<i>wax</i> <sup>+</sup>
7B-3C	<i>wax</i> <sup>-</sup>
10A-2C	<i>wax</i> <sup>+</sup>
10A-3C	<i>wax</i> <sup>+</sup>
11B-2A	<i>wax</i> <sup>+</sup>
12A-2D	<i>wax</i> <sup>+</sup>
12B-5E	<i>wax</i> <sup>-</sup>
13A-3F	<i>wax</i> <sup>+</sup>
13A-5E	<i>wax</i> <sup>-</sup>
13B-4D	<i>wax</i> <sup>-</sup>

enzy

restr

numb

the n

were

disti

were

homoc

Wow

deter

comp

Wow

as W

have

foun

sizes

the c

inser

phen

of 10

cosmi

enzymes due to their large size (Figures 3-3 and 3-4). It was found that many of the restriction enzymes that were tried (i.e. HindIII, EcoRV and PstI) resulted in a large number of bands making it very difficult to order them on the map. Comparison of the restriction patterns of the two different cosmids (1A-3F and 4A-55) when they were digested with a variety of different enzymes indicated that the cosmids were distinct and had no obvious overlap. Additionally, when the end fragments of 1A-3F were used as hybridization probes against the cosmid 4A-55 (data not shown), no homology was evident. This implies that the cosmids do not overlap, and therefore, *Wow1* and *Wow15* represent mutations at two different loci.

Next, the cosmid 1A-3F was mated into all of the different *Wow* mutants to determine if it was able to complement any of the other mutants. Besides complementing *Wow1*, the cosmid was also observed to complement *Wow13* and *Wow14*. Both of these mutants were class I null mutants (*wax*<sup>-</sup>), the same phenotype as *Wow1*. This leaves only two other class I, null mutants, *Wow2* and *Wow28* that have not been complemented. A similar experiment using 4A-55, the cosmid that was found to complement *Wow15* has not yet been completed.

**Transposon mutagenesis of complementary cosmids.** Because of the large sizes of the cosmids (55 kb), the genes were localized on the cosmids by mutagenizing the cosmids with a transposon. The mutagenized cosmids were then screened for insertions that eliminated the ability of the cosmid to complement the mutant phenotype. Mutagenesis of 4A-55 with a Tn-10 derived transposon, produced a total of 10 insertions out of a total of 192 that resulted in the loss of the ability of the cosmid to complement the *wow15* phenotype. Two of the 10 mutations resulted in



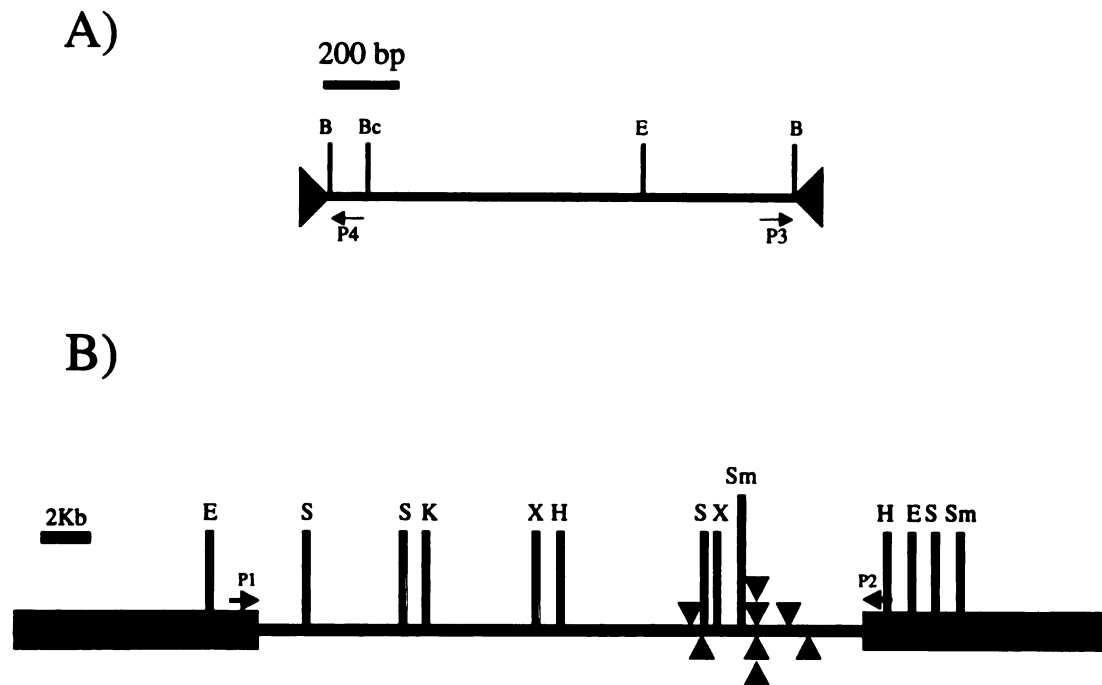


**Figure 3-3: Restriction map of cosmid 4A-55 and locations of the transposon insertions.** The transposon, mini-Tn10Cm, illustrated in Panel A (Kleckner et al., 1991) was used to generate mutants of 4A-55 which were unable to complement the *wow15* phenotype. The approximate position of primers used in mapping the positions of the insertions by extended PCR are illustrated as P3 and P4. The triangles at the ends of the transposon represent the inverted repeats of the transposon.. Panel B represents the cosmid 4A-55, which was found to complement the *wow15* phenotype. The insert DNA is represented by the lighter shaded line, while the vector portion of the cosmid is the darker shaded line. The arrows facing the insert portion of the cosmid (P1 and P2) symbolize the primers that were constructed with specificity to the *Km<sup>r</sup>* cassette of pLA2917 and were used with P3 and P4 (above) to map the location of the transposon insertions. The small triangles indicate the sites of transposon insertions that were found to inactivate the ability of 4A-55 to complement the mutant phenotype. The approximate location of the transposon insertions were determined by extended PCR. The restriction sites are *EcoRI* (E), *BamHI* (B), *HpaI* (H), *KpnI* (K), *SalI* (S), *ScaI* (Sc), *SmaI* (Sm) and *XhoI* (X).

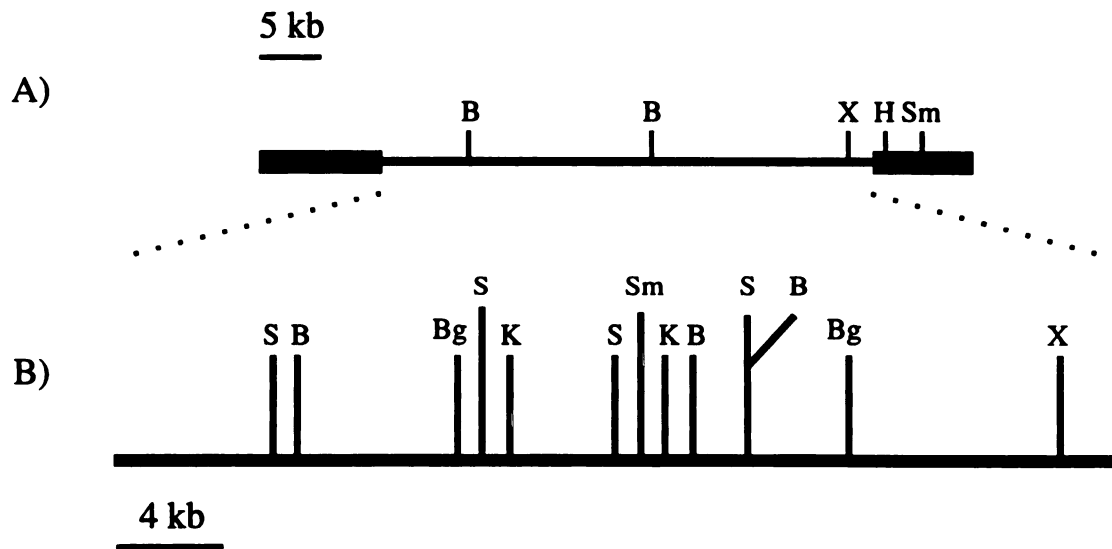


Figure 3-4: Restriction map of cosmid 1A-3F. This cosmid was found to complement the *wow1* mutation. Panel A shows the insert DNA in respect to the cosmid vector, pLA2917 (darker line). The insert was subcloned into the *Bgl*III site of pLA2917 as a *Sau*III A fragment, destroying the site. Panel B is an enlargement of the insert region showing the following restriction sites, *Bam*HI (B), *Bgl*III (Bg), *Hpa*I (H), *Kpn*I (K), *Sal*I (S), *Sma*I (Sm) and *Xho*I (X).

some sort of deletion or rearrangement in the cosmids that were evident when they were analyzed by restriction analysis. This left 8 insertions of interest. Mutagenesis of the other cosmid, 1A-3F, has resulted in a total of 3 insertions that inactivate the ability of the cosmid to complement the *wow1* phenotype.

The approximate location of the insertions relative to the restriction map have been highlighted in Figure 3-3 for the cosmid 4A-55. The location of the insertions in 1A-3F have not yet been determined. Delineation of the transposons on the map was possible by using extended PCR primed with oligonucleotides that were complementary to the transposon (P3 and P4, Table 3-3) in combination with primers (P1 and P2, Table 3-3) sharing homology to the region surrounding the *Bgl*III site of pLA2917 (Figure 3-3). It was observed that the transposons had inserted 2.0-6.5 kb away from P2 primer by determining the size of the extended PCR products on an agarose gel. The localization of all of the insertions to a small region of the cosmid's DNA indicated that the *wow15* gene probably did not reside within an operon, or if it did, it was near the beginning of the operon. Localization of the transposons on the restriction map showed that there was no single restriction fragment of practical size that would encompass the region containing all of the transposon insertions (Figure 3-3).

**Delineation of the complementary region from cosmid 4A-55.** In order to subclone a fragment corresponding to the region that contained all of the transposon insertions, the insertional mutants of cosmid 4A-55 were digested with several different enzymes (i.e. *EcoRV*, *Cla*I, and *Nhe*I that are not on the restriction map) and the restriction pattern compared to that of the wild type cosmid. Digestions with *EcoRV*

resul

cost

Fig-

ind-

size

app

Eco

diff

part

hyb

cost

of f

that

inte

nes

exo

info

bas

Ger

are

to er

resulted in a shift (of the predicted size) of a band in the transposon mutagenized cosmids, that was not present in the wild type cosmid, 4A-55 (Figure 3-5). As seen in Figure 3-5 the fragment that was shifted, did not disappear from the mutagenized lines, indicating that there were two or more EcoRV fragments of approximately the same size.

Wild type cosmid DNA was digested with EcoRV, resolved on a gel, and the approximately 4.0 kb band was electroeluted. The resulting DNA was ligated to EcoRV digested Bluescript vector and transformed into *E. coli* strain DH5 $\alpha$ . Two different isolates, designated pSR2 and pSR6, were identified based on restriction patterns with enzymes other than EcoRV. These two different samples were used as hybridization probes against wild type cosmid DNA and transposon mutagenized cosmid DNA digested with EcoRV (Figure 3-6). It can be seen from panels A and B of Figure 3-6 that the transposons have inserted into two different EcoRV fragments that were subcloned as constructs pSR2 and pSR6. This indicated that the region of interest spanned these two fragments.

In order to expedite the process of sequencing the two EcoRV fragments, nested deletions of the fragments were made using Promega's Erase-a-Base exonuclease kit. Single strand passes through the fragments provided enough sequence information to distinguish a total of six open reading frames which were identified based on their sequence similarity to identified open reading frames deposited in GenBank (Appendix A, this text). The six sequence similarities reported by GenBank are summarized in the table of Figure 3-7. The open reading frame that was thought to encode the gene of interest was localized to the end of the EcoRV fragment used in



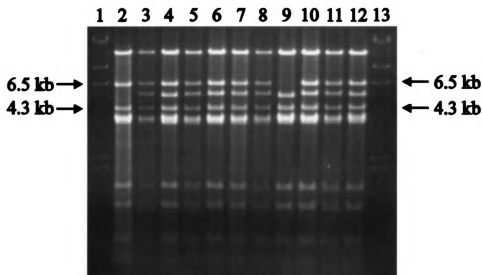


Figure 3-5: *EcoRV* digestions of 4A-55 and transposon containing derivatives of 4A-55. *EcoRV* digestions of 4A-55 (lane 2), the cosmid which complements the *wow15* phenotype, and the 4A-55 derivatives, SER101-110 (lanes 3-12, respectively) which contain mini-Tn10Cm. These transposon insertions were observed to inactivate the ability of the cosmid to complement the *wow15* phenotype. A 6 kb fragment is observed in all of the transposon mutagenized cosmids, that is not seen in the 4A-55 complementary cosmid. This 2 kb difference is anticipated upon insertion of the transposon. Also observed is the presence of several other fragments of approximately 4 kb in size. These 4 kb fragments were gel purified from *EcoRV* digestions of the complementary cosmid, 4A-55, and subsequently subcloned.

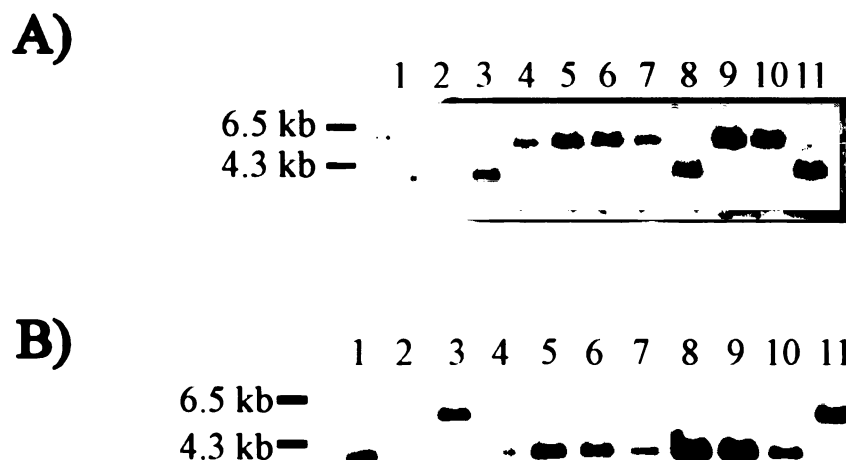
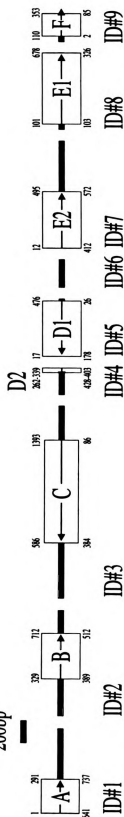


Figure 3-6: Southern analysis of transposon mutagenized cosmids. Cosmids containing the mini-Tn10Cm from  $\lambda$ NK1324 which inactivates their ability to complement the *wow*<sup>15</sup> phenotype were digested with *Bgl*II. The blots were probed with the subcloned EcoRV fragment, pSR6 (panel A), and pSR2 (panel B), each of which had been subcloned from the original complementary cosmid 5A-F1. Wild type cosmid DNA, 4A-55, that is able to complement the *wow*<sup>15</sup> phenotype has been loaded in lanes labelled lane 1. Cosmids SER101-110 (lanes 2-11, respectively) contain the transposable element.



Figure 3-7: Map showing sequence ID#1-9 in respect to one another. The boxed regions highlight regions of homology that were detected between the sequence and GenBank release 92.0 by BLASTX analysis (Altschul et al., 1990). These data are summarized in the table below the map. The numbers surrounding the boxes indicate the start of the similarity between the DNA query sequence (the numbers above the line) and the amino acid numbers in the matching protein from GenBank (the numbers below the line). This is to give some sense of the encoded protein over the whole restriction fragment, and also helps to determine the amount of DNA sequence missing between gaps. The gene, *acr1*, spans sequence ID#3-4 with the promoter residing on the very end of ID#4, and was first found to match *cmal* from *Mycobacterium tuberculosis*. Sequence ID#1-3 are from pSR2 and ID#4-9 come from pSR6. The table summarizes the GenBank information giving the length of the matching protein, accession number of the matching protein, the BLASTX score, probability score and the name of the protein as reported by GenBank. Cases where the description of the first match is ambiguous, second and third matches are included. Contig maps and actual DNA sequences can be found in Appendix A of this text.

200bp



Seq. ID#	Region Highlighted Above	Matches Accession Number	Name of Match as Given by GeneBank	BLAST Score	Probability Score	Protein Length of Matching Prot. (amino acids)
1	A	L09189	<i>Neisseria meningitidis</i> dTDP-D-glucose 4,6-dehydratase, glucose-1-phosphate thymidyl transferase and UDP-glucose-4-epimerase pseudogene	289	$8.4 \times 10^{-32}$	757
2	B	D64004 S51764	Hypothetical protein from <i>Synechocystis</i> High affinity sulphate transporter from <i>Stylosanthes hamata</i>	165 140	$7.9 \times 10^{-16}$ $5.5 \times 10^{-10}$	556 667
3	C	U27357	<i>Mycobacterium tuberculosis</i> cyclopropane mycolic acid synthase ( <i>cma1</i> ) gene	579	$3.4 \times 10^{-76}$	384
4	D2	U19394	O-Acetyl-L-homoserine sulphydrylase from <i>Emmericella nidulans</i>	94	$2.5 \times 10^{-4}$	437
5	D1	P06106	O-Acetylhomoserine sulphydrylase from Yeast	359	$4.8 \times 10^{-52}$	443
6	N/A	N/A	No Matches	N/A	N/A	N/A
7	E2	P10343	Hypothetical 42.6 KD Protein in <i>Isomylase 3'</i> Region from <i>Pseudomonas</i>	340	$2.2 \times 10^{-54}$	396
8	E1	L47693 P07003	Pyruvate Oxidase from <i>E. coli</i> Pyruvate Oxidase from <i>E. coli</i>	330 223	$4.9 \times 10^{-51}$ $4.1 \times 10^{-35}$	548 572
9	F	J01566	Plasmid ColE1	207	$3.3 \times 10^{-38}$	123

Figure 3-7

the

pSR

321

with

open

fract

my

sequ

con

calc

FA

pro

to

that

(30

cin

(Ar

OR

trif

inv

con

way

the construction of pSR6, and the promoter region of the gene resided on the end of pSR2. This is in keeping with the previous finding that the region of interest, delineated by the transposon insertions, spanned the two EcoRV fragments as witnessed by the results presented in Figure 3-6, panels A and B. Additionally, the open reading frame was of interest because of its strong similarity to an open reading frame identified in *Mycobacterium tuberculosis* that is thought to be involved in mycolic acid biosynthesis. Therefore, this open reading frame and its surrounding sequence was completely sequenced on both strands (Figure 3-8 and Appendix A for contig maps).

Comparison of the fully sequenced open reading frame identified from *A. calcoaceticus* with ORF2 from *Mycobacterium tuberculosis* resulted in an optimized FASTA score of 609 (Figure 3-9) indicating a very strong similarity between the two proteins. ORF2 from *Mycobacterium tuberculosis* was sequenced as part of an effort to characterize *cmal*, cyclopropane mycolic acid synthase. It is an open reading frame that resides just downstream of *cmal*. ORF2 is reported to be homologous to ActIII (30% identity over 188 amino acids), a  $\beta$ -ketoacyl reductase from *Streptomyces cinnamonensis* (a gene involved in chain elongation during polyketide biosynthesis) (Arrowsmith et al., 1992). Based on this similarity and its location between *cmal* and ORF3, an open reading frame with 35% identity (over 278 amino acids) to a trifunctional hydratase/dehydrogenase/epimerase from *Candida tropicalis* which is involved in peroxisomal degradation of fatty acids, Yuan et. al. (Yuan et al., 1995) concluded that the probable role of ORF2 was in mycolic acid metabolism. A three-way alignment of *wow15*, ORF2 from *Mycobacterium tuberculosis* and ActIII from

Figure 3-8: DNA and protein sequence of the region containing *acr1*. A conserved Shine Delgarno sequence is indicated in bold, underlined type (346-349 bp), while possible promoter elements are highlighted in underlined italics (-10 box) and in italics (-35 box). The EcoRV site which divides the two EcoRV fragments which were subcloned to give pSR2 and pSR6 is highlighted at 336-341 bp. Priming sites used for PCR to generate pSER2:*acr1* and pET21:*acr1* are double underlined (P5, 25-42 bp; P7, 202-225 bp; P6 and P8, 1325-1342 bp (complementary strand)).

```

1  CAG AAG ATA TGG TTC GGT TAT CGG TTG GGA TTG AAC ATA TTG ATG ATT TGA TTG CAG ATC
61  TGG AAC AAG CAT TGG CCA CAG TTT GAG CGT AAA TTT TAT AAA AAA CCT CTG CAA TTT CAG
121 AGG TTT TTT TAT ATT TGC TTT ATT ATC GTA TGA TGT TCA TAA TTG ATC TAG CAA ATA ATA
181 AAA ATT AGA GCA ATT ACT CTA AAA ACA TTT GTA ATT TCA GAT ACT TAA CAC TAG ATT TTT
241 TAA CCA AAT CAC TTT AGA TTA ACT TTA GTT CTG GAA ATT TTA TTT CCC TTT AAC CGT CTT

301 CAA TCC AAA TAC AAT AAT GAC AGC CTT TAC AGT TTG ATA TCA ATC AGG GAA AAA CGC GTG
1  Met
361 AAC AAA AAA CTT GAA GCT CTC TTC CGA GAG AAT GTA AAA GGT AAA GTG GCT TTG ATC ACT
2  Asn Lys Lys Leu Glu Ala Leu Phe Arg Glu Asn Val Lys Gly Lys Val Ala Leu Ile Thr
421 GGT GCA TCT AGT GGA ATC GGT TTG ACG ATT GCA AAA AGA ATT GCT GCG GCA GGT GCT CAT
22  Gly Ala Ser Ser Gly Ile Gly Leu Thr Ile Ala Lys Arg Ile Ala Ala Ala Gly Ala His
481 GTA TTA TTG GTT GCC CGA ACC CAA GAA ACA CTG GAA GAA GTG AAA GCT GCA ATT GAA CAG
42  Val Leu Leu Val Ala Arg Thr Gln Glu Thr Leu Glu Glu Val Lys Ala Ala Ile Glu Gln
541 CAA GGG GGA CAG GCC TCT ATT TTT CCT TGT GAC CTG ACT GAC ATG AAT GCG ATT GAC CAG
62  Gln Gly Gly Gln Ala Ser Ile Phe Pro Cys Asp Leu Thr Asp Met Asn Ala Ile Asp Gln
601 TTA TCA CAA CAA ATT ATG GCC AGT GTC GAT CAT GTC GAT TTC CTG ATC AAT AAT GCA GGG
82  Leu Ser Gln Gln Ile Met Ala Ser Val Asp His Val Asp Phe Leu Ile Asn Asn Ala Gly
661 CGT TCG ATT CGC CGT GCC GTA CAC GAG TCG TTT GAT CGC TTC CAT GAT TTT GAA CGC ACC
102 Arg Ser Ile Arg Arg Ala Val His Glu Ser Phe Asp Arg Phe His Asp Phe Glu Arg Thr
721 ATG CAG CTG AAT TAC TTT GGT GCG GTA CGT TTA GTG TTA AAT TTA CTG CCA CAT ATG ATT
122 Met Gln Leu Asn Tyr Phe Gly Ala Val Arg Leu Val Leu Asn Leu Leu Pro His Met Ile
781 AAG CGT AAA AAT GGC CAG ATC ATC AAT ATC AGC TCT ATT GGT GTA TTG GCC AAT GCG ACC
142 Lys Arg Lys Asn Gly Gln Ile Ile Asn Ile Ser Ser Ile Gly Val Leu Ala Asn Ala Thr
841 CGT TTT TCT GCT TAT GTC GCG TCT AAA GCT GCG CTG GAT GCC TTC AGT CGC TGT CTT TCA
162 Arg Phe Ser Ala Tyr Val Ala Ser Lys Ala Ala Leu Asp Ala Phe Ser Arg Cys Leu Ser
901 GCC GAG GTA CTC AAG CAT AAA ATC TCA ATT ACC TCG ATT TAT ATG CCA TTG GTG CGT ACC
182 Ala Glu Val Leu Lys His Lys Ile Ser Ile Thr Ser Ile Tyr Met Pro Leu Val Arg Thr
961 CCA ATG ATC GCA CCC ACC AAA ATT TAT AAA TAC GTG CCC ACG CTT TCC CCA GAA GAA GCC
202 Pro Met Ile Ala Pro Thr Lys Ile Tyr Lys Tyr Val Pro Thr Leu Ser Pro Glu Glu Ala
1021 GCA GAT CTC ATT GTC TAC GCC ATT GTG AAA CGT CCA ACA CGT ATT GCG ACG CAC TTG GGT
222 Ala Asp Leu Ile Val Tyr Ala Ile Val Lys Arg Pro Thr Arg Ile Ala Thr His Leu Gly
1081 CGT CTG GCG TCA ATT ACC TAT GCC ATC GCA CCA GAC ATC AAT AAT ATT CTG ATG TCG ATT
242 Arg Leu Ala Ser Ile Thr Tyr Ala Ile Ala Pro Asp Ile Asn Asn Ile Leu Met Ser Ile
1141 GGA TTT AAC CTA TTC CCA AGC TCA ACG GCT GCA CTG GGT GAA CAG GAA AAA TTG AAT CTG
262 Gly Phe Asn Leu Phe Pro Ser Ser Thr Ala Ala Leu Gly Glu Gln Glu Lys Leu Asn Leu
1201 CTA CAA CGT GCC TAT GCC CGC TTG TTC CCA GGC GAA CAC TGG TAA AAT TTA TAA AAG AAG
282 Leu Gln Arg Ala Tyr Ala Arg Leu Phe Pro Gly Glu His Trp
1261 CCT CTC ATA CCG AGA GGC TTT TTT ATG GTT ACG ACC ATC AGC CAG ATT TAG AGG AAA TTG
1321 ACT TTT CCT GTT TTT ACA TCA TAA ATC GCA CCA ACA ATA TCA ATT TCT TTG CGA TCC AGC
1381 ATA TCT TTA AGT ACA GAA CTA TGC TGA ATA ATG TAT TGA ATA TTA TAG TGA ACA TTC ATA
1441 GCA GTC ACC TGA TCA ATA AAT GCT TTG CTT AAT TCA CGC GGT TGC ATA ATA TCA AAT ACA
1501 CTG CCA ACC GAA TGC ATG AGT GGC CCA AGC ACG TAT TGG ATG TGT GGC ATT TCC TGA ATA
1561 TCG GAA ATC TGC TTA TGT TGC AAT CTT AAC TGG CAT GCG CTG GTG ACC GCA CCA CAG TCG
1621 GTA TGT CCC AAA ACC AGA ATC ACT TTG GAA CCT TTG GCT TGA CAG GCA AA

```

Figure 3-8

Se T  
REF:

ACAP  
REF:

ACAP  
REF:

ACAP  
REF:

ACAP  
REF:

ACAP  
REF:

Figure  
FAS  
Myco  
optim  
44.79  
indica  
where

No.	Target file	Definition	Match%	Over.	INIT	OPT 1
ORF2.AMI			44.7	264	597	609
ACAR1.AMI	10	20	30	40	50	60
ORF2.AMI	80	90	100	110	120	130
ACAR1.AMI	70	80	90	100	110	120
ORF2.AMI	140	150	160	170	180	190
ACAR1.AMI	130	140	150	160	170	180
ORF2.AMI	200	210	220	230	240	250
ACAR1.AMI	190	200	210	220	230	240
ORF2.AMI	260	270	280	290	300	310
ACAR1.AMI	250	260	270	280	290	
ORF2.AMI	320	330	340	350	360	

Figure 3-9: Optimized FASTA alignment between *acr1* and ORF2. An optimized FASTA alignment between *acr1* (ACAR1.AMI) and ORF2 (ORF2.AMI) from *Mycobacterium tuberculosis* was prepared using the Lipman-Pearson algorithm. The optimized FASTA score for these two protein sequences is observed to be 609 and is 44.7% identical over 264 amino acids. Symbols used in the above alignment are (:) indicating a full query/target match, (.) denotes a partial match and (X) represents where the homologous region between the two sequences starts and stops.



Step

align

ACA

and

acids

fram

inter

the b

actin

keto

sequ

bas

246

GTC

cons

Fig

seq

init

(P5

The

Bam

*Streptomyces cinnamonensis* is shown in Figure 3-10. It can be observed from this alignment that the open reading frame identified from *A. calcoaceticus* (labelled ACAR.1) is more similar to ORF2 than ActIII (optimized FASTA alignment between *acr1* and ActIII is observed to produce a score of 274, 29.8% identity over 245 amino acids, Figure 3-11). Thus based on the similarity between the identified open reading frame and ORF2 from *Mycobacterium tuberculosis*, it was my feeling that the gene of interest may encode some sort of  $\beta$ -ketoacyl reductase. This would be in keeping with the biochemical model outlined in Figure 3-12, where acyl-CoA (or acyl-ACP) is acting as the substrate for the encoded enzyme and the ketone group, which is a  $\beta$ -ketone, is being reduced.

**Cloning of *acr1*:** Examination of the open reading frames present in the gene sequence indicate that the largest protein, 32468 KDa, would be encoded using GTG (base pairs 358-360, Figure 3-8) as a translational initiation codon as compared to a 24655 KDa protein when ATG (base pairs 583-585 on Figure 3-8) is used. Use of GTG as an initiation codon is further supported by the presence of a strongly conserved Shine Delgarno sequence of AGG from -10 to -13 bp (base pairs 346-349 of Figure 3-8) upstream of the predicted start site, while there is no such conserved sequence upstream of the first ATG codon.

The open reading frame predicted by the use of GTG as the translational initiation codon was subcloned by PCR from the complementary cosmid using primers (P5, P6, P7 and P8) specific to the regions illustrated in Figure 3-8 (also Table 3-3). The amplified product resulting from primers P5 and P6 was subcloned into the BamHI site of pSER2 (construction of pSER2 is detailed in appendix B of this text),

Fi  
an  
Th  
Di  
pe  
pe

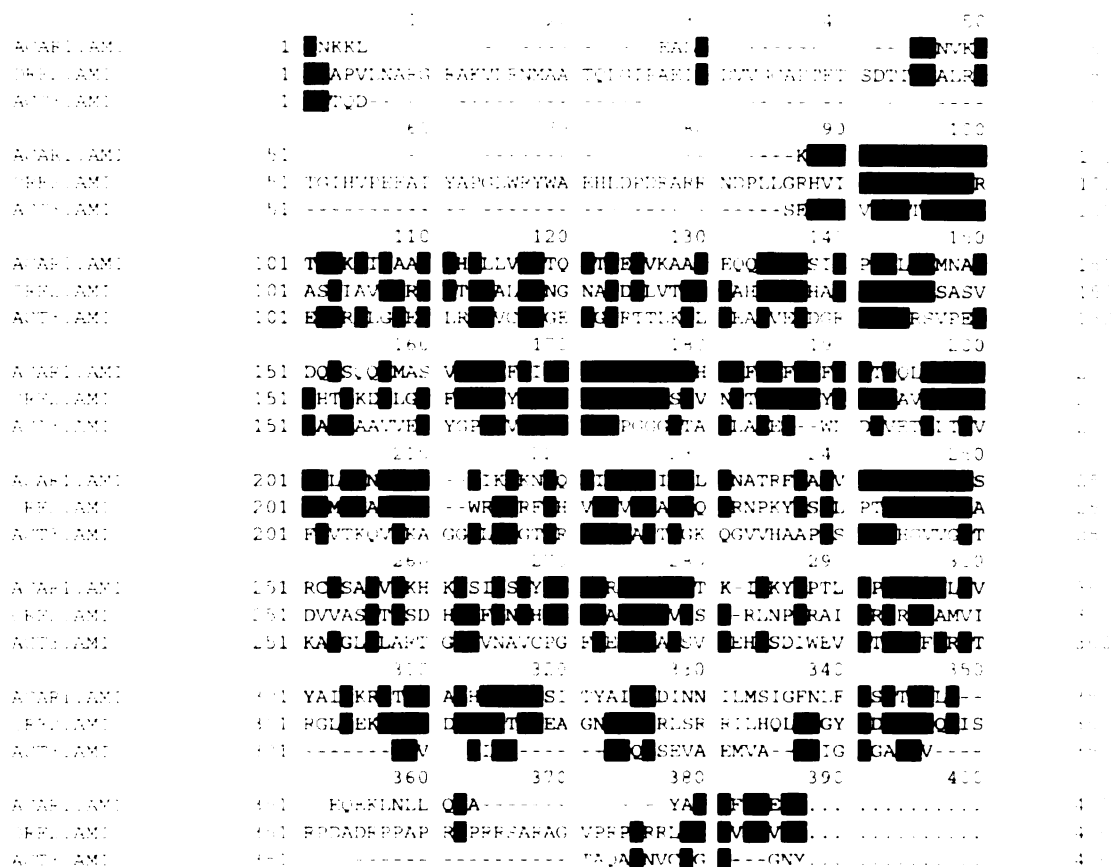


**Figure 3-10: Three-way alignment of *acr1* (ACAR1.AMI), ORF2 from *Mycobacterium tuberculosis* (ORF2.AMI) and ActIII from *Streptomyces cinnamonensis* (ACT3.AMI). The alignment is based on the Higgins and Sharp algorithm (CLUSTAL4) using the DNASIS for Windows software package (Hitachi Software) with the following parameters: gap penalty of 5, top diagonals of 5, fixed gap penalty of 10, floating gap penalty of 10, K-tuple of 2 and a window size of 5.**

No.	Target file	Definition	Match%	Over.	INIT	OPT
2	ACT3.AMI		29.8	245	237	274
		10          20          30          40          50          60				
ACAR1.AMI		RENVKGKVALITGASSGIGLTIAKRIAAGAHVLLVARTQETLEEVKAAIEQQGGQASIF ..X:::.....:::.....:::.....:::.....:::.....:::.....:::				
ACT3.AMI		MATQDSEVALVTGATSGIGLEIARRLGKEGLRVFVCARGEELRTTLKELREAGVEADGR 10                20                30                40                50                60				
		70          80          90          100         110         120				
ACAR1.AMI		PCDLTDMNAIDQLSQQIMASVDHVDLINNAGRSIRRAPHESFDRF-HDFERTMQLNYFG .:...:~::~:~::~:~::~:~::~:~::~:~::~:~::~:~::~:~::~:~::~:~::~:~::~:				
ACT3.AMI		TCDVRSVPEIERALVAAVVERYGPVDVLVNNA GRPGGATAELADELWLDDVVETNL TG VFR 70                80                90                100                110                120				
		130         140         150         160         170         180				
ACAR1.AMI		AVRLVLNLLPHMIKRKNQGIIINISSIGVLANATRFSA YVASKAALDAF S RCLSAEVLKHK .:...:~::~:~::~:~::~:~::~:~::~:~::~:~::~:~::~:~::~:~::~:~::~:~::~:				
ACT3.AMI		VTKQVLK-AGGMLERG TGRIVNIASTGGKQGVVHAAPYSASHGVVGPTKALGLELARTG 130                140                150                160                170				
		190         200         210         220         230         240				
ACAR1.AMI		ISITSYIMPLVRTPMIAPTK-IYKYVPTLSPEEAADLIVYAIVKRPTRIATHLGRLASIT .:...:~::~:~::~:~::~:~::~:~::~:~::~:~::~:~::~:~::~:~::~:~::~:~::~:				
ACT3.AMI		ITVNAVCPGFVPETPMAASVREHYSDIEWSTEEAFDRITARVP IGRYVQPSEVAEM--VA 180         190         200         210         220         230				
		250         260         270				
ACAR1.AMI		YAIAPDINNILMSIGFNLFPSSTA .:...:~::~:~::~:~::~:~::~:~::~:~::~:~::~:~::~:~::~:~::~:~::~:~::~:				
ACT3.AMI		YLIGPGA AAVTAQALNVCGGLGNY 240         250         260				

**Figure 3-11: Optimized FASTA alignment between *acr1* and ActIII. An optimized FASTA alignment between *acr1* (ACAR1.AMI) and ActIII (ACT3.AMI) from *Streptomyces cinnamonensis* was prepared using the Lipman-Pearson algorithm. The optimized FASTA score for these two protein sequences is observed to be 274 and is 29.8% identical over 245 amino acids. Symbols used in the above alignment are (:) indicating a full query/target match, (.) denotes a partial match and (X) represents where the homologous region between the two sequences starts and stops.**

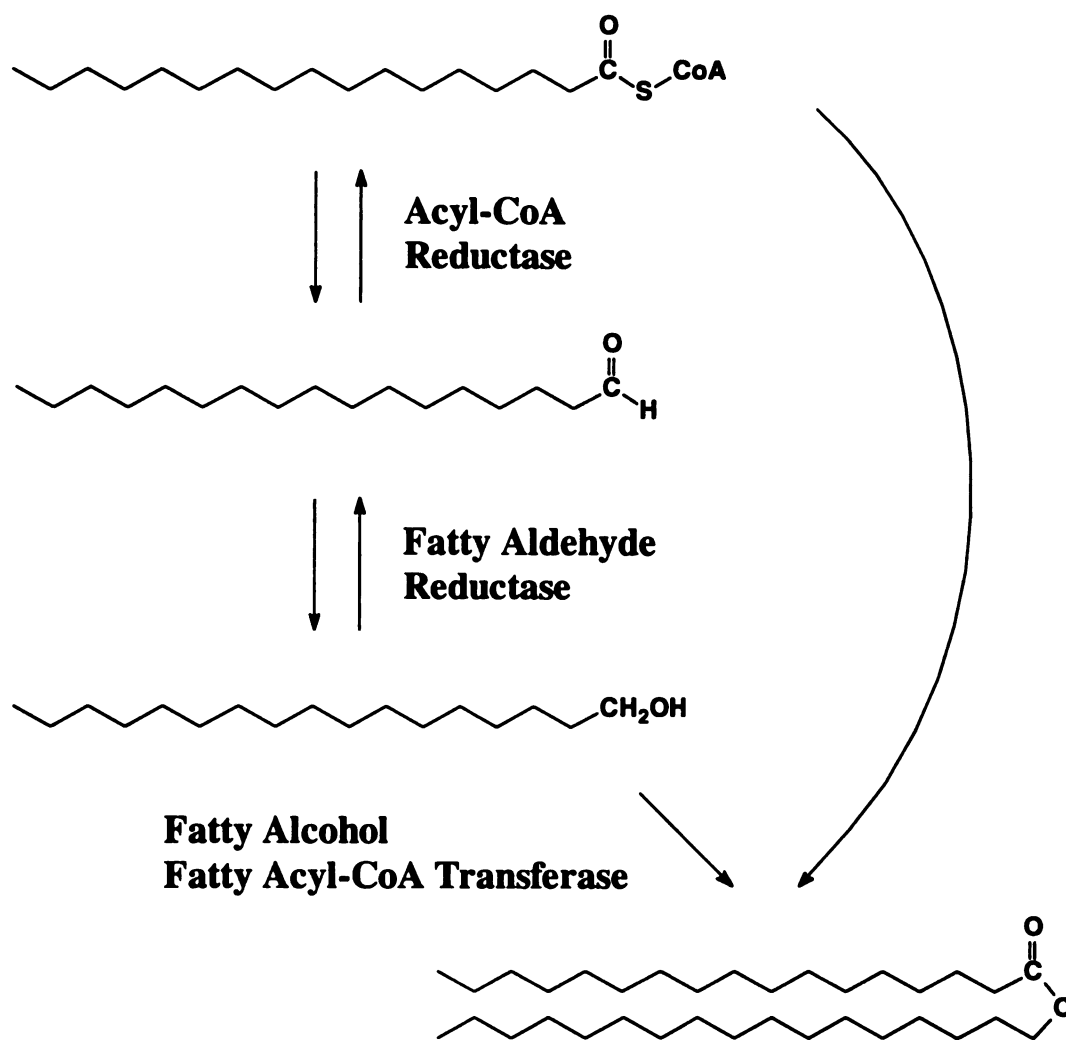


Figure 3-12: Proposed pathway for wax ester biosynthesis in *Acinetobacter calcoaceticus* strain BD413.

an *A. calcoaceticus*/*E. coli* shuttle vector, to give pSER2:*acr1*. This construct was used to transform *E. coli* strain DH5 $\alpha$  for amplification and analysis, followed by subsequent transformation into the *A. calcoaceticus*, mutant *Wow15*. Transformants were grown under wax inducing conditions, collected and extracted with chloroform/methanol for isolation of lipid compounds. Resolution of the lipid fraction by TLC indicated that *Wow15* transformed with pSER2:*acr1* was now able to synthesize wax esters (Figure 3-13), indicating that correct open reading frame had been identified, and that the gene responsible for the *wow15* mutation had been cloned.

**Hydropathy analysis.** Hydropathy analysis of the protein sequence via the Kyte and Doolittle prediction (DNASIS for Windows, Hitachi Software) (Kyte & Doolittle, 1982) is illustrated in Figure 3-14. Panel A shows the hydropathy plot when a window of 21 amino acids was used to identify putative membrane-spanning domains. Since it has been observed that wax ester inclusions are surrounded by a single membrane (Scott & Finnerty, 1976), hydropathy prediction was repeated using a window of 10 amino acids (Panel B, Figure 3-14). The use of a 20 amino acid window showed the protein to be very hydrophobic, suggesting the possibility that the majority of the protein is associated with a hydrophobic environment. Use of a 10 amino acid window gave strong indication of several potential membrane spanning domains.

***In vitro* reductase activity assays.** To test the enzymatic function of the *wow15* gene product *in vitro*, the gene was subcloned into pET21. The P7 and P8 primers (Table 3-3) specific to the region illustrated in Figure 3-8 were used to





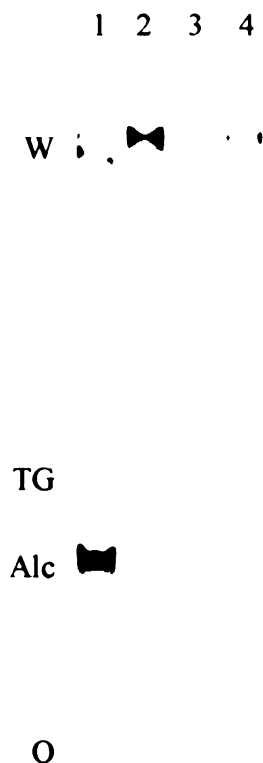
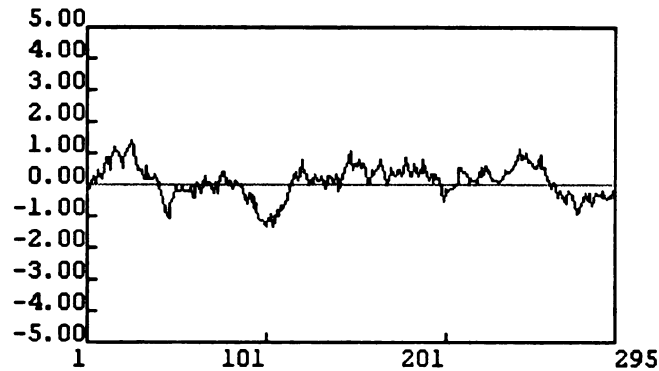
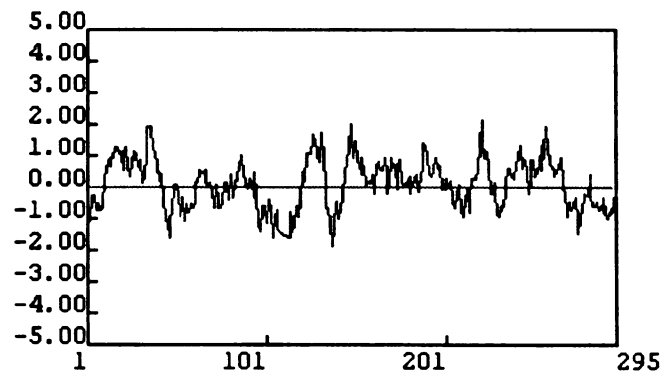


Figure 3-13: Complementation of the mutant *Wow15* with pSER2:*acr1*. Wild type (lane 2), the mutant *Wow15* (lane 3) and the mutant transformed with pSER2:*acr1* (lane 4) were grown under nitrogen limited conditions. The neutral lipids were extracted with chlorform:methanol, spotted onto the TLC and separated. The lipids were visualized by spraying the plate with 50% sulfuric acid and charring the plate at 160°C. Lane 1 contains 0.2 mg of wax esters (W), triacylglycerol (TG), and hexadecanol (Alc) standards. The origin is shown at (O) and the solvent front is at (SF).

**A)** File: *acr1.ami* 1 - 295  
 Table: Kyte & Doolittle  
 Window: 21 Average: 0.14 Threshold Line: 0.00



**B)** File: *acr1.ami* 1 - 295  
 Table: Kyte & Doolittle  
 Window: 10 Average: 0.14 Threshold Line: 0.00



**Figure 3-14: Kyte and Doolittle plots of the protein sequence from *acr1*. A window size of 21 amino acids, the length of an alpha helix needed to span a double phospholipid membrane, was used in panel A. The window size was reduced to 10 amino acids in panel B under the assumption that the protein may be localized to the wax ester inclusion bodies. Wax ester inclusion bodies have been observed to contain only a single phospholipid membrane. Kyte and Doolittle plots were generated using the software package DNASIS for Windows (Hitachi Software).**

remove the native promoter of the gene. The PCR product was subcloned directionally into the BamHI, EcoRI sites of pET21 to give the pET21:*acr1* construct. In this expression system the gene is under the transcriptional control of a *T7lac* promoter which can be induced by the addition of IPTG. Based on the sequence information for the *wow15* gene, it was predicted that the size of the induced protein should be approximately 32 kDa. Following induction of the system with IPTG, a protein of the predicted size was observed primarily in the insoluble protein fraction (Figure 3-15) implying the protein is being localized to the membrane, or is in the form of inclusion bodies. Assays for acyl-CoA, acyl-ACP and palmitic acid reductase activity were run on all the protein fractions by incubating the extracts in the presence of  $^{14}\text{C}$  labelled substrate. The greatest amount of enzymatic activity was associated with the insoluble fraction where the induced protein was observed to be localized (Figure 3-16). Additionally, enzymatic activity was observed in the presence of acyl-CoA, but not acyl-ACP, implying the enzyme is specific for acyl-CoA (Figure 3-17). Experiments aimed at determining the cofactor specificity of the enzyme showed that catalytic activity was observed when the enzyme was incubated in the presence of NADPH but not NADH (Figure 3-18).  $^{14}\text{C}$  labelled fatty alcohol was also observed to be associated with protein extracts derived from *E. coli* transformed with pET21:*acr1*. This implies that the enzyme is not only able to catalyze the reduction of acyl-CoA to the corresponding aldehyde, but it is also able to reduce the aldehyde to the corresponding alcohol. To verify this result, a time course was run using the same enzymatic conditions, but removing a fraction of the reaction every 2.5 minutes (and every 30 seconds in a separate experiment). The results of that experiment are shown

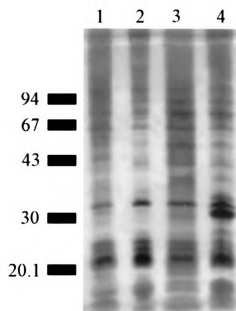


Figure 3-15: SDS-PAGE gel showing protein induction. Protein fractions from *E. coli* containing pET21 was compared to protein fractions prepared from *E. coli* transformed with pET21:*acr1*, following induction with 0.1 M IPTG. Lanes 1 and 2 show soluble fraction 1 from *E. coli* transformed with pET21 and pET21:*acr1*, respectively. Lanes 3 and 4 show the insoluble protein fraction from induced *E. coli* samples transformed with pET21 and pET21:*acr1*, respectively. Lanes were loaded with 1  $\mu$ g of protein. The gel was electrophoresed and silver stained as per materials and methods. Size standards are shown to the left of the gel and are in kilodaltons.

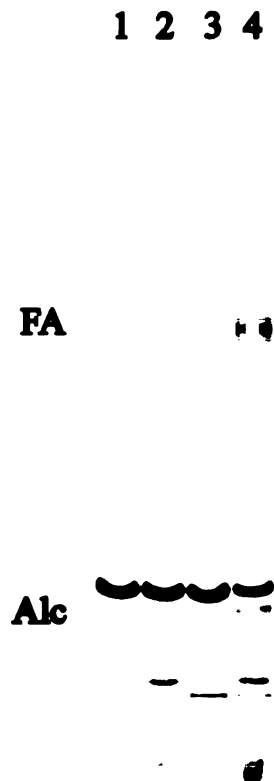
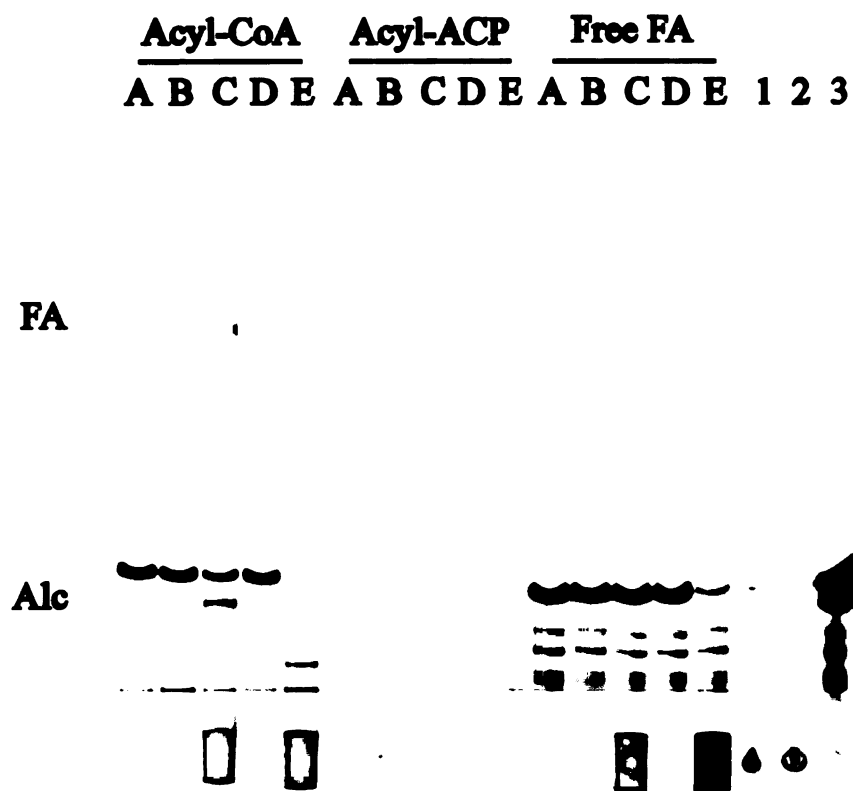
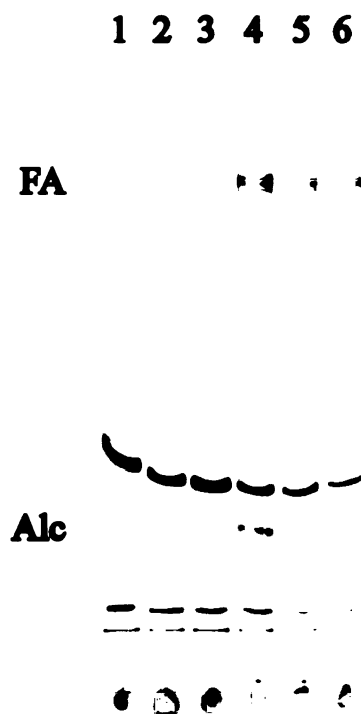


Figure 3-16: *In vitro* acyl-CoA reductase assay. Soluble (lane 1) and insoluble (lane 2) protein fractions from *E. coli* containing pET21 were compared to soluble (lane 3) and insoluble (lane 4) protein preparations from *E. coli* transformed with pET21:*acr1*. Reactions contained 13.5 ug of protein and were incubated in the presence of 0.04 uCi of palmitoyl-1-<sup>14</sup>C-coenzyme A (30 uM) at 30°C for 15 minutes. Neutral lipids were separated by TLC and radiolabelled products were visualized by exposing the TLC plate to a phosphorimaging cassette. Fatty aldehyde (FA) and fatty alcohol (Alc).



**Figure 3-17: Demonstration of an *in vitro* assay showing reductase activity of *acr1* with different radiolabelled substrates.** Soluble and insoluble protein extracts from *E. coli* strain DE3(BL21) transformed with pET21:*acr1* in comparison to protein fractions from untransformed *E. coli* strain DE3(BL21). Reactions contained 13.5 ug of the indicated protein extract, 30 uM palmitoyl-1-<sup>14</sup>C-coenzyme A, 0.83 mM ATP, 100 uM NADH and 100 uM NADPH were incubated at 30°C for 15 minutes. Neutral lipids were collected by chloroform:methanol extraction and spotted onto TLC plates. Radiolabelled lipids were visualized by exposing the TLC plate to a phosphorimaging cassette. Soluble protein extract 1 (A), soluble extract fraction 2 (B) and the insoluble extract (C) were from *E. coli* strain DE3(BL21) transformed with pET21:*acr1*. Soluble protein extract 1 (D) and the insoluble extract (E) were from untransformed *E. coli* strain DE3(BL21). Palmitoyl-1-<sup>14</sup>C-coenzyme A (30 uM), palmitoyl-1-<sup>14</sup>C-ACP (10000 dpm compared to 70000 dpm for palmitoyl-CoA) and 1-<sup>14</sup>C-palmitic acid (65 uM) were used as substrates in the indicated sets. Additionally, one half of the volume used for each reaction was spotted in lanes 1, 2 and 3, respectively. Fatty aldehyde (FA) and fatty alcohol (Alc).



**Figure 3-18: Cofactor dependence of acyl-CoA reductase. *In vitro* reductase assays were carried out with three different cofactors. The insoluble protein fraction (13.5 ug per reaction) was incubated in the presence of 30 uM palmitoyl-1-<sup>14</sup>C-coenzyme A for 15 minutes at 30°C. In addition to the protein extract from *E. coli* transformed with pET21:*acr1* was the addition of no cofactors (lane 1), 0.83 mM ATP (lane 2), 100 uM NADH (lane 3), 100 uM NADPH (lane 4), 100 uM NADH plus 100 uM NADPH (lane 5) and 0.83 mM ATP, 100 uM NADH and 100 uM NADPH (lane 6). Fatty aldehyde (FA) and fatty alcohol (Alc).**

in Figure 3-19. It was observed that fatty aldehyde accumulation can be detected as early as 1.5 minutes into the assay, while fatty alcohol formation is not observed until about 7.5 minutes into the assay.

The ability of the Acr1 protein to convert fatty aldehyde to the alcohol was tested directly. Radiolabelled aldehyde was recovered from the TLC plate by scrapping off the silica, eluting with chloroform/methanol, then drying under nitrogen gas. The resulting radiolabelled fatty aldehydes were resuspended in 2% Triton-X100 (0.2% final concentration) for use as the substrate in an enzyme assay under the conditions detailed above. The results of this experiment are shown in Figure 3-20 where the presence of fatty alcohols is associated solely with protein extracts prepared from *E. coli* transformed with pET21:*acr1*.

**Protein motifs.** Analysis of the protein sequence using the program MotifFinder (Ogiwara, unpublished), which searches the primary sequence for amino acid motifs that are conserved among families of proteins, indicated the presence of a region that is conserved among short chain alcohol dehydrogenase proteins. Figure 3-21 shows predicted secondary structure using DNASIS for Windows (Hitachi Software). Amino acids that were noted to be conserved by the family of short chain alcohol dehydrogenases by Persson et. al. are highlighted in the Figure 3-21 (Persson et al., 1991). The conserved glycine residues at positions 22, 26 and 28 are consistent with a nucleotide binding domain, in this case NADPH. These observations support the idea that the isolated gene encodes a protein which is able to catalyze the production of fatty alcohol from an acyl-CoA substrate.



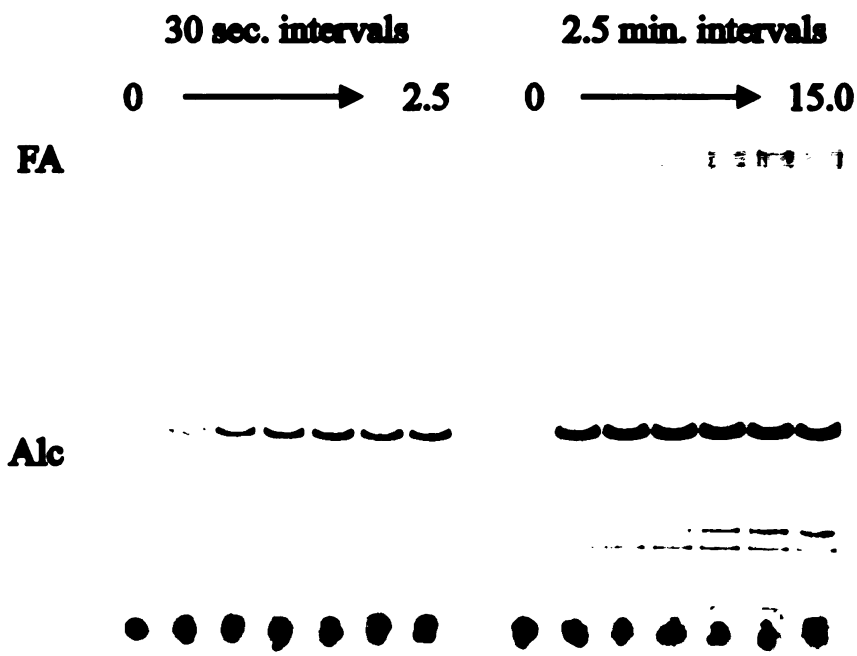


**Figure 3-19: *In vitro* acyl-CoA reductase timecourse.** A total of 13.5 ug of insoluble protein from *E. coli* transformed with pET21:*acr1* was incubated in the presence of 30 uM palmitoyl-1-<sup>14</sup>C-coenzyme A at 30°C for 15 minutes. Time points were collected at 30 second intervals up to 2.5 minutes as shown on the left side of the figure. The same conditions were used in a second experiment, where time points were collected at 2.5 minute intervals up to 15 minutes as shown on the right side of the figure. Five microliters of the reaction was removed at each time point and the neutral lipids were isolated by chloroform:methanol (50:50) extraction and spotted onto the TLC plate. Following separation, the radiolabelled products were visualized by exposing the TLC plate to a phosphorimaging screen. Fatty aldehydes (FA) and fatty alcohols (Alc).



Figure 3-20: *In vitro* enzyme assay testing for reductase activity using 1-<sup>14</sup>C-palmitoyl aldehyde. Reactions contained 13.5 ug of protein and were incubated in the presence 100 uM NADPH and the aldehyde for 15 minutes at 30°C. Samples were then chloroform:methanol (50:50) extracted and separated on a TLC plate before being visualized using a phosphorimager. Lane 1 contains the radiolabelled aldehyde that was used as a substrate, lane 2 represents the reaction run with proteins prepared from *E. coli* transformed with pET21. Lane 3 is from the reaction containing proteins from *E. coli* transformed with pET21:*acr1*. Fatty aldehyde (FA) and fatty alcohol (Alc).

```

File: acrl.ami
Size: 295 aa
Seq: 1 - 295
Function: Chou and Fasman
      10      20      30      40      50      60      70
      *      *      *      *      *
VNNKLEALFRENVKGKVALITGASSGIGLTIAKRIAAGAHVLLVARTQETLEEVKAAIEQQGGQASIFP
HELIX HHHHHHHHHHHH hhhhhh HHHHHHHHHHHHHHHHHHHHHHHHHHHHHHH hH
SHEET sssss sSSSS sSSSSssss sssssssssssssss sss sSSSSs
TURN TTTT TTTTT
COIL

      80      90      100      110      120      130      140
      *      *      *      *      *
CDLTDMAIDQLSQQIMASVDHVDFLINNAGRSIRRAVHESFDRFHDFFERTMQLNYFGAVRLVLNLLPHM
HELIX HHHHHHHHHHHHHHHHHHHHHHHHHHHHHHHHHHHHHHHHHHHHHHHHHHHHHHH
SHEET sSSSSs sssssssssss sSSSS TTTTTT SSSSSSSssssSSSSSSSSSSSS
TURN TT C C TTTT
COIL

      150      160      170      180      190      200      210
      *      *      *      *      *
IKRKNGQIINISSIGVLNATRFSAIVVASKAALDAFSRCLSAEVLKHKISITSIMPLVRTPMIAPTKEY
HELIX HH hHHHHHHHHHHHHHHHHHHHHHHHHHHHHHHHHHHHHHHHHHHHHHHHHHH
SHEET s sSSSSSSSSSS sSSSS sSSSS sSSSSSSSSSSSSSSSSSSSSSSSSSS
TURN TTTT TTTT TTTT TTTT
COIL

      220      230      240      250      260      270      280
KYVPTLSPEEAADLIVYAIVKRPTRIATHLGRSLATYAIAPDINNILMSIGFNLFPSSSTAALGEQEKLN
HELIX HHHHHHHHHHHHHHHHHHHHHHHHHHHHHHHHHHHHHHHHHHHHHHHHHHH
SHEET SSSSSs SSSSSSSSSSSSSSSSSSSSSSSSSSS sSSSSSSSSSSs SS
TURN TTTT TTTT TTTTTT TTTT
COIL

      290
LLQRAYARLFPGEHW
HELIX hhhhhhhhhhhh hh
SHEET SSSSSSSSSs
TURN TTTTTT
COIL

```

Figure 3-21: Secondary structure prediction for *acrl* and conserved amino acid residues specific to the family of short chain alcohol dehydrogenases. This figure shows predicted  $\alpha$ -helices (H and h),  $\beta$ -sheets (B and b), turns (T and t) and coils (C and c) in context to the protein sequence. Upper case letters represent a higher probability of the indicated secondary structure, while lower case letters represent a possibility of the structural element being present. This secondary prediction was calculated using the Chou-Fasman algorithm with a beta-turn probability value of  $7.5 \times 10^{-6}$  using the DNASIS for Windows software package (Hitachi Software). Amino acid residues that are highlighted with (\*) were found to share homology and spacing requirements observed by Persson et. al. (Persson et al., 1991) to be associated with short-chain alcohol dehydrogenase family of enzymes. Amino acids in bold type are the same as those found by Persson to be 100% conserved throughout the family. Also of particular interest are glycine residues 22, 26 and 28 which make up the nucleotide binding motif and are associated with a helix-turn-helix region of the predicted secondary structure as described by Persson et. al. (Persson et al., 1991).

**Enzyme mechanism.** The time course experiment outlined above provided useful information about the mechanism of the Acr1 protein. The observation that alcohols do not accumulate in parallel with aldehydes suggests several things. This result might be interpreted to mean that there is a single active site which carries out both the conversion of acyl-CoA to aldehyde and aldehyde to alcohol. The emergence of alcohols later in the assay would suggest that acyl-CoA is a preferred substrate over fatty aldehyde. Another possible explanation is that the enzyme possesses two active sites, one for the conversion of acyl-CoA to aldehyde, and another which catalyzes the conversion of the fatty aldehydes to alcohol. To address these questions, the time course experiment was repeated in the presence of unlabelled *cis*-11-hexadecenal. If the single site on the enzyme is substrate specific, an overabundance of unlabelled aldehyde should be able to out compete acyl-CoA for the reactive site, and the formation of radiolabelled aldehydes should be inhibited. If there is a second reaction site, then addition of an overabundance of aldehyde should have no effect on the accumulation of radiolabelled aldehyde during the timecourse. The timecourse experiment was repeated in saturating amounts of unlabelled *cis*-11-hexadecenal. The results of the experiment are shown in Figure 3-22. It can be seen that aldehyde accumulation is not inhibited even in the presence of saturating amounts of unlabelled aldehyde. As would be predicted, radiolabelled alcohols are absent. This suggests that the enzyme might contain two active sites, one that converts acyl-CoA to aldehyde, and a second site that catalyzes the conversion of aldehyde to alcohol. This finding is supported by the phenotype of the *Wow15* mutant during nutritional supplementation experiments. Observation that the mutant is unable to synthesize waxes when grown

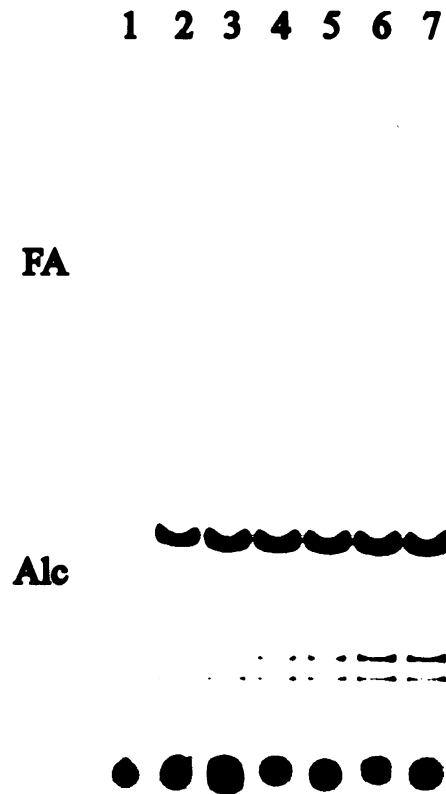


**Figure 3-22: *In vitro* acyl-CoA reductase assay carried out in the presence of unlabelled *cis*-11-hexadecenal. A total of 13.5 ug of protein was incubated in the presence of 30 uM palmitoyl-1-<sup>14</sup>C-coenzyme A at 30°C for 15 minutes. Samples were collected at time 0 (lane 1), 2.5 min. (lane 2), 5.0 min. (lane 3), 7.5 min. (lane 4), 10.0 min. (lane 5), 12.5 min. (lane 6) and 15.0 min. (lane 7). The neutral lipids were collected by chloroform:methanol (50:50) extraction and spotted onto the TLC plate. Following separation, the radiolabelled products were visualized by exposing the TLC plate to a phosphorimaging screen. Fatty aldehydes (FA) and fatty alcohols (Alc).**

in the presence of hexadecane and Tween-40, but accumulates wax esters when grown with *cis*-11-hexadecenal, is consistent with an enzymatic model involving two active sites.

## CONCLUSIONS

A cosmid genomic library was constructed and used to complement two class I, wax<sup>-</sup> mutants, *Wow1* and *Wow15*. DNA from the ends of one of the cosmid's inserts was labelled and used as a probe against digested DNA from the other cosmid. No cross hybridization was evident, indicating that the insert DNAs in the cosmids represented two different areas of the *A. calcoaceticus* genome and that the mutants were affected in two different loci. This was further proven by the observation that the two different cosmids had different restriction patterns.

In order to delineate the complementary region and subclone the gene of interest, I mutagenized the complementary cosmids with a Tn10 derived transposon, mini-Tn10Cm. Three insertions in 1A-3F led to an inability of that cosmid to complement the mutant phenotype of *Wow1*. These insertions have not yet been mapped on the cosmid. Eight insertions in 4A-55 eliminated the ability of the cosmid to complement the *Wow15* mutant. These mutagenized cosmids were used to delineate the gene of interest by comparing their restriction patterns to that of the wild type when it was digested with EcoRV. The insertions were found to span two different EcoRV fragments, which were subcloned and sequenced.

An open reading frame of interest was identified based on its location on the EcoRV fragments and its strong similarity to an open reading frame from

*Mycobacterium tuberculosis*, ORF2, which is thought to encode a  $\beta$ -ketoacyl reductase involved in mycolic acid biosynthesis. The open reading frame from *A. calcoaceticus* was PCR amplified from the complementary cosmid, subcloned into pSER2, an *E. coli*/*A. calcoaceticus* shuttle vector constructed for this purpose, and used to transform *Wow15*. The transformed mutant was able to synthesize wax esters indicating that the complementary gene, designated *acr1*, had been isolated.

Because of the strong sequence similarity of *acr1* to a  $\beta$ -ketoacyl reductase, more chemical complementation experiments were carried out to determine if the mutant was unable convert acyl-CoA to its corresponding aldehyde. Incubation of the mutant, *Wow15*, in the presence of Tween-40, under wax inducing conditions, resulted in no wax production. Growth of *Wow15* in the presence of *cis*-11-hexadecenal resulted in the production of wax esters. These observations, together with the previously noted observation that waxes were not synthesized by *Wow15* when it was cultured in the presence of hexadecane led to the conclusion that *Wow15* was most likely the result of a mutation in the gene encoding the enzyme for acyl-CoA reductase.

To investigate the enzymatic properties of the cloned *acr1* gene, it was transformed into an inducible *E. coli* transcriptional expression system. An induced protein of the appropriate size was observed to be present in the insoluble fraction of proteins prepared from these induced transformants. This enzyme catalyzed the conversion of acyl-CoA to the corresponding alcohol, via an aldehyde intermediate. The enzyme was substrate specific for acyl-CoA, and not acyl-ACP, and utilized NADPH (but not NADH) as a cofactor. The primary sequence of the protein

contained recognizable motifs that match signatures of the short chain alcohol dehydrogenase family.

I have named the gene encoding this enzyme *acr1*, for *acyl-CoA reductase*. It represents a novel enzyme that has not been detailed previously in the scientific literature.

Experiments are currently under way to ascertain the function of the gene residing on the cosmid that was found to complement *Wow1*. Because of the discovery that *acr1* is able to catalyze both of the reduction steps involved in wax ester biosynthesis, it seems unlikely that the *Wow1* mutation is affected in either one of these steps. This is in contradiction to the chemical complementation experiments which characterized it as a reductase mutant. The other activity left in the pathway involves the acyl-CoA fatty alcohol transferase. However, experiments in which the *Wow1* mutant was fed hexadecanol indicated that it was still able to synthesize waxes, implying this gene had not been disrupted. It is possible that this mutant has been affected in a regulatory protein that is specific to controlling wax ester production and not triacylglycerol production. Although this does not seem very likely, it is one explanation that can be put forth with the evidence in hand. It will be interesting to pursue this mutant further and determine what gene has been disrupted.

## REFERENCES

- Allen, L. N. and Hanson, R. S.. 1985. Construction of Broad-Host-Range Cosmid Cloning Vectors: Identification of Genes Necessary for Growth of *Methylobacterium organophilum* on Methanol. *J. Bact.* 161(3):955-962.
- Altschul, S. F., Gish, W., Miller, W., Myers, E. W. and Lipman, D. J.. 1990. Basic Local Alignment Search Tool. *J. Mol. Biol.* 215: 403-410.



- Arrowsmith, T. J., Malpartida, F., Sherman, D. H., Birch, A., Hopwood, D. A. and Robinson, J. A.. 1992. Characterization of *acrl*-Homologous DNA Encoding Polyketide Synthase Genes from the Monensin Producer *Streptomyces cinnamonensis*. *Mol. Gen. Genet.* 234:254-264.
- Bachmann, B. J. 1987. In *Escherichia coli* and *Salmonella typhimurium*, Cellular and Molecular Biology. Eds. Neidhardt F. C. et. al., ASM.
- Figurski, D. and Helinski, D. R.. 1979. Replication of an Origin-Containing Derivative of Plasmid RK2 Dependent on a Plasmid Function *in trans*. *Proc. Natl. Acad. Sci., U.S.A.* 76:1648-1652.
- Fixter, L. M. and Sherwani, M. K.. Energy Reserves in *Acinetobacter*. In The Biology of *Acinetobacter*: Taxonomy, Clinical Importance, Molecular Biology, Physiology, Industrial Relevance. Plenum Press, New York, New York. 1991. Eds. Towner, K. J., Bergogne-Bérézin, E., and C. A. Fewson.
- Juni, E. 1972. Interspecies Transformation of *Acinetobacter*: Genetic Evidence for a Ubiquitous Genus. *J. of Bact.* 112:917-931.
- Kleckner, N., Bender, J. and Gottesman, S.. 1991. Uses of Transposons with Emphasis on Tn10. In Methods of Enzymology: Bacterial Genetic Systems. Vol. 204. Miller, J. H. (ed.). Academic Press Inc., San Diego, California.
- Kyte, J. and Doolittle, R. F.. 1982. A Simple Method for Displaying the Hydropathic Character of a Protein. *J. Mol. Biol.* 157: 105-132.
- Maniatis, T., Fritsch, E. F., and Sambrook, J.. 1982. In Molecular Cloning, A Laboratory Manual. Cold Spring Harbor Laboratory Press, New York, New York.
- Ogiwara, A. MotifFinder can be accessed via the World Wide Web at the following address, which is current at the time of this manuscript:  
<http://www.genome.ad.jp/SIT/MOTIF.html>. Unpublished.
- Persson, B., Krook, M., and Jörnvall H.. 1991. Characteristics of Short-Chain Alcohol Dehydrogenases and Related Enzymes. *Eur. J. Biochem.* 200:537-543.
- Raleigh, E. A., Lech, K. and Brent, R.. 1989. In Current Protocols in Molecular Biology. Eds. Ausubel, F. M. et al. Publishing Associates and Wiley Interscience, New York.
- Scott, C. C. L. and Finnerty, W. R.. 1976. Characterization of Intracytoplasmic Hydrocarbon Inclusions from the Hydrocarbon-Oxidizing *Acinetobacter* Species H01-N. *J. Bact.* 127(1):481-489.
- Yuan, Y., Lee, R. E., Besra, G. S., Belisle, J. T. and Barry, C. E.. 1995.

Identification of a Gene Involved in the Biosynthesis of Cyclopropanated Mycolic Acids in *Mycobacterium tuberculosis*. *Proc. Natl. Acad. Sci., U.S.A.* 92:6630-6634.

Zilsel, J., Ma, P. H. and Beatty, J. H.. 1992. Derivation of a Mathematical Expression Useful for the Construction of Complete Genomic Libraries. *Gene* 120:89-92.

## CHAPTER 4

### ISOLATION AND CHARACTERIZATION OF TRANSPOSON MUTANTS FROM *A. CALCOACETICUS* STRAIN BD413

#### ABSTRACT

It has previously been observed that when *A. calcoaceticus* strain BD413 is grown under nitrogen limited conditions it accumulates both wax esters and triacylglycerol. In the previous chapter I described the isolation of mutants of *A. calcoaceticus* that were deficient in triacylglycerol accumulation via chemical mutagenesis. However, it was not possible to complement the mutant phenotypes with the cosmid genomic library that had been constructed. Therefore, another round of mutagenesis was performed on *A. calcoaceticus* strain BD413, using a transposon derivative of Tn10 called mini-Tn10PttKm. A total of four mutants were isolated, two of these were class II (tag<sup>-</sup>) mutants, and the other two were class III (wax<sup>-</sup>tag<sup>-</sup>) mutants. One of these tag<sup>-</sup> mutants, 11-C7, was selected for further study.

DNA flanking the transposon insertion was amplified by extended inverse PCR (IPCR). The IPCR product was subcloned and used to identify cosmids from the genomic library that shared homology to the flanking DNA regions. A BglII fragment from one of these cosmids (5A-F1) was observed to share homology to the flanking sequences surrounding the transposon insertion. The BglII fragment from the cosmid was subcloned and used as a probe against genomic DNA prepared from wild type

*A. calcoaceticus* and the mutant, 11-C7. A shift in molecular weight, appropriate to the size of the expected transposon was observed. The BglII fragment was sequenced and three open reading frames could be identified. The approximate location of the insertion was mapped via extended PCR. From this information it was determined that the transposon inserted into an open reading frame that shares considerable homology to a gene called *glnE* that has been identified in many different organisms. Since *glnE* has been implicated in the regulation of nitrogen, it is considered likely that the 11-C7 phenotype is not the result of a mutation in a triacylglycerol structural gene, but rather is the result of a mutation to a gene involved in nitrogen regulation or response.

## INTRODUCTION

During the course of selecting a strain of *A. calcoaceticus* to work with in studying wax ester biosynthesis it was observed that *A. calcoaceticus* strain BD413 also accumulated triacylglycerol when grown under low nitrogen conditions (Chapter 2, this text). This represented an opportunity to not only screen for wax ester mutants, but at the same time to screen for mutants that failed to accumulate triacylglycerol.

It was our hope to identify mutants that were affected in triacylglycerol production, but were unaffected in wax ester accumulation. This would help eliminate the possibility that mutants affected in nitrogen sensing and response would be recovered. In recovering such mutants we hoped to identify mutants that had been affected in structural genes for enzymes involved in triacylglycerol biosynthesis, particularly the gene encoding the enzyme diacylglycerol acyl transferase (DGAT).

DGAT plays a very important part in triacylglycerol production. It is

responsible for the final conversion of diacylglycerol to triacylglycerol via the addition of an acyl group to the sn3 position of diacylglycerol. It is believed that this might be a key regulatory step in triacylglycerol production in higher organisms, primarily plants, since it would regulate the flow of carbon between phospholipid production and triacylglycerol accumulation.

A similar approach to that outlined in the previous chapter for the isolation and characterization of the wax mutant, *Wow15*, was also carried out for chemically induced mutants affected in triacylglycerol accumulation. Complementation using the genomic library that was known to complement two class I mutants and a tryptophan auxotrophic mutant, was used to try to complement *Wow7*, a class II (tag<sup>-</sup>) mutant, but was unsuccessful. This raised the possibility that the cosmid library was incomplete, or that the *wow7* phenotype was the result of a dominant mutation that could not be complemented by the library. Therefore, a new approach involving mutagenizing *A. calcoaceticus* with a transposon was tried in an attempt to generate new tag<sup>-</sup> mutants.

There are several benefits of using a transposon mutagenesis compared to chemical mutagenesis. One reason is that by generating mutants with a transposon, only a single mutational event occurs that is the result of the transposon inserting into the gene of interest. By contrast, chemical mutagenesis can cause many mutational events throughout the genome depending on the amount of mutagen used and the duration of exposure. Another reason is that once the desired phenotype is isolated, the transposons can be rescued from the genome of the mutant, usually together with flanking genomic sequence. This can be done either by plasmid rescue, if the transposon contains an origin of replication, or by inverse PCR. The flanking

sequence can then be used as a probe to identify the full length gene.

The reason transposon mutagenesis was not used initially, was simply because there had not been a transposon available for use with *A. calcoaceticus*. That changed when a Tn10 derivative, mini-Tn10PttKm, was used to generate lipase mutants in *A. calcoaceticus* strain RAG-1 (Leahy et al., 1993). Another reason not to use transposon mutagenesis is simply the amount of work required to screen for the desired phenotype. Because the mutagenesis typically produces one insertional event per colony (i.e. one mutagenic event), it is necessary to screen more samples than in the chemical mutagenesis to find the desired phenotype.

In this chapter I describe the mutants isolated by transposon mutagenesis of *A. calcoaceticus* strain BD413. I will discuss the characterization of these mutants by Southern analysis, and finally describe the isolation of flanking DNA surrounding the insertion in the tag<sup>+</sup> mutant 11-C7 and what this DNA possibly encodes.

## MATERIALS AND METHODS

**Bacterial stains and plasmids.** The bacterial strains used in the experiments described in this chapter are shown in Table 4-1. The source of the plasmids used in this chapter, or in the construction of novel plasmids is presented in Table 4-2.

**Growth and culture conditions.** Conditions have been previously described in Chapter 2.

**Transposon Mutagenesis.** Fifty milliliter cultures of *A. calcoaceticus* strain BD413 and the transposon donor *E. coli* strain SM10 containing the transposon mini-

Table 4-1: Bacterial strains used in Chapter 4.

Bacterial Strains	Relevant Characteristics	Source or Reference
<b><i>A. calcoaceticus</i></b>		
ATCC #33305, strain BD413	wild type used during these studies, unencapsulated mutant of <i>A. calcoaceticus</i> strain BD4	ATCC stock center
<i>Wow7</i>	tag <sup>-</sup> null mutant of BD413	this study, chapter 2
3-A9	mini-Tn10PttKm mutant of strain BD413 that is wax <sup>-</sup> tag <sup>-</sup> and found to have multiple insertions	this study
6A-H5	mini-Tn10PttKm mutant of strain BD413 that is wax <sup>-</sup> and found not to have an insertion	this study
9-C3	mini-Tn10PttKm mutant of strain BD413 that is tag <sup>-</sup> and found to have multiple insertions	this study
11-C7	mini-Tn10PttKm mutant of strain BD413 that is tag <sup>-</sup>	this study
11-C7:Rif <sup>r</sup>	spontaneous Rif <sup>r</sup> mutant of 11-C7	this study
11-D12	mini-Tn10PttKm mutant of strain BD413 that is tag <sup>-</sup> and found not to have an insertion	this study
30-F10	mini-Tn10PttKm mutant of strain BD413 that is tag <sup>-</sup>	this study
30-F10:Rif <sup>r</sup>	spontaneous Rif <sup>r</sup> mutant of 30-F10	this study

Table 4-1 (cont'd)

30-G9	mini-Tn10PttKm mutant of strain BD413 that is wax <sup>-</sup> tag <sup>-</sup>	this study
35-G5	mini-Tn10PttKm mutant of strain BD413 that is wax <sup>-</sup> tag <sup>-</sup>	this study
<i>E. coli</i>		
HB101	F <sup>-</sup> proA2 recA13 mcrB	(Maniatis et al., 1982)
DH5 $\alpha$	F'/endA1 recA1 $\Delta$ (lacZYA-argF) U169 ( $\phi$ 80dlac $\Delta$ (lacZM15)	(Raleigh et al., 1989)
MM294	F <sup>-</sup> endA1 hsdR17 thi-1	(Bachmann, 1987)
SM10 $\lambda$ pir	Km <sup>r</sup> thi-1 thr leu tonA lacY supE recA::Rp4-2-Tc::Mu $\lambda$ pir	(Miller & Mekalanos, 1988)

---



Table 4-2: Plasmid sources and derivations for Chapter 4.

<b>Plasmid</b>	<b>Description or Construction</b>	<b>Source or Reference</b>
pBS-KS <sup>+</sup> , pBS-KS <sup>-</sup>	Bluescript Vector	Stratagene
pRK2013	Km <sup>r</sup> self-transmissible RK2 derivative containing ColE1 replicon and transfer functions to mobilize RK2 derivatives	(Figurski & Helinski, 1979)
pLA2917	Cosmid Vector (Tet <sup>r</sup> ) derived from RK2	(Allen & Hanson, 1985)
5A-F1	pLA2917 derived cosmid clone with homology to flanking sequences surrounding the insertion found in the strain 11-C7	this study
pLOFPttKm	Plasmid vehicle carrying mini-Tn10PttKm	(Herrero et al., 1990)
pGEM-T	T-vector for facilitating the subcloning of PCR fragments	Promega
pSR10	pGEM-T derivative containing flanking sequence surrounding the insertion site of the Tn from the 11-C7 mutant	this study
pSR11	Bluescript derivative containing the BglII fragment from the cosmid 5A-F1 that shared homology with flanking sequence surrounding the insertion site of the Tn from the 11-C7 mutant. Gave rise to sequence ID#10-11	this study, chapter 4 for construction and appendix A for sequence information

Table 4-2 (cont'd)

pSR12	Bluescript derivative containing a BglII fragment from 5A-F1 that lies upstream of the BglII fragment contained in pSR11. Gave rise to sequence ID#12-14	this study, chapter 4 for construction and appendix A for sequence information
-------	--	--

---

Tn10PttKm on plasmid pLOFPttKm were grown in LB at 30°C to an OD<sub>600</sub> of 0.6. The cells were collected by centrifugation, washed twice with LB medium, and resuspended in the original volume. Fifty milliliters of *A. calcoaceticus* culture was then mixed with 25 ml of the transposon donor strain and collected on 0.45 µ sterile 85 mm cellulose acetate filter producing an even lawn of bacteria. The resulting filter was transferred to an LB plate containing 500 µM IPTG to induce the mobilization of the transposon. The diparental mating was incubated at 30°C for 8 hours. The bacteria were then removed from the filter by washing the filter in 10 ml of 10 mM MgSO<sub>4</sub>. The sample was concentrated by centrifugation and resuspended in 10 mM MgSO<sub>4</sub>. Transconjugates containing the transposon were selected by plating the cells on LB plates containing rifampicin to select against the presence of *E. coli*, plus kanamycin to select for the presence of the transposon in *A. calcoaceticus*.

**Mutant and complementation screening using the lipophilic dye Sudan black B.** Methods have been previously described in Chapter 3.

**Thin layer chromatography (TLC).** Method has been previously described in Chapter 2.

**Library Construction.** Library construction was described in Chapter 3.

**Triparental filter matings.** Matings were carried out in the manner previously described in Chapter 3. The cosmid library was contained in *E. coli* strain HB101 and was Tet<sup>r</sup> due to the presence of the cosmid. MM294 is a strain containing pRK2013, a helper plasmid that enables triparental mating through its *mob* genes. The pRK2013 plasmid imparts Km<sup>r</sup>. Finally, the mutant strain 11-C7:Rif<sup>r</sup> is the target of the mating and is a Rif<sup>r</sup> strain of 11-C7. It was obtained by plating 11-C7 on rifampicin plates and looking for the presence of spontaneous Rif<sup>r</sup> colonies. The neutral lipid profiles of these Rif<sup>r</sup> strains were examined to make sure they matched those of the original 11-C7 mutant. At the end of the mating, 11-C7:Rif<sup>r</sup> mutants containing the cosmid can be selected by plating the product of the cross onto LB medium containing rifampicin, to select for 11-C7:Rif<sup>r</sup>, and tetracycline to select for the presence of the cosmid. MM294 and the HB101 donor will fail to grow because they are not resistant. The 11-C7 strain and MM294 were grown overnight as 3 ml cultures, and the library was grown in 96 well titer plates as replicates of the original. The day of the mating, 0.5 ml of MM294 was used to inoculate a 50 ml of culture, and 3 ml of 11-C7 was used to inoculate a 50 ml culture. Cultures were collected at an OD<sub>600</sub>=0.6, washed and then resuspended in 50 ml of LB. Twenty five milliliters of MM294 was combined with 50 ml of the 11-C7 strain. Ten milliliters of this mixture was drawn through a sterilized 45μ filter (85 mm in diameter) via a vacuum apparatus creating an even lawn of bacteria. The filter was then removed and placed on to an LB plate. Using a sterilized set of prongs arranged to match 48 wells of the 96 well titer plates containing the library, the library was stamped onto the lawn of bacteria and matings were allowed to incubate at 30°C overnight. Filters were then transferred to selective

medium containing rifampicin (100 µg/ml) and tetracycline (15 µg/ml) to select for 11-C7:Rif<sup>r</sup> containing the cosmids. The resulting patches were then restreaked onto a master plate containing the selective medium, before being replica plated onto minimal, low nitrogen, triacylglycerol inducing medium for subsequent analysis by lipophilic staining and TLC.

**Inverse PCR.** In the hope of creating intramolecular recircularization events, genomic DNA from the class II mutants, 11-C7 and 30-F10 were digested to completion with BglII and XbaI, respectively. Fragments were size selected by separating the digested products on a 0.8% agarose gel, cutting out an agarose block containing the appropriately sized fragments, and purifying the DNA fragments away from the agarose by electroelution (Maniatis et al., 1982). The DNA fragments were recircularized by diluted them to a concentration of 0.6 ng/µl in a 200 µl ligation volume containing 3 units of T4 DNA ligase (Boehringer Mannheim) and 20 µl of 10x ligation buffer (660 mM Tris-HCl (pH 7.6), 50 mM MgCl<sub>2</sub>, 10 mM dithioerythritol and 10 mM ATP (pH 7.5)). Three microliters of this ligation reaction was used with Boehringer Manneheim's Expand Long Template PCR System. Reactions contained 350 µM of dNTP's, 300 nM of each primer, 5 µl of 10x buffer 1 (17.5 mM MgCl<sub>2</sub>, 500 mM Tris-HCl, pH 9.2, 160 mM (NH<sub>4</sub>)<sub>2</sub>SO<sub>4</sub>), 3.0 µl of the ligation reaction described above was used as template DNA and 0.75 µl of the supplied enzyme mix in a total volume of 50 µl. Cycling was carried out in the following manner:

Step 1: 94°C for 2 minutes

Step 2: 94°C for 10 seconds

Step 3: 65°C for 30 seconds

Step 4: 68°C for 7 minutes

Step 5: repeat from step 2 10 more times

Step 6: 94°C for 10 seconds

Step 7: 65°C for 30 seconds

Step 8: 68°C for 7 minutes + 20 seconds each cycle

Step 9: repeat from step 6 15 more times

Step 10: 68°C for 7 minutes

Step 11: Hold at 4°C

**Extended PCR.** Mapping the location of the BglII fragment that was found to share homology to flanking sequences surrounding the transposon insertion in 11-C7 in respect to the cosmid was possible using Boehringer Mannheim's extended PCR.

Primers were constructed on either end of the BglII site of pLA2917 facing in toward the insert. Additionally, primers specific to both ends of the BglII fragment were constructed to face out, toward the edge of the insert DNA. Using one anchor on the cosmid in conjunction with the primers specific to the BglII sequence (Table 4-3), it was possible to amplify the DNA in between the primers allowing me to assign a distance from the end of the fragment relative to the anchoring (cosmid specific) primer (Figure 4-1). Long PCR products were obtainable using Boehringer Mannheim's Expand Long Template PCR System. Reactions contained 350 µM of dNTP's, 300 nM of each primer, 5 µl of 10x buffer 1 (17.5 mM MgCl<sub>2</sub>, 500 mM Tris-HCl, pH 9.2, 160 mM (NH<sub>4</sub>)<sub>2</sub>SO<sub>4</sub>), 0.15 µg of template DNA and 0.75 µl of the supplied enzyme mix in a total volume of 50 µl. Cycling was carried out in the following manner:

- Step 1: 94°C for 2 minutes
- Step 2: 94°C for 10 seconds
- Step 3: 65°C for 30 seconds
- Step 4: 68°C for 7 minutes
- Step 5: repeat from step 2 10 more times
- Step 6: 94°C for 10 seconds
- Step 7: 65°C for 30 seconds
- Step 8: 68°C for 7 minutes + 20 seconds each cycle
- Step 9: repeat from step 6 15 more times
- Step 10: 68°C for 7 minutes
- Step 11: Hold at 4°C

**Colony lifts for hybridization.** Method was described in Chapter 3.

**Restriction digestions and southern blot analysis.** Methods were previously described in Chapter 3.

**Nested deletions and DNA sequencing.** Methods were previously described in Chapter 3.

**Database analysis of DNA sequences.** Methods were previously described in Chapter 3.

Table 4-3: List of synthetic oligonucleotides used in this Chapter 4.

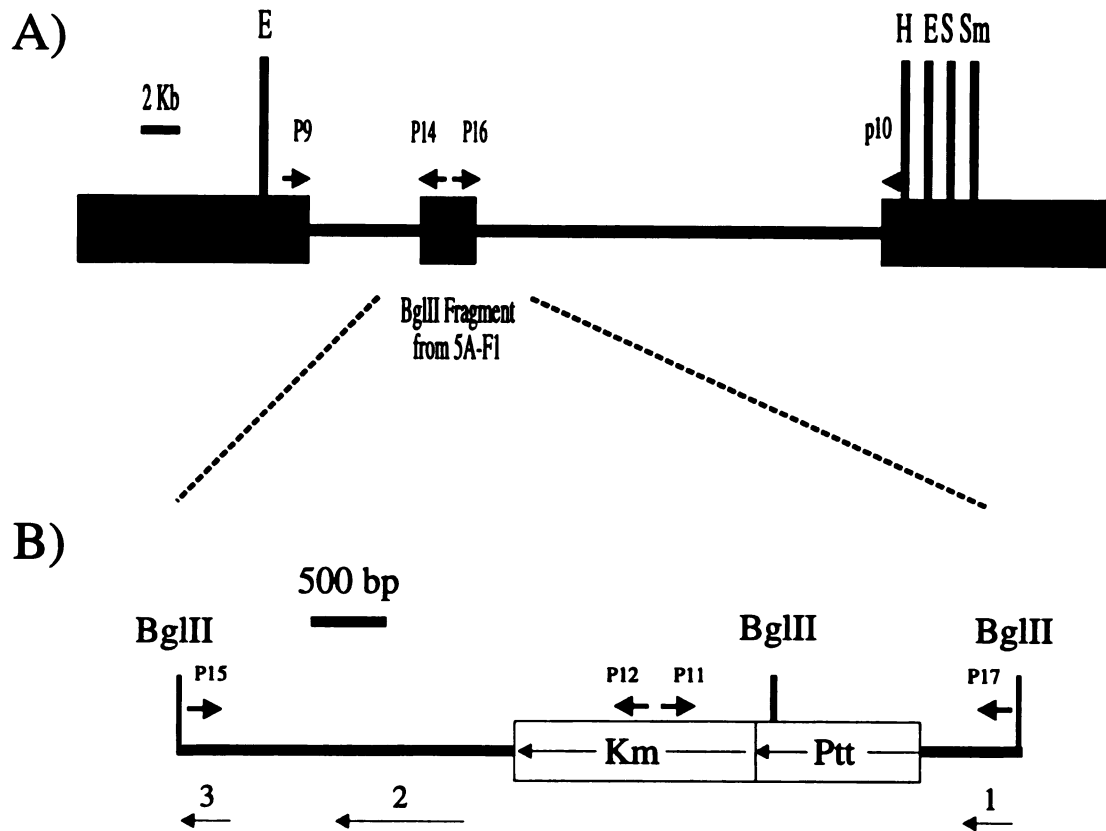
Name of primer	Sequence (5'-3')	Description
P9	CTTTCTTGCCGCCA AGGATCTGATG	Primer used in mapping the location of BglII fragment containing <i>glnE</i> in 4A-55. Specific to 5' side of BglII site of pLA2917 in the Km cassette which originated from Tn-5. Faces toward BglII site (Figure 4-1).
P10	GGCCGGAGAACCT GCGTGCAAT	Same as 5' Km Tn-5 but specific to the 3' side of the BglII site (Figure 4-1).
P11	TCGCGGCCTCGAGC AAGACGT	Primer used for inverse PCR experiments and for mapping the location of Tn with respect to BglII fragment from 5A-F1. Primer is specific to 5' end of Km cassette in mini-Tn10PttKm. Km cassette is from Tn903. Primer faces out (Figure 4-1).
P12	CTGCCTCGGTGAGT TTTCTCC	Same as SER-5', except primer is located further into Km cassette (Figure 4-1).
P13	GATTCGGCCACCGC TTCCAAA	Used for the same purposes and in conjunction with SER-5' and SER-3'. Specific to 5' region of the Ptt cassette of mini-Tn10PttKm

Table 4-3 (cont'd)

P14	CTTTTGCGGTGTGG TGTATAA	Primer designed with specificity to end of Sequence ID#10. Primer faces out toward BglII site of pLA2917 (Figure 4-1).
P15	ACACCGCAAAAGA GAAAGGTT	Primer designed with specificity to end of Sequence ID#10. Primer faces in toward mini-Tn10PttKm (Figure 4-1).
P16	TTCGGCTCGTTCAC GTAGATA	Primer designed with specificity to end of Sequence ID#11. Primer faces out toward BglII site of pLA2917 (Figure 4-1).
P17	AGCCGAAAGCCAC CGTTTAGC	Primer designed with specificity to end of Sequence ID#11. Primer faces in toward mini-Tn10PttKm (Figure 4-1).

---





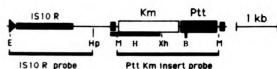
**Figure 4-1: Positional mapping of the BglII fragment in the cosmid 5A-F1.** The location of the BglII fragment cloned from cosmid 5A-F1, in relation to 5A-F1's insert DNA, was determined by extended PCR using primers specific to the cosmids Km' cassette (P9 and P10) in conjunction with primers specific to identified sequence from the BglII fragment (P14 and P16) (Panel A). The location of the transposon insertion relative to the BglII fragment was determined by PCR mapping using genomic DNA as a template and primers specific to the transposon, mini-Tn10PttKm (P11 and P12) in combination with primers specific to determined sequence from the ends of the BglII fragment (P15 and P17) (Panel B). By testing the different combinations of primers it was possible to finally come to the orientation shown above and determine that the transposon had inserted into the open reading frame encoding *glnE*. The approximate positions of the open reading frames present on the BglII fragment illustrated in panel B are represented by arrows below the fragment showing direction of transcription. These are glutamate-ammonia-ligase adenylyltransferase from *E. coli* (1), putative branched-chain-amino-acid transaminase from *E. coli* (2) and an unidentified open reading frame (3).

## RESULTS AND DISCUSSION

**Transposon mutagenesis.** To measure the frequency of transposition, it was determined that the number of recipient cells at the time of infection with the transposon measured  $1.3 \times 10^7$  cfu/ml. The number of resulting colonies after selection for the presence of the transposon in the recipient, *A. calcoaceticus* strain BD413:Rif<sup>r</sup> was observed to be 3000 cfu/ml. By dividing the number of chloramphenicol resistant transformants by the number of recipients, the frequency of transposition was estimated to be  $2.3 \times 10^{-5}$ . It was noted that when the chloramphenicol resistant lines resulting from the mutagenesis were plated out onto selective medium, a variety of colony morphologies were evident. This was one indication of the success of the mutagenesis. Additionally, when the transposon mutagenized colonies were transferred to low nitrogen, minimal medium plates for staining with Sudan black B, several colonies were unable to grow. This suggested the presence of auxotrophic mutants. To confirm if transposition had occurred and whether it was random, nine colonies were selected and genomic DNA was prepared. The genomic DNA from these suspected transposon mutagenized lines was digested with HindIII, an enzyme known to cut internal to the transposon, and separated on a 0.8% agarose gel. The samples were then probed with the MluI fragment from the Km<sup>r</sup> marker from the transposon (Figure 4-2, panel A). The MluI fragment hybridized to two bands in each sample as predicted due to the presence of a HindIII site in the transposon (Figure 4-2, panel B). It was also observed that the fragments were all of different sizes implying that each colony carried an insertion at a different site.

**Mutant screening.** A total of over 3000 transposon-mutagenized colonies

A)



B)

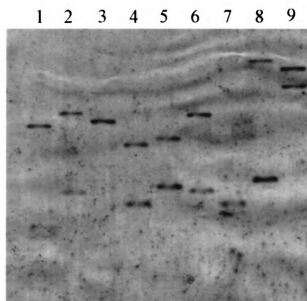


Figure 4-2: Southern blot analysis of 9 random colonies following mutagenesis with mini-Tn10PttKm transposon. Genomic DNA was digested with HindIII and probed with the cassette illustrated in panel A. (A) An abbreviated restriction map of pLOFPttKm, the plasmid carrying mini-Tn10PttKm the transposon used in the mutagenesis. The region between the two MluI sites was used as a probe against the blot illustrated in panel B (B, BglII, E, EcoRI, Hp, HpaI, M, MluI and Xh, XhoI). The two small rectangles in panel A represent the inverted repeats of the transposon. Note that there is a HindIII site internal to the transposon, thus giving rise to the presence of two bands on the blot.

were directly screened by TLC analysis of their neutral lipid composition. A total of 8 mutants were recovered. These 8 mutants could be divided into the 3 different phenotypic classes that were similarly observed in the chemically mutagenized samples. One class I mutant (wax<sup>-</sup>), four class II mutants (tag<sup>-</sup>) and three class III mutants (wax<sup>-</sup>tag<sup>-</sup>) were recovered. Genomic DNA from the eight mutants was prepared and then digested with PstI, which is known not to cut the transposon. The DNA was then Southern blotted and probed with the transposon (Figure 4-3). The transposon was absent in 2 of the 8 mutants, indicating that their phenotype's were either the result of a spontaneous mutation, or more likely, that the transposon excised itself from the genome. Two of the mutants were observed to contain multiple bands on the Southern blot indicating multiple insertions. This left a total of four mutants with single insertions. Although the mutants containing multiple insertions could be analyzed, I decided to simplify the matter and investigate the mutants harboring single insertions. Two of these were class II mutants and the other two were class III mutants. The class III mutants were dismissed as nitrogen regulatory mutants and only the class II mutants were pursued for further analysis.

It is important to note that when the two class II mutants, 11-C7 and 30-F10, were cultured under low nitrogen conditions, little to no growth occurred. Identification of the mutant phenotype was possible by scrapping colonies off of an LB plate and then culturing the cell paste in low nitrogen medium. In this manner, it was possible to identify them as class II mutants in a reproducible manner.

**Inverse PCR.** Genomic DNA from the two class II mutants, 11-C7 and 30-F10, was digested with several different restriction enzymes, the fragments were

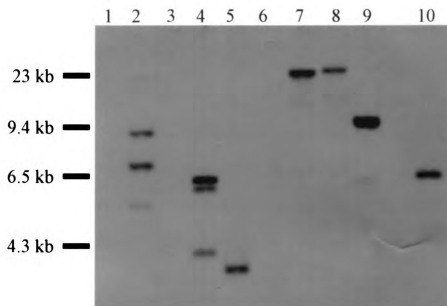


Figure 4-3: Southern analysis of isolated mutants carrying mini-Tn10PttKm. Genomic DNA from the isolated mutants was digested with *Pst*I and probed with the *Mlu*I fragment of the transposon (Figure 4-2, panel A). There are no *Pst*I sites internal to the transposon as witnessed in lane 10 which contains pLOFPttKm digested with *Pst*I. *A. calcoaceticus* strain BD413 wild type DNA (lane 1), 3-A9 (lane 2), 6A-H5 (lane 3), 9-C3 (lane 4), 11-C7 (lane 5), 11-D12 (lane 6), 30-F10 (lane 7), 30-G9 (lane 8), 35-G5 (lane 9). The identification of multiple bands in lanes 2 and 4 indicates the presence of multiple insertions in these strains, while the absence of bands in lanes 3 and 6 can be interpreted to mean that these mutants have lost the transposable element.

separated by electrophoresis through an agarose gel, and a Southern blot was probed with the transposon (Figure 4-4). The purpose of this experiment was to identify a fragment of convenient size that could be size-selected and recircularized for inverse PCR (IPCR). Digestion of 30-F10 with XbaI and 11-C7 with BglII, respectively, produced the desired results. A restriction fragment of approximately 6.5 kb was observed for 30-F10 when it was digested with XbaI and a fragment of about 4.0 kb was seen for 11-C7 when it was cut with BglII.

Genomic DNA was digested with the appropriate enzyme, and fragments of approximately 6.5 kb in the case of 30-F10 and 4.0 kb for 11-C7 were diluted to a concentration of 0.6 ng/ $\mu$ l and then recircularized for IPCR. By taking advantage of extended PCR using Boehringer Mannheim's Expand Long Template PCR polymerase and buffer mixture, it was possible to amplify a single band of the appropriate size from each of the samples (Figure 4-5). The resulting 3.5 kb band amplified from the 11-C7 sample was successfully subcloned into Promega's pGEM-T vector producing pSR10. However, problems arose in trying to subclone 30-F10's IPCR product, probably because of its larger size (approximately 6 kb). Therefore, because of the ease in subcloning the fragment from 11-C7 and in the interest of proceeding forward, further analysis was focused on 11-C7. To verify that the subcloned IPCR fragment in pSR10 was the correct product, genomic DNA from the wild type *A. calcoaceticus* and the tag<sup>-</sup> mutant 11-C7 was cut with BglII. The DNA was Southern blotted and probed with pSR10. A shift in molecular weight of the predicted size was observed in the mutant indicating the presence of the transposon and verifying that the subcloned IPCR fragment in pSR10 was the right product (Figure 4-6).

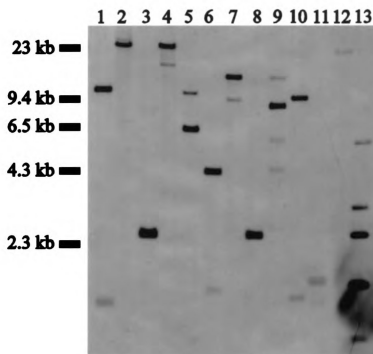
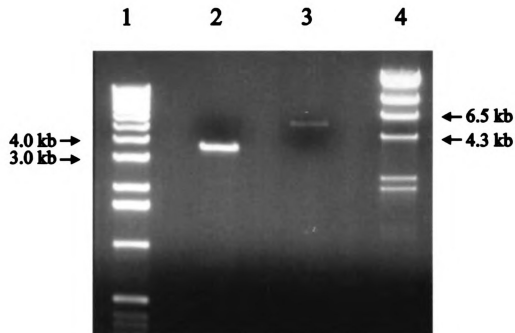


Figure 4-4: Southern analysis of genomic DNA from 30-F10 and 11-C7. Both tag mutants, were cut with *Bgl*III (lane 1), *Kpn*I (lane 2), *Mlu*I (lane 3), *Sal*I (lane 4) and *Xba*I (lane 5). Genomic DNA from 11-C7 was also cut with the same enzymes, *Bgl*III (lane 6), *Kpn*I (lane 7), *Mlu*I (lane 8), *Sal*I (lane 9) and *Xba*I (lane 10). The blot was probed with the *Mlu*I fragment from the transposon, mini-Tn10PtKm (Figure 4-2, A). Lane 11 contains 1 kb ladder size standard and Lane 12 contains Lambda DNA cut with *Hind*III. Finally, lane 13 is a positive control containing pLOFPtKm digested with *Mlu*I and *Xba*I.



**Figure 4-5: Extended IPCR of 11-C7 and 30-F10.** Extended IPCR reactions were run on recircularized DNA samples from 11-C7 (lane 2) and 30-F10 (lane 3). Lane 1 contains 0.5 ug of 1 kb ladder and lane 4 shows 0.4 ug of Lambda/*Hind*III size standards. The solitary bands observed in lanes 2 and 3 were gel purified and used in subsequent cloning.



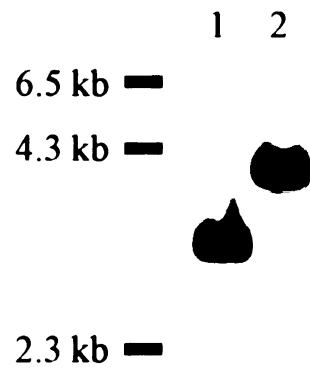


Figure 4-6: Southern analysis of 11-C7 with pSR10. Southern blot analysis of *A. calcoaceticus* wild type genomic DNA (lane 1) and the tag mutant, 11-C7 genomic DNA (lane 2) cut with *Bgl*II. The blot was probed with pSR10.

**Library screening.** The subcloned IPCR fragment was labelled with digoxigenin-11-UTP and used to probe filter replicas of the cosmid genomic library. In the first round of screening, colorimetric detection was used via nitro-blue-tetrazolium to identify cosmids that shared homology with the probe. This resulted in the identification of a single cosmid (5A-F1) that shared homology to the IPCR fragment. Subsequent screening, taking advantage of luminescent detection, has allowed the identification of 10 other cosmids that share homology to the subcloned fragment (1B-B6, 2B-F3, 2B-G4, 2B-G5, 4A-E4, 4A-F4, 4A-F5, 4A-G2, 4A-G5 and 9B-B5). Attempts to complement the mutation with the first cosmid (5A-F1) that was found was unsuccessful. Cosmid DNA preparations of the mutant, 11-C7, transformed with the cosmid indicated that the cosmid is present in the mutant. Examination of all the exconjugates transformed with the other identified cosmids has been hampered by the poor growth response of the exconjugates in low nitrogen medium. The observation that the exconjugates fail to grow under low nitrogen conditions, could be interpreted to indicate that the cosmids do not complement the mutant phenotype. Another possibility is that there is a second site mutation, the result of a spontaneous event, that is contributing to the mutants poor growth response under low nitrogen conditions.

Based on these assumptions I decided to sequence the region disrupted by the transposon. To do this, the cosmid that was found to share homology with pSR10 was digested with several restriction enzymes and the products were separated on an agarose gel to make a Southern blot. This blot was then probed with pSR10 to find a fragment of convenient size for sequencing. As can be seen in Figure 4-7, digestion

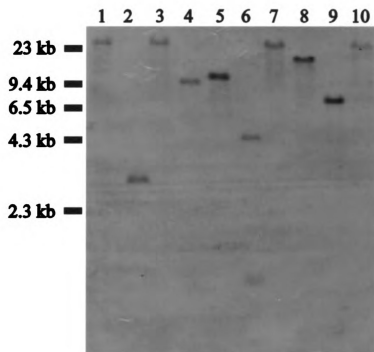
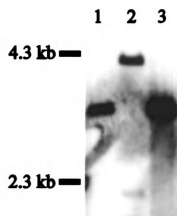


Figure 4-7: Southern analysis of 5A-F1 cosmid DNA. The cosmid, 5A-F1, which homology to the IPCR product from the tag<sup>-</sup> mutant, 11-C7 was digested with several different restriction enzymes, blotted and probed with pSR10. *Bam*HI (lane 1), *Bgl*II (lane2), *Cla*I (lane3), *Eco*RI (lane 4), *Eco*RV (lane 5), *Hind*III (lane 6), *Kpn*I (lane 7), *Sal*I (lane 8), *Xba*I (lane 9) and *Xho*I (lane 10).

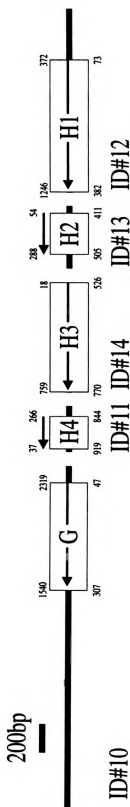
of 5A-F1 with BglII yielded such a fragment. This fragment was subcloned into Bluescript producing pSR11. To ensure that the proper fragment had been subcloned, pSR11 was used as a probe against BglII digested wild type, mutant (11-C7) and cosmid (5A-F1) DNA. The results of the experiment are shown in Figure 4-8. Based on the shift in molecular weight observed in the mutant lane, it was concluded that the proper fragment had been subcloned. At this same time another band of approximately the same size was also subcloned in bluescript to give pSR12. This fragment was originally subcloned because it was believed to be the BglII fragment of interest, but was later discovered not to be by Southern analysis. However, upon sequencing this fragment (see below) it was determined that this fragment resided next to the BglII fragment subcloned in pSR11. It was possible to determine this because they both shared homology to the same gene identified in GenBank release 92.0 (glutamate-ammonia-ligase adenylyltransferase from *E. coli*, accession #P30870).

Exonuclease digestions of pSR11 and pSR12 were carried out to create nested deletions. The deletion series was then sequenced allowing for the identification of 3 open reading frames on the DNA (Figure 4-9). One of these shared no homology to anything in the GenBank database. The other two showed significant homology to proteins involved in nitrogen regulation and amino acid biosynthesis. One of these was homologous to *E. coli glnE*, the gene which encodes glutamate-ammonia-ligase adenylyltransferase (BLAST score of 317 with a probability score of  $1.6 \times 10^{-183}$ ). The other open reading frame matched a branched-chain-amino-acid transaminase from *E. coli* (BLAST score of 448 with a probability score of  $7.1 \times 10^{-69}$ )



**Figure 4-8: Southern analysis of 11-C7 with pSR11.** Southern blot analysis of genomic DNA prepared from wild type *A. calcoaceticus* (lane 1), tag mutant, 11-C7 (lane 2) and the cosmid clone 5A-F1 (lane 3). DNA was probed with pSR11, a clone carrying the *Bgl*II fragment from 5A-F1.

Figure 4-9: Map showing sequence ID#10-14 in respect to one another. The boxed regions highlight regions of homology that were detected between the sequence and GenBank release 92.0 by BLASTX analysis (Altschul et al., 1990). These data are summarized in the table below the map. The numbers surrounding the boxes indicate the start of the similarity between the DNA query sequence (the numbers above the line) and the amino acid numbers in the matching protein from GenBank (the numbers below the line). This is to give some sense of the encoded protein over the whole restriction fragment, and also helps to determine the amount of DNA sequence missing between gaps. The gene, *glnE*, spans sequence ID#11-14. Sequence ID#10-11 were from pSR11 and Sequence ID#12-14 are from pSR12. The table summarizes the GenBank information giving the length of the matching protein, accession number of the matching protein, the BLASTX score, probability score and the name of the protein as reported by GenBank. Cases where the description of the first match is ambiguous, second and third matches are included. Contig maps and actual DNA sequences can be found in Appendix A of this text.



Seq. ID#	Region Highlighted Above	Matches Accession Number	Name of Match as Given by as Given by GeneBank	BLAST Score	Probability Score	Protein Length of Matching Prot. (amino acids)
10	G	S30668	Branched-chain-amino-acid transaminase from <i>E. coli</i>	448	$7.1 \times 10^{-69}$	309
11	H4	P30870	Glutamate-ammonia-ligase adenylyltransferase from <i>E. coli</i>	160	$5.0 \times 10^{-15}$	945
12	H1	P30870	Glutamate-ammonia-ligase adenylyltransferase from <i>E. coli</i>	317	$1.5 \times 10^{-62}$	945
13	H2	P44419	Glutamate-ammonia-ligase adenylyltransferase from <i>Haemophilus influenzae</i>	80	0.01	981
14	H3	P30870	Glutamate-ammonia-ligase adenylyltransferase from <i>E. coli</i>	275	$3.4 \times 10^{-61}$	945

Figure 4-9

**Mapping the location of the transposon relative to the BglII fragment.** To determine why the cosmid (5A-F1) is unable to complement the mutant phenotype, and to determine which of the open reading frames was directly affected by the insertion of the transposon, I mapped the location of the insertion in the genome and extrapolated its position in respect to the cosmid. One simple explanation for why the cosmid does not complement the 11-C7 phenotype would be if the gene was at the extreme end of the cosmid's insert DNA. Another possibility would be if the complementary gene resided in an operon and the operon was at an the extreme end of the cosmid's insert so that the complementary gene was not, in fact, on the cosmid. If either of these situations were the case, then it might be possible that the rest of the coding sequence of the gene, or the operon, is not present on the insert DNA of cosmid 5A-F1. Thus, the reason that it can not complement 11-C7 is because the entire coding region of the gene or the operon simply is not present. To determine if this was the case, extended PCR was carried out as outlined below to map the location of the BglII fragment in the cosmid, and at the same time, determine the location of the transposon relative to the BglII fragment.

To map the location of the sequenced region relative to the end of the insert DNA of the cosmid, primers that faced in toward the cosmid's insert DNA (P9 and P10, Table 4-3) were used in conjunction with primers that were specific to the ends of the BglII fragment that faced out (P14 and P16, Table 4-3) (Figure 4-1, Panel A). Using extended PCR with the cosmid, 5A-F1 as a template, it was possible to amplify a fragment of approximately 6.0 kb when using a primer specific for the transposon in conjunction with an anchoring primer specific for the cosmid. This maps one end of



the BglII fragment that was sequenced approximately 6.0 kb from the end of the cosmids insert DNA.

Mapping the location of the transposon relative to the BglII fragment to determine which open reading frame it inserted into involved using primers specific to the transposon that faced out (P11 and P12, Table 4-3), in combination with primers with specificity to the ends of the sequence obtained from the BglII fragment (P15 and P17, Table 4-3) (Figure 4-1, Panel B). Using genomic DNA prepared from the mutant, 11-C7, it was determined that the transposon had inserted into the third open reading frame. This open reading frame shares considerable homology to *glnE*, glutamate ammonium ligase adenylyltransferase, that has been identified from many different organisms.

## CONCLUSION

Transposon mutagenesis based on a Tn10 derivative was used to identify mutants in triacylglycerol biosynthesis in *A. calcoaceticus*. This second attempt at isolating triacylglycerol deficient (*tag*<sup>-</sup>) mutants was performed following attempts to complement *tag*<sup>-</sup> mutants generated by NTG mutagenesis had failed for unknown reasons. It is possible that the mutants that were generated using NTG resulted in dominant mutations that could not be complemented through the addition of the wild type gene. Therefore, I decided to try to generate tagged mutants in triacylglycerol biosynthesis, subclone the flanking regions around the transposon insertion and identify the gene of interest by DNA sequencing.

The transposon mutagenesis was successful. A total of 8 mutants were

identified, however only 4 of these were clearly due to a single insertion of the transposon. The other 4 mutants were removed from study because they did not contain the transposon or had multiple insertions. Two of the remaining four mutants were class II (tag<sup>-</sup>) mutants and the other two were class III (wax<sup>-</sup>tag<sup>-</sup>) mutants. The class II mutants were further pursued because of their interesting phenotype. The class III mutants were again dismissed based on the belief that they might be nitrogen regulatory mutants since they do not accumulate either waxes or triacylglycerol when induced under low nitrogen conditions.

Using IPCR it was possible to subclone the DNA flanking the transposon insertion from the mutant 11-C7. By labelling the IPCR product and using it as a probe against the cosmid genomic library it was possible to identify 9 cosmids that shared homology to the DNA. One of these cosmids, 5A-F1 was selected for further analysis based on the simple fact that it was identified first. Attempts at complementing the mutant, 11-C7, with any of the cosmids has been complicated by the fact that the mutant does not grow, or grows poorly, when cultured under low nitrogen conditions. The reason that the mutant was identified at all was probably the result of culturing the mutant on LB plates and then transferring a large amount of cell paste to liquid medium for analysis by TLC. Attempts at culturing (in low nitrogen medium) the exconjugates obtained from mating the cosmids with homology to the IPCR fragment into the mutant has not been successful. Most attempts have been tried with the cosmid 5A-F1, but complementation of the mutant phenotype, in terms of growth defect, or triacylglycerol accumulation has never been observed. Additional attempts at complementing the mutant with the other cosmids will need to be repeated

before they can be completely ruled out.

Through extended PCR it was determined that the transposon inserted into an open reading frame that is highly homologous to *glnE*. This gene product adenylates glutamate synthase, thus down regulating its activity in the presence of high nitrogen levels. Interestingly, *glnE* was found to be strongly repressed in the presence of excess nitrogen and carbon limited conditions in *E. coli*. One phenotypic characteristic of *glnE* mutants in *E. coli*, is their inability to grow in low nitrogen medium after being transferred from a high nitrogen medium. This is a growth characteristic that is also true of 11-C7 and 30-F10, the two class II mutants that were identified, loosely implying that the phenotypes that are observed are due to mutations in nitrogen sensing and response. This growth characteristic together with the observation that the transposon inserted into an open reading frame encoding an enzyme with a high degree of similarity to *glnE* of *E. coli* is evidence, although not conclusive, that the 11-C7 mutation is a result of a mutation in *glnE*. However, this interpretation is complicated by the fact that a cosmid, 5A-F1, presumably containing a wild type copy of *glnE* does not complement the mutant phenotype (either its ability to grow in low nitrogen medium, or its ability to accumulate triacylglycerol).

Examination of the region in the cosmid where the transposon inserted, shows the presence of three open reading frames that are all being transcribed in the same direction. Additionally, the first two genes are involved in amino acid biosynthesis (Figure 4-9). The first open reading frame is *glnE* and the second shares strong homology to a branch chained amino acid transaminase. These two observations hint at the possibility that these genes are organized in an operon. If this is so, then the

possibility exists that the operon is not entirely located on the cosmid's insertion. To determine if this was a possibility the insertion site of the transposon was mapped relative to the cosmid. First, the transposon was situated relative to the BglII fragment that was cloned and sequenced, and then the BglII fragment was placed relative to its location in the cosmid. The results of this mapping experiment placed the BglII fragment approximately 6.0 kb from the end of the cosmids insert, and therefore the third open reading frame identified in this fragment is 6.0 kb from the end of the cosmid.

The results from this experiment fall in the gray area of interpretation. Although the distance from the end of the last open reading frame to the end of the insert DNA is considerable (a distance of 6.0 kb), there are many examples of much larger operons. There are 4 known examples of operons in *A. calcoaceticus*. The lengths of these operons range from about 3.5 kb to over 10 kb. Thus, it seems likely that the cosmid does not complement the phenotype because the entire operon is not present and therefore is not being fully transcribed.

The fact that the third open reading frame does not share strong homology to anything in the database leaves open the possibility that it could be a gene involved in triacylglycerol accumulation. Since there are no known genes for diacylglycerol acyltransferase (DGAT), it is possible that this unknown open reading frame is DGAT. It can be imagined that the gene encoding DGAT would be situated in an operon that might be transcriptionally controlled by nitrogen levels in the medium, since it is observed that *A. calcoaceticus* accumulates triacylglycerol under low nitrogen conditions. However, it would not be straight forward to test the function of this open

reading frame and there is a high probability that the outcome would not be the identification of DGAT, but rather another gene involved in amino acid biosynthesis. Therefore, because of the lack of promise that lies in the direction of this project, I decided to bring it to a close.

## REFERENCES

- Allen, L. N. and Hanson, R. S.. 1985. Construction of Broad-Host-Range Cosmid Cloning Vectors: Identification of Genes Necessary for Growth of *Methylobacterium organophilum* on Methanol. *J. Bact.* 161(3):955-962.
- Altschul, S. F., Gish, W., Miller, W., Myers, E. W. and Lipman, D. J.. 1990. Basic Local Alignment Search Tool. *J. Mol. Biol.* 215: 403-410.
- Bachmann, B. J. 1987. In *Escherichia coli* and *Salmonella typhimurium*, Cellular and Molecular Biology. Eds. Neidhardt F. C. et. al., ASM.
- Figurski, D. and Helinski, D. R.. 1979. Replication of an Origin-Containing Derivative of Plasmid RK2 Dependent on a Plasmid Function *in trans*. *Proc. Natl. Acad. Sci., U.S.A.* 76:1648-1652.
- Herrero, M., de Lorenzo, V. and Timmis, K. N.. 1990. Transposon Vectors Containing Non-Antibiotic Resistance Selection Markers for Cloning and Stable Chromosome Insertion of Foreign Genes in Gram-Negative Bacteria. *J. Bact.* 172, 6557-6567.
- Leahy, J. G., Jones-Meehan, J. M., Pullias, E. L. and Colwell, R. R.. 1993. Transposon Mutagenesis in *Acinetobacter calcoaceticus* RAG-1. *J. Bact.* 175(6): 1838-1840.
- Maniatis, T., Fritsch, E. F., and Sambrook, J.. 1982. In Molecular Cloning, A Laboratory Manual. Cold Spring Harbor Laboratory Press, New York, New York.
- Miller, V. and Mekalanos, J.. 1988. A Novel Suicide Vector and its Use in Construction of Insertion Mutations: Osmoregulation of Outer Membrane Proteins and Virulence Determinants in *Vibrio cholerae* Requires *toxR*. *J. Bact.* 170, 2575-2583.
- Raleigh, E. A., Lech, K. and Brent, R.. 1989. In Current Protocols in Molecular Biology. Eds. Ausubel, F. M. et al. Publishing Associates and Wiley Interscience, New York.

## CHAPTER 5

### CONCLUSIONS AND PERSPECTIVES

The work described here has provided new insight into wax ester biosynthesis. It has long been believed that in *A. calcoaceticus*, wax ester biosynthesis is alkane oxidation run in reverse, requiring three separate enzymatic steps. This work dispels this notion through biochemical and genetic evidence. It is now evident that wax ester biosynthesis is carried out in two enzymatic steps. With the cloning of *acr1*, I have shown that the starting substrate for wax ester biosynthesis is acyl-CoA, that reduction is dependent on a NADPH cofactor, and that a single enzyme catalyzes the conversion of acyl-CoA to fatty alcohol.

This is a very interesting observation and provides the potential for many interesting experiments. It would be nice to know how this enzyme catalyzes both reactions. Future experiments could address whether the reaction is carried out by a single catalytic site, or if there are two separate sites on the enzyme. Steps in this direction have already been taken by running timecourse experiments and substrate competition experiments. It might be important to know if the enzyme is acting alone as a single subunit or as a multimer. Based on the substrate competition assays it appears that aldehyde does not compete with acyl-CoA. Thus, it appears, at this time, that the enzyme contains two active sites.

Other biochemical experiments that should be conducted involve measuring the kinetics and substrate specificity of the enzyme. Kinetic studies will be difficult to pursue given the extremely hydrophobic nature of the substrates. Fatty aldehydes and fatty alcohols are very insoluble in an aqueous environment. This makes determination of the actual free substrate concentration nearly impossible. Experiments aimed at substrate specificity are much easier to carry out. By using different carbon length acyl-CoA's it will be possible to determine which substrates can be utilized by the enzyme and preferred substrates can be determined by measuring the amount of radiolabelled product. Substrates can be varied based on the length of the acyl chain and the degree of unsaturation. Highly unsaturated substrates may even provide some rudimentary insight into the organization of the active site. For instance, once the preferred carbon length substrate is determined (most likely palmitoyl-CoA since waxes made from this is substrate are the major product in wild type), multiple *cis* and *trans* double bonds can be added to bend the acyl chain. Because of these double bonds the acyl chain is predominantly in a bent position, and it might be predicted that if the active site is a narrow opening then "bent", unsaturated acyl chains will not be readily converted because of their inability to reach the active site.

As described, the *Wow15* mutant was the result of a point mutation in the gene *acr1*. This mutation effected the ability of the Acr1 protein to convert acyl-CoA to aldehyde, but had no effect on the enzymes ability to convert aldehyde to alcohol. An important experiment aimed at determining the *in vivo* activity of the Acr1 protein would be to subclone the mutant *acr1* gene from the *Wow15* mutant. Based on the results described in this study, the mutant allele should encode a protein product that is

able to convert fatty aldehyde to alcohol, but should not be able to catalyze the conversion of acyl-CoA to fatty aldehyde. Additionally, by carrying out nutritional supplementation experiments on the other wax<sup>-</sup> mutants that were isolated, it may be possible to identify mutants which contain point mutations in the *acr1* gene which effect the proteins ability to catalyze the conversion of aldehydes to alcohols, but has not effect on the conversion of acyl-CoA to aldehyde.

Alteration of the pET21:*acr1* construct to eliminate the translational stop region from the native coding sequence, would allow the protein product to be His tagged (there is a His tag encoded on the pET21 vector allowing for C-terminal His tag fusions). This would provide an easy means of purifying large amounts of recombinant protein from *E. coli*. With purified protein it would be possible to raise antibodies specific to *acr1*. This could lead to the localization of the protein in *A. calcoaceticus* either by cell fractionation or by *in situ* hybridization using immunogold labelling. Because of the novel activity of this protein, possible presence of two active sites and potential industrial applications, further structural studies may provide important insights into the catalytic domain. This could be coupled with experiments dealing with site directed mutagenesis to produce altered enzyme specificities.

One of the desired goals of this work was to be able to transfer the knowledge gained from *A. calcoaceticus* wax biosynthesis and apply it to other organisms, particularly *Arabidopsis*. Efforts in this direction have already begun in the form of identifying ESTs (expressed sequence tags) from the GenBank library that share homology to *acr1*. The results from such a search have already yielded an EST (Figure 5-1) that has an optimized BLASTX score of 137 (Figure 5-2). This EST has



FILE NAME : T21872.SEQ

SEQUENCE : 565BP; 154 A; 121 C; 123 G; 150 T.

\*\*\* SEQUENCE LIST \*\*\*

(SINGLE)

10	20	30	40	50	60
5' AGAAAAAAAA	AAGATTGAAA	TGGAGAAGAA	GCTACCGAGA	AGATTGGAAG	GCAAAGTCGC
70	80	90	100	110	120
GATTGTNACG	GCTTCGACGC	AAGGGATTGG	TTTCGGAATC	ACTGAGCGTT	TCGGTCTCGA
130	140	150	160	170	180
AGGCGCTTCC	GTCGTCGTCT	CTTCCCGCAA	ACAGGCAAAT	GTTGATGAGG	CAGTAGCAAA
190	200	210	220	230	240
ACTCAAATCC	AAAGGGATTG	ATGCATATGG	AATCGTCTGT	CATGTTTCCA	ATGCTCAACA
250	260	270	280	290	300
TCGCCGCAAT	CTTGTCGAAA	AGACGGTTCA	GAAATATGGG	AAGATAGATA	TCGTTGTCTG
310	320	330	340	350	360
TAACGCTGCT	GCCAATCCAT	CTACAGACCC	AATCTTGTCT	AGCAAAGAAG	CTGTTCTTGA
370	380	390	400	410	420
CAAGCTTTTG	GGAAATCAAT	GTCAAATCCT	CTATACTTCT	CCTGCAAGGA	TATGGCTCCT
430	440	450	460	470	480
CACCTTGAGN	AGGGGTTCCT	CTGTTATCTT	CATAACTTCC	TATTTGCTGG	NTTTCACCAC
490	500	510	520	530	540
AAGGNNCTAT	TNGCTATGTA	TNGNGCACTA	AAACTNCNTT	NTNNGNCTAA	CTAAGNGNTT
550	560				
CTTCCTAGAT	GCCCCGATCA	NGGTC	3'		

Figure 5-1: DNA Sequence of *Arabidopsis* EST T21872.

No.	Target file	Definition	Match%	Over.	INIT	OPT
1	T21872.AMI		25.8	97	130	137
		10 20 30 40 50 60				
ACR1.AMI	LEALFRENVKGKVALITGASSGIGLTIAKRIAAAGAHVLLVARTQETLEEVKAAIEQQGG					
T21872.AMI	MEKKLPRRLEGKVAIVTASTQGIGFGITERFGLEGASVVSSRKQANVDEAVAKLKSKEI	10 20 30 40 50 60				
		70 80 90 100 110 120				
ACA1.AMI	QASIFPCDLTDMNAIDQLSQQIMASVDHVDFLINNAGRSIRRAVHESFDRFHDFFERTMQL					
T21872.AMI	DAYGIVCHVSNAQHRRNLVEKTVQKYGKIDIVVCNAAANPSTDPISSKEAVLDKLLGNQ	70 80 90 100 110 120				
		130 140 150				
ACA1.AMI	NYFGAVRLVLNLLPHMIKRKNGQIINISSIGVLAN					
T21872.AMI	CQILYTSPARIWLLTLXRGSSVIFITSYLLXFTTR	130 140 150				

Figure 5-2: Optimized FASTA alignment between Acr1 and the *Arabidopsis* EST, T21872. FASTA alignment was done using the software package, DNASIS for Windows (Hitachi Software).

been classified as a putative ketoacyl reductase, because of its similarity to granaticin polyketide synthase putative ketoacyl reductase. Rough mapping of this EST has already been done, and was found to map to the upper portion of chromosome 4, near the *hy4* locus. None of the mapped *cer* mutants have been localized to this region of the genome. It is important to note that only 9 of the 21 known *cer* mutants have mapped. Therefore, although it is disappointing that the EST does not map near a *cer* locus, it definitely is not conclusive that this EST is not a gene involved in wax ester biosynthesis. The EST can also be used to make an antisense construct which could be used to transform *Arabidopsis*. Resulting plants could be easily screened for the glossy phenotype which is indicative of a *cer* mutation. Additionally, it would be very interesting to transform *Arabidopsis* with *acr1* and see what affects this might have on the plant. It would be expected that the Acr1 protein product would reduce acyl-CoA to its corresponding fatty aldehydes and fatty alcohol. It is not clear what sort of phenotypic affect this might have on the plant, however, it might be predicted that fatty aldehydes and fatty alcohols, which are not normally found within plant cells, may accumulate in significant levels to produce inclusion bodies in the cells. If expressed in leaves, alterations in epicuticular wax composition might occur. Although the mechanism of wax deposition on leaves is not known, it is possible that by increasing the amount of fatty aldehydes and fatty alcohols present in epicuticular cells, that epicuticular wax composition might be altered. This might lead to a better understanding of the mechanisms involved in epicuticular wax deposition by examining where Acr1 is localized. Additionally, by measuring the lipid composition of the epicuticular waxes in transgenic plants, it might be determined if alterations in

fatty aldehyde and fatty alcohol concentrations have any effects on the concentrations of other wax components, such as wax esters and free fatty acids. Observed alterations in wax composition could lead to investigations of this effect on insect and pathogen resistance. Finally, *acr1* could also be expressed in seeds where it might cause a decrease in triacylglycerol accumulation by siphoning off acyl-CoA and converting it to fatty aldehydes and alcohols. This might lead to a decrease in seed viability because of the lack of an available carbon source for growth.

Other directions leading from this work deal with more immediate questions dealing with wax biosynthesis in *A. calcoaceticus*. As described in Chapter 2, *Wow15*, was not the only wax<sup>-</sup> mutant complemented by the cosmid genomic library. The mutant *Wow1* was complemented by the cosmid 1A-3F. With the observation that this cosmid is able to complement two other wax<sup>-</sup> mutants besides *Wow1* it is imperative that further analysis be conducted on this cosmid. Transposon insertions have already been identified which inactivate the ability of this cosmid to complement the mutant phenotype. Additionally, there have been several other cosmids which have been found that share homology with this cosmid, some of which do and do not complement the mutant phenotype. With all of these resources available, discovery of the region of interest should be straightforward. It will be interesting to discover what the gene of interest encodes. Nutritional supplementation experiments on this mutant suggested that it is deficient in one of originally proposed reductase steps. With the discovery of *acr1* this now seems unlikely. Possible roles for the mutated gene may involve nitrogen response and regulation that is specific to wax ester biosynthesis or perhaps the gene product serves as an acyl-CoA:ACP transacylase which converts

acyl-ACP to acyl-CoA, which then gets fed into wax ester biosynthesis.

Two other wax<sup>-</sup> null mutants, *Wow2* and *Wow28* have not been complemented. It is possible that cosmids which complements the *Wow15* mutant, might also complement these mutants. Investigation of these mutants may yield more insight into wax ester biosynthesis of *A. calcoaceticus*.

It is disturbing that a mutant was never identified that seemed deficient in an acyl-CoA:fatty alcohol transferase reaction. It is possible, although unlikely, that the same enzyme which catalyzes this reaction also catalyzes the formation of triacylglycerol. This idea might prompt a reexamination of the class III mutants (wax<sup>-</sup> tag<sup>-</sup>) that have been isolated, in terms of experiments aimed at trying to complement some of these mutants. The transposon-mutagenized tag<sup>-</sup> mutants may be an excellent place to start since flanking sequence can be easily cloned and sequenced by inverse PCR. Additionally, nutritional supplementation experiments should be carried out on all of the transposon marked lines. With a source of readily available, inexpensive fatty aldehyde (*cis*-11-hexadecenal, Aldrich), chemical complementation experiments using this compound as a carbon source, should be performed for all of the mutants to further characterize their deficiencies.

Although not promising in terms of understanding triacylglycerol production, the tag<sup>-</sup> transposon mutant, 11-C7, should be pursued one further step. The observation that the region surrounding the transposon insertion contains genes involved in amino acid biosynthesis, and that these genes might be organized as an operon leaves the possibility of another gene, perhaps involved in triacylglycerol biosynthesis, further downstream in the operon. Subcloning and expressing *glnE* in the

11-C7 mutant can bring this question to a close. If this gene is found to complement the mutation, then there is little doubt that the tag<sup>-</sup> phenotype is the result of the insertion in the *glnE* gene. If not, then experiments aimed at identifying and subcloning open reading frames further downstream may provide the answer. A valuable tool for such experiments will be pSER200-1 and pSER200-4, two transcriptional expression vectors that can be used in *A. calcoaceticus* and *E. coli*. The construction of these vectors is detailed in Appendix B of this text. Experiments aimed at investigating the 30-F10 phenotype (the other tag<sup>-</sup>, transposon generated mutant) should probably be avoided, if the goal is to investigate structural genes involved in triacylglycerol production. The reason for this caution is the observation that this mutant exhibits poor growth under nitrogen limited conditions, similar to 11-C7. This hints at the possibility that this mutant may also be affected in nitrogen sensing and response.

In conclusion it is apparent that this work has answered some of the questions dealing with wax biosynthesis in *A. calcoaceticus*. It has provided a tool for the investigation of similar pathways in other organisms, and opened new avenues for scientific investigation. It is my honest wish that work will continue to be focused on wax ester and triacylglycerol biosynthesis in *A. calcoaceticus* so that more insights and discoveries are gained.

## **APPENDIX**

## **APPENDIX A**



## APPENDIX A

### DNA SEQUENCE INFORMATION AND CONTIG MAPS

In the course of identifying the genes of interest involved in wax ester and triacylglycerol biosynthesis, a number of open reading frames were identified. This appendix lists the sequence data that was generated in the course of sequencing the fragments that contained the genes of interest (Figures A-1 through A-14). For the most part they represent single stranded reads that were obtained using Perkin Elmer's automated sequenator, the ABI310. The contigs that were sequenced are highlighted in Figures A-15 through A-18. Contigs were assembled using Perkin Elmer's Sequence Navigator software. Double stranded sequencing was conducted on the region encoding *acr1* and is indicated by reverse arrows.

FILE NAME : ID1.DNA

SEQUENCE : 746BP; 243 A; 146 C; 172 G; 185 T.

\*\*\* SEQUENCE LIST \*\*\*

(SINGLE)

5'	10	20	30	40	50	60
	ATGCAGCTCG	AAGGTGTTGT	GACTAATGTG	ACTAACTTTG	GCGCGTTTGT	GGATATTGGT
	70	80	90	100	110	120
	GTGCATCAGG	ACGGTCTGGT	ACACATTTCT	GAGCTAGCTA	ACGAGTTTGT	GTCAGATCCA
	130	140	150	160	170	180
	CATAAAGTGG	TGAAACCAGG	TCAGATTGTG	CAGGTTTCGTG	TGATTCAAGT	CGATGCAGAG
	190	200	210	220	230	240
	CGTAAGCGTG	TCAATTTGAG	TATGCGTCCA	GAAGGTGCAG	AAGCTCCAGC	GAAGACACAA
	250	260	270	280	290	300
	CGACCACCAC	GTCGTGAGCA	ACAAGAACAG	CGCGGTGAAC	GTAAGCCGCA	GCCAAAACGT
	310	320	330	340	350	360
	CCACAGGCTG	CACGTTCAAA	TGATCAGGCT	AAAAAGCCAC	AACGTGCCAA	GCAAGAAAAA
	370	380	390	400	410	420
	CCACAAGAGC	AAATTTTGGT	GGGTTGGGCG	CATTATTGCT	ACAAGCTGGA	ATTACTGGTT
	430	440	450	460	470	480
	CTAAATAATT	TTAGTCCTGT	TTAAGAAGAA	AAAACCACCT	TCGGGTGGTT	TTTTCTTATG
	490	500	510	520	530	540
	TGCATTGACG	CTGCTTTAAA	TTAAATTTAT	TGTCATGAGA	ATAAAGATGA	GGCGATTCTG
	550	560	570	580	590	600
	AAGATCAACA	AAAAAAAGTG	AAAACATTCG	GCATCGTCAC	AACAGCACAG	CATAACTCAA
	610	620	630	640	650	660
	CTATGAGCCA	TAAAAAATGT	CAGACAAGAT	CACACCGCTT	GAGATCAAAA	ACATCGGGTT
	670	680	690	700	710	720
	TTCGATATAA	GAAACTCAAG	GAATGCGTCA	ACTTTTTTAT	TGAATGGTTA	TTTAATGACA
	730	740				
	ACCCCCAGGT	CAGAAACAAG	TTTCAT	3'		

Figure A-1: Sequence ID#1

FILE NAME : ID2.DNA

SEQUENCE : 930BP; 238 A; 202 C; 202 G; 287 T.

\*\*\* SEQUENCE LIST \*\*\*

(SINGLE)

5'	10	20	30	40	50	60
	GCGCTATTCA	ATTCTGGCTT	GGGACAGTAG	TCCACTCAAA	AAATGGGTAT	TGCCTTCTGC
	70	80	90	100	110	120
	TTTAATTGCA	GTCGTGGCTG	CTGCGCTGCT	CAATTATCTA	CTGGTTTATT	TTCAGTCACC
	130	140	150	160	170	180
	CTGGGCGATT	CAGCCTAATA	ATCTGATTCA	GTTACCCAAA	ATCCTAGACG	CACCTGAAAG
	190	200	210	220	230	240
	TGTGATGATC	TATCCAGATT	TCAGTGCGCT	CAGTAATCCA	CTCATTTACA	CAGGTGCTAT
	250	260	270	280	290	300
	TACGCTGGCA	GTTGTTGCTT	CTTTAGAAAC	GTTATTAAAT	CTTGAAGCAG	CAGACAAGCT
	310	320	330	340	350	360
	TGACCCTCAA	AAACGTTCTC	CACCACCCAA	TCGTGAATTA	TGGGCGCAAG	GTACAGGCAA
	370	380	390	400	410	420
	TATCGTGTC	GGCTTCATTG	GTGGAATGCC	AATCACTTCG	GTCATTGTGC	GTAGTTCGGT
	430	440	450	460	470	480
	CAATGCCAAT	ACTGGTGCGC	GTAGCAAATG	TTCAACGATT	ATTTCATGGCG	TATTACTGTT
	490	500	510	520	530	540
	ACTGGCAGTT	TTATGGGGTG	TGCCATTAAT	GAATATGATT	CCATTATCCG	CACTGGCTGC
	550	560	570	580	590	600
	GATCCTGATT	CTTACAGGTT	TTATACTTAC	TCATCCCAAG	ATGTTTAAAA	NGCTGTATCA
	610	620	630	640	650	660
	ACAAGGCTGG	AAGCAGTTTA	TACCATTTAT	CATTACGCTA	GTTGGAATGT	TGATCACC GA
	670	680	690	700	710	720
	CCTTCTCATC	GGAATGTTGA	TTGGGCTAGC	CACCAGTATC	GCTTTTATT	TGTACGGAAA
	730	740	750	760	770	780
	TTTGCATAGA	GGGCGTGCGC	GTGTACAAGG	AAAAACATTT	GCATGGTGTC	ATAACACGTA
	790	800	810	820	830	840
	TTGAGTTGCC	GACTCAAGTA	ACTTTTCTAA	CATCGTGGCG	GTGCTTATTT	CTGCGCTAGA
	850	860	870	880	890	900
	CCGACTTCAT	CGCAATGAAA	AGCTGGTGAT	TGATGCCACC	CAGTCAGATA	GCATTGATT
	910	920	930			
	TGATATTCAT	CAGGTGATAC	AGGATTATCA	3'		

Figure A-2: Sequence ID#2

FILE NAME : ID3.DNA  
 SEQUENCE : 1708BP; 499 A; 322 C; 383 G; 504 T.

10	20	30	40	50	60
5' GTGGGCTGTA	TGGATTACAG	TGCACCAACA	GAAATGGTGT	TTGATGTGGG	CATTGGTGAC
70	80	90	100	110	120
TTATTTAGTT	TGAGAATCGC	GGGGTAATAT	TGCGGGGCAG	AAAGTCCTTG	GATCATTGGA
130	140	150	160	170	180
GTTTTGCCTG	TCAAGCCAAA	GGTTCCAAAG	TGATTCTGGT	TTTGGGACAT	ACCGACTGTG
190	200	210	220	230	240
GTGCGGTCAC	CAGCGCATGC	CAGTTAAGAT	TGCAACATAA	GCAGATTTC	GATATTTCAGG
250	260	270	280	290	300
AAATGCCACA	CATCCAATAC	GTGCTTGGGC	CACTCATGCA	TTCGGTTGGC	AGTGTATTTG
310	320	330	340	350	360
ATATTATGCA	ACCGCGTGAA	TTAAGCAAAG	CATTTATTGA	TCAGGTGACT	GCTATGAATG
370	380	390	400	410	420
TTCACTATAA	TATTCAATAC	ATTATTTCAGC	ATAGTTCTGT	ACTTAAAGAT	ATGCTGGATC
430	440	450	460	470	480
GCAAAGAAAT	TGATATTGTT	GGTGCGATTT	ATGATGTAAA	AACAGGAAAA	GTCAATTTCC
490	500	510	520	530	540
TCTAAATCTG	GCTGATGGTC	GTAACCATAA	AAAAGCCTCT	CGGTATGAGA	GGCTTCTTTT
550	560	570	580	590	600
ATAAATTTTA	CCAGTGTTTCG	CCTGGGAACA	AGCGGGCATA	GGCACGTTGT	AGCAGATTCA
610	620	630	640	650	660
ATTTTTCCTG	TTCACCCAGT	GCAGCCGTTG	AGCTTGGGAA	TAGGTTAAAT	CCAATCGACA
670	680	690	700	710	720
TCAGAATATT	ATTGATGTCT	GGTGCGATGG	CATAGGTAAT	TGACGCCAGA	CGACCCAAGT
730	740	750	760	770	780
GCGTCGCAAT	ACGTGTTGGA	CGTTTCACAA	TGGCGTAGAC	AATGAGATCT	GCGGCTTCTT
790	800	810	820	830	840
CTGGGGAAAG	CGTGGGCACG	TATTTATAAA	TTTTGGTGGG	TGCGATCATT	GGGGTACGCA
850	860	870	880	890	900
CCAATGGCAT	ATAAATCGAG	GTAATTGAGA	TTTTATGCTT	GAGTACCTCG	GCTGAAAGAC
910	920	930	940	950	960
AGCGACTGAA	GGCATCCAGC	GCAGCTTTAG	ACGCGACATA	AGCAGAAAAA	CGGGTCGCAT
970	980	990	1000	1010	1020
TGGCCAATAC	ACCAATAGAG	CTGATATTGA	TGATCTGGCC	ATTTTACGCG	TTAATCATAT
1030	1040	1050	1060	1070	1080
GTGGCAGTAA	ATTTAACACT	AAACGTACCG	CACCAAAGTA	ATTCAGCTGC	ATGGTGCGTT
1090	1100	1110	1120	1130	1140
CAAAATCATG	GAAGCGATCA	AACGACTCGT	GTACGGCACG	GCGAATCGAA	CGCCCTGCAT
1150	1160	1170	1180	1190	1200
TATTGATCAG	GAAATCGACA	TGATCGACAC	TGGCCATAAT	TTGTTGTGAT	AACTGGTCAA
1210	1220	1230	1240	1250	1260
TCGCATTTCAT	GTCAGTCAGG	TCACAAGGAA	AAATAGAGGC	CTGTCCCCCT	TGCTGTTCAA
1270	1280	1290	1300	1310	1320
TTGCAGCTTT	CACTTCTTCC	AGTGTTCCTT	GGGTTCGGGC	AACCAATAAT	ACATGAGCAC
1330	1340	1350	1360	1370	1380
CTGCCGCAGC	AATTCTTTTT	GCAATCGTCA	AACCGATTCC	ACTAGATGCA	CCAGTGATCA
1390	1400	1410	1420	1430	1440
AAGCCACTTT	ACCTTTTACA	TTCTCTCGGA	AGAGAGCTTC	AAGTTTTTTG	TTACGCGGTT
1450	1460	1470	1480	1490	1500
TTTCCCTGAT	TGATATCAAA	CTGTAAAGGC	TGTCATTATT	GTATTTGGAT	TGAAGACGGT
1510	1520	1530	1540	1550	1560
TAAAGGGAAA	TAAAATTTCC	AGAACTAAAG	TTAATCTAAA	GTGATTTGGT	TAAAAAATCT
1570	1580	1590	1600	1610	1620
AGTGTTAAGT	ATCTGAAATT	ACAAATGTTT	TTAGAGTAAT	TGCTCTAATT	TTTATTATTT
1630	1640	1650	1660	1670	1680
GCTAGATCAA	TTATGAACAT	CATACGATAA	TAAAGCAAAT	ATAAAAAAAC	CTCTGAAATT
1690	1700				
GCAGAGGTTT	TTTATAAAAT	TTACGCTC	3'		

Figure A-3: Sequence ID#3

FILE NAME : ID4.DNA

SEQUENCE : 339BP; 125 A; 52 C; 50 G; 112 T.

\*\*\* SEQUENCE LIST \*\*\*

(SINGLE)

10	20	30	40	50	60
5' ATCAA	ACTGT	AAAGG	CTGTC	ATTATT	GTAT
70	80	90	100	110	120
ATTTCC	CAGAA	CTAAAG	TTAA	TCTAAAG	TGA
130	140	150	160	170	180
GAAATT	ACCA	ATGTTT	TTAG	AGTAATT	GCT
190	200	210	220	230	240
GAACAT	CATA	CGATAA	TAAA	GCAAAT	TATA
250	260	270	280	290	300
TAAAAT	TTAC	GCTCAA	ACTG	TGGCCA	ATGC
310	320	330			
ATGTT	CAATC	CCAACC	GATA	ACCGA	ACCAT
			ATCTT	CTGA	3'

Figure A-4: Sequence ID#4

FILE NAME : ID5.DNA

SEQUENCE : 511BP; 143 A; 111 C; 115 G; 142 T.

\*\*\* SEQUENCE LIST \*\*\*

(SINGLE)

10	20	30	40	50	60
5' ATTGT	CGACT	ACCAC	AGGGT	ACGCC	CATATT
70	80	90	100	110	120
CGATAA	TATT	ACCTA	ATGGA	TTGCC	CAATCG
130	140	150	160	170	180
CAATTAA	ACT	GCGTA	ATTGC	TCGGG	CTGCT
190	200	210	220	230	240
GTTTG	GGGAG	GGTAT	GCGCA	AATAA	ATTAT
250	260	270	280	290	300
CAATATT	GTC	GCCTG	CTTCG	GTTAT	CGTCT
310	320	330	340	350	360
ATGCC	CAGCG	CAAAG	CACCA	ATTCC	GCCTT
370	380	390	400	410	420
CCGTG	GTTGG	ATTCAT	GATT	CGAGT	TATAAA
430	440	450	460	470	480
TCTGC	ACCAT	GTTGT	GTATT	GTCAAA	AGCA
490	500	510			
AACAG	CTTTC	GTGGT	TGGTT	CTGGT	GAAATA
					A 3'

Figure A-5: Sequence ID#5

FILE NAME : ID6.DNA

SEQUENCE : 351BP; 120 A; 59 C; 65 G; 103 T.

\*\*\* SEQUENCE LIST \*\*\*

(SINGLE)

5'	10	20	30	40	50	60
	CATATTCTGT	ATGCTTAATT	TATCTATTTN	TATGAGGAGT	TCAGCTTTTT	TAAGAATAAC
	70	80	90	100	110	120
	NGATTAAAAA	TTTACTTCAT	TTCTAATGCT	TGATTTCAAT	TTACATGATG	TTGAGAGAAC
	130	140	150	160	170	180
	GCCACAAAAA	CTTACTCGGC	AGTCTGGGGC	TAGCAAGACC	ACTATAAAAA	ACNAAAGTAA
	190	200	210	220	230	240
	TTCAAATCAT	GATAAAAAAG	CTGGAGAATT	GACCTAATGA	GTAATCAAAA	AGTATCCGAT
	250	260	270	280	290	300
	ATTATCATCG	GAAGTGCTTG	AGCAAGCAGG	CGTTCAGCGC	TGTTACGGTA	TTGTGGGTGA
	310	320	330	340	350	
	CACTTAAACC	ATGTCACCGA	CTCCATGTCA	AAAAGCAAGA	TTGANTGGAT	C 3'

Figure A-6: Sequence ID#6

FILE NAME : ID7.DNA

SEQUENCE : 953BP; 260 A; 199 C; 207 G; 273 T.

\*\*\* SEQUENCE LIST \*\*\*

(SINGLE)

5'	10	20	30	40	50	60
	CGGNCCANTG	CATGCCCCAG	GCGCTTGGCG	CACAAAAAGC	TTCCCNCAAT	CGCCAGATTA
	70	80	90	100	110	120
	TTGNGCTGTG	TGGCGATGGT	GGATTAGCCA	TGTTACTTGG	TGATTTACTC	ACTACGATTC
	130	140	150	160	170	180
	AGGAAAAATT	ACCGATTAAA	ATTGTGGTAT	TTAACAACAG	CTCGCTTAAT	TTTGTGAGC
	190	200	210	220	230	240
	TTGAACAAAA	AGTCGAAGGC	TTGCTTGATC	ATTATACCGA	CTTGCTCAAT	CCTGATTTTG
	250	260	270	280	290	300
	GGCAAGCTTG	CCAGTGTGAT	CGGGCTACAT	GGGCAGACTG	TGACGCATGG	CGATGGCTTG
	310	320	330	340	350	360
	GAGCAGGCAG	TTGAAAACCT	CTTAAAGCAT	GATGGTCCAG	CATTACTCAA	TGTGCATACC
	370	380	390	400	410	420
	AATCCGATGG	AACTGGTGAT	GCCGCCAGAT	CCGANTCTGA	ATCAAGTCTC	GTCCACTTCA
	430	440	450	460	470	480
	CTTTATGCAA	TTAAGGCCTT	GATGTCGGGT	CGAGTAGATG	ACGTTAAAAA	TTTGTGCGTC
	490	500	510	520	530	540
	AATAATTTCA	TTAAATAAAT	TTANTGAACA	CAAGTCANCT	CAGGGCACAN	CTATAAGTTA
	550	560	570	580	590	600
	AAAATGCATG	ATCTAGCGTC	ATGCATCCNT	TATATCAGGA	AACANNNNAG	ACAACATTTA
	610	620	630	640	650	660
	TCAGTCATAA	AAACCGATTA	AACTCAATCA	CGCCTTATTT	TTTTACGGTA	TTCAGCATAT
	670	680	690	700	710	720
	AATAGATGCT	ATTTTTCGCT	CATTGCGATG	TATTGGTTTT	TCTATTGAGG	AGTCCTAAGT
	730	740	750	760	770	780
	GGCCCAATAT	ATTTATACGA	TGAACCGAGT	ATCCAAGATG	GTTCCGCCGA	AGCGCGAAAT
	790	800	810	820	830	840
	CCTCAAGGAT	ATCAAGCTTA	TCGATACCGT	CGACCTCGAG	GGGGGGCCCG	GTACCAGCTT
	850	860	870	880	890	900
	TTGTTCCCTT	TAGTGAGGGT	TANTTTTCGAG	CTTGCGGTAA	TCATGGTCAT	AGCTGTTTCC
	910	920	930	940	950	
	TGTGTGAAAT	TGTTATCCGC	TCACAATTCC	ACACAACATA	CGAGCCGGAA	GCA 3'

Figure A-7: Sequence ID#7

FILE NAME : ID8.DNA

SEQUENCE : 681BP; 183 A; 146 C; 161 G; 184 T.

\*\*\* SEQUENCE LIST \*\*\*

(SINGLE)

5'	10	20	30	40	50	60
	GCCTTTCGAC	GAAATGGNAG	GNTTTATNGA	CTTTCCGNAA	TACGTCGATT	TTAAATCGNG
	70	80	90	100	110	120
	TTTATGCGAA	AAATTCGGTC	TTCTGTGAAG	NAAATTACTC	AACCCTCACA	AGCTAGNACA
	130	140	150	160	170	180
	TATCATGAGC	ATGGCCTGTC	AGGCAGCACT	CAATAAACGC	GGTGTGCTG	TGGTCATCGT
	190	200	210	220	230	240
	GCCAGCCAAT	ATCAGTGAAG	CATCGGCTGA	AGCGGGTCTA	CCTTTCGTGC	CACGTCATGT
	250	260	270	280	290	300
	TGAACCTGAT	ATGTTGCCAA	ACAAAGCTGA	ACTGCATCAA	ATGGTTGAGC	TGATTTCCCA
	310	320	330	340	350	360
	GCATCAAAAA	ATTGGAATTT	ATGCAGGTGC	GGGGTGTGAA	GGCGCACATG	ATCAGTTAAT
	370	380	390	400	410	420
	TGCGTTTGCT	GAAAAGTTAA	AAGCCCCTGT	GGCGCATACC	TCACGTGCCA	AAGATTTTGT
	430	440	450	460	470	480
	GGAGTACGAT	AACCCATACA	ACATGGGCAT	GACGGGTATT	GTTGGCAATA	AAGCAGGTTA
	490	500	510	520	530	540
	TCACACGCTC	ATGGATTGTG	ATTTACTGAT	TTTGCTGGGT	GCCGATTTTG	CATGGGCACA
	550	560	570	580	590	600
	GTAATATCCA	AGTCATGCCA	AATTCCTTGCA	GATTGATATT	GATCCGACAC	ATTTAGGGCG
	610	620	630	640	650	660
	ACGTCACCAA	TTACACTGGG	TGCGGTAGGT	AAAATCTCAT	CGACGCTCGA	TGCCTTATTA
	670	680				
	CCATTGCTTG	AAACGCGTCA	A	3'		

Figure A-8: Sequence ID#8



FILE NAME : ID9.DNA

SEQUENCE : 354BP; 87 A; 100 C; 96 G; 71 T.

\*\*\* SEQUENCE LIST \*\*\*

(SINGLE)

10	20	30	40	50	60
5' TCGGTCGTTT	GGGTGAGTGA	GAGAGGCATC	AGCTCACTCA	AAGGGGGTAA	TACGGTTATC
70	80	90	100	110	120
CACAGTAATC	AGGGTGATAA	CGCAGGAAAG	AACATGTGAG	CAAAAGGCCA	GCAAAAGGCC
130	140	150	160	170	180
AGGAACCGTA	AAAAGGCCGC	GTTGCTGGCG	TTTTTCCATA	GGCTCCGCCC	CCCTGGACGA
190	200	210	220	230	240
GCATCACAAA	AATCGACGCT	CAAGTCAGAG	GTGGCGAAAC	CGACAGGACT	ATAAAGATAC
250	260	270	280	290	300
CAGGCGTTTC	CCCCTGGAAG	CTCCCTCGTG	CGCTCTCCTG	TTCCGACCCT	GCCGTTACCG
310	320	330	340	350	
GATACCTGTC	CGCTTTCTCC	CTTCGGGAAG	CGTGGCGCTT	TCTCATAGCT	CACG 3'

Figure A-9: Sequence ID#9

FILE NAME : ID10.DNA

SEQUENCE : 2341BP; 681 A; 532 C; 432 G; 687 T.

\*\*\* SEQUENCE LIST \*\*\*

(SINGLE)

10	20	30	40	50	60
5' TTTTATAAAT	TTTTCTCTCT	CTGGTTCTTT	ATACACCACA	CCGCAAAAGA	GAAAGGTNTT
70	80	90	100	110	120
ATCTGTATTA	ANATTTTAA	ATTGAATTAA	GCTTTCAACA	TTACGATGCC	CGATATTGGG
130	140	150	160	170	180
CATATACGCT	GCACTCAAAT	GTGGCTGTTT	TAACTTTGCT	ANATATTCCC	CTGCAGTAGT
190	200	210	220	230	240
ACNAAAGACG	CATCCAGATA	GGGAGAAAAC	GCTTTTACAA	AATCCAGCTT	ATGTTCAAGA
250	260	270	280	290	300
TATAATGGAT	CGACATACCA	AAACGCAATT	TTGGTTTCTG	GAAACTGCTG	TTTGATCTGC
310	320	330	340	350	360
TTAAGCACTT	CAGGACTCAT	CAGGTCGCTG	TGCCCCGATCA	ATACCAAATC	AGGCTCGAGG
370	380	390	400	410	420
TTATTACAA	TTTTTAAAAT	TTCTTTGTTG	GCCCAACTCG	CACCGAGTTT	TTTGGTTTTA
430	440	450	460	470	480
AAAATTGTGC	CCATGCGCGC	CATGTCACGA	AAACTAAAAT	CGTAAACAAA	ATGTCCATTT
490	500	510	520	530	540
TCTACCAGCC	CCGCCGAAAT	TTTACGATCG	GTGCAGTAGA	AATGCGCGCC	TTGCTTGTTA
550	560	570	580	590	600
AAACCAAAT	TTGCAATGTG	CAATATTTTC	ATTTAATTAA	AAACTCGATG	AGTCCAATAT
610	620	630	640	650	660
TTGAGATGCT	ACACGACTTG	CTTCATTGAG	TGGAGCCGAG	TTTGCAGCA	CACGCATGAC
670	680	690	700	710	720
ACCAATATTC	TGCTCAAAAG	GCAATTGATC	AATCATTTGA	GTAATTCTAT	CAGATTTTAA
730	740	750	760	770	780
ACGATCCATT	GCAATCCACA	CCTACACGGC	AGCCTGCAGT	CAATGCTTCA	AAAATCATGG
790	800	810	820	830	840
AAACACTATC	CTCTGTGACC	CATACCGTGG	CCGCCAACTG	CATTTGTTCA	AATATCCAGC
850	860	870	880	890	900
CTTGAGGGGT	TTCTTCAACA	GGAAAGAGCT	GTAATTGCTG	TGCACAAGGC	AATGTTTTTA
910	920	930	940	950	960
AATGTGATAT	AAAATTTACA	GGCGTACGTC	GTGAGGTCGT	CAAAATAATA	TGGGTATCTG
970	980	990	1000	1010	1020
GATAGTCTCG	AACAATATTT	TGAATAGACG	TTAAAACTTT	TTCTTGATTG	CATTGATGTC
1030	1040	1050	1060	1070	1080
GTTTGGAGTC	GCCGCCTAGG	GCAATCAAAA	TTGATTAGT	GTCGTGACGA	TGCTCATTTA
1090	1100	1110	1120	1130	1140
CGATTGGATT	CAGCGCCCCC	TGTGTCACAA	TGACTCGATC	AGATGCAGCC	ACACCATCAT
1150	1160	1170	1180	1190	1200
GCTCAGGAAT	AACTGCATAA	TTAAACCAAT	GTATCGGTAA	GCTTGGCTTC	ATCAAAATAA
1210	1220	1230	1240	1250	1260
TCGTTTTTCGC	CTGAGGATAA	ATTTTTCCAA	GTAACCACAC	TCGAAAATGC	GTATGACTTC
1270	1280	1290	1300	1310	1320
CTACCCCAA	TATAAAATCC	AGGCGGCTGC	TTGATCTGTG	ATACCTGATG	TGTAAACAGC
1330	1340	1350	1360	1370	1380
CCCTTCAAGA	TCGTTAATAA	TGGCAACTGC	TGTAGAGGAA	TTTCCTCAAA	ACGGCTATGG
1390	1400	1410	1420	1430	1440
ATAACGAGTT	TATGCATTGC	CTGATACAGG	CCTAAAGCTT	GTGATCGGTG	TCCTGCTTTT
1450	1460	1470	1480	1490	1500
CCATCACTCA	CATACACAAC	ATGCATATTT	TTTCCTAAAA	ACATCAATAA	AAAAGGCGAA
1510	1520	1530	1540	1550	1560
ACATGTGTTT	CGCCTTGATC	TTAACGGATT	CGCTTACTTC	ACGTAAGTTA	ACCAGTGTTT
1570	1580	1590	1600	1610	1620
ATATTTTGCA	TTTTTGCCCT	GAACCGCATC	GAAAAAGGTT	TTCTGGATTT	CTGTGGTAAT

Figure A-10: Sequence ID#10

Figure A-10 (cont'd)

1630	1640	1650	1660	1670	1680
TGGGCCACGG	CATCCTTCAC	CAATTTTCACG	GTCATCGTAT	TCACGAATTG	GCGTCACTTC
1690	1700	1710	1720	1730	1740
TGCGGCAGTA	CCAGTAAAGA	ATGCTTTCATC	TGCAATGTAG	AATTCATCAC	GGGTAATACG
1750	1760	1770	1780	1790	1800
ACGCTCAACC	ACTTCGTATC	CTAAATCTTT	TGCAATGGTA	ATAACTGTTT	GACGGGTAAT
1810	1820	1830	1840	1850	1860
CCCTTCTAAT	GCACCACCAG	CCAAATCAGG	GGTATGCAAC	ACGCCATCTT	TAATCAAGAA
1870	1880	1890	1900	1910	1920
CACGTCCTCG	CCTGCACCTT	GACACACAAA	GCCTTGTGGA	TCTAGCAACA	TCGCTTTCATC
1930	1940	1950	1960	1970	1980
ATAACCTGAA	CGCGCTACTT	CCTGATGTGC	CAAGATCGAC	ACAGTATAGT	TGCCACATGC
1990	2000	2010	2020	2030	2040
TTTTGCCTTA	CACATCGTCA	CGTTTGGATG	ATGATGCGTA	AACGAAGATG	TTTTTACACG
2050	2060	2070	2080	2090	2100
AATACCACGT	GCCATTGCCT	CTTCACCAAG	GTAAGCACCC	CAGCCCCATG	CCGCAACGGC
2110	2120	2130	2140	2150	2160
AGCATGAATA	CTATTTTCAG	TGGCAGCAAT	ACCTAATTTT	TCAGAACCGA	TCCAGATCAA
2170	2180	2190	2200	2210	2220
TGGACGCAAG	TAACAAGATG	CTAATTTATT	TTCACGAACC	ACATCAATTT	GAGCTTGCTC
2230	2240	2250	2260	2270	2280
AAGTGTCGCT	TGATCAAATG	GAACTTTCAT	TTGATAAATT	TTTGCAGAGT	TTAACAAACG
2290	2300	2310	2320	2330	2340
CCTNGTGTGA	TCTTGGANAA	CAAAAATTGC	NGTGGCTTTA	AGANTTTCAT	NAGGGCCGGA

C 3'

FILE NAME : ID11.DNA

SEQUENCE : 325BP; 74 A; 76 C; 73 G; 98 T.

\*\*\* SEQUENCE LIST \*\*\*

(SINGLE)

	10	20	30	40	50	60
5'	CTCTCGGGTA	TGGCGCCACT	GTGCAGCATT	CACNTGCANG	GATTGATTTG	CAAGGGNTAA
	70	80	90	100	110	120
	ACGTGGCTTT	CGGCTCGTTC	ACGTAGATAA	GCATGCATTA	ATGCTGTGGC	ATCTTCACTG
	130	140	150	160	170	180
	GATAAGCAGC	CTGCTTGAGC	AGCATCTTCT	AGAATTCTTA	CATTGTCGGA	AAAATGGGCG
	190	200	210	220	230	240
	AGATCAGGAT	TCGCTCCACT	CCATGCAAGC	ACCATATACT	GTGCCATAAA	TTCGATGTCA
	250	260	270	280	290	300
	ACGATACCAC	CTGCATCCTG	TTTTAAATGA	TGCCATGTTT	TTTTTGCTCA	TTGGATGATC
	310	320				
	CCAGATGTCT	TTCNTCTTGT	GGCGC	3'		

Figure A-11: Sequence ID#11

FILE NAME : ID12.DNA

SEQUENCE : 1300BP; 355 A; 227 C; 338 G; 376 T.

\*\*\* SEQUENCE LIST \*\*\*

(SINGLE)

5'	10	20	30	40	50	60
	GGCGATTGGC	TGTGTAAGCG	GTTTGTGCGAT	CTTAATCTCG	GTGCAATTTC	AGTCACCTCC
	70	80	90	100	110	120
	AAAGAAGGTG	AAGGTACTGT	ATTTACGGNG	ACCTTACCTA	TTGCCCAGAA	TGTTGCAGAG
	130	140	150	160	170	180
	ATTTATGCGG	AAAAGCAGGT	GAGTGAAGAA	AAATTGGTTT	AAATAGAACT	CCCTAAACAT
	190	200	210	220	230	240
	GCCTGCAACT	GCTATAACTA	TGCAAAACAA	AGGTTGCAGG	TTTTTTATGA	ATACTGAGCA
	250	260	270	280	290	300
	GTTGCAAAAA	ACATTAAGAT	CAAGTCAGTA	CGCAGAACAG	GTTTTAGGAT	TACATCAGCT
	310	320	330	340	350	360
	TTATTTAGAA	CAAGATTATC	AAATTGATCA	GTGTTGCTGC	TCCGCTTTTCG	AGAGAGAATA
	370	380	390	400	410	420
	TCTTCCAGTC	AGTTGAAAAT	GAATTAAAAA	ACATTCAGGA	TGAAAGTCAG	TGGATGCGAG
	430	440	450	460	470	480
	TAGTTCGTAT	TCTGCGTGCG	CGTTTAATGT	TCCGTTGGTT	CTGGCAAGAT	GCCAATCGAC
	490	500	510	520	530	540
	TCACCAATGT	GGTGAGTTTG	ACGCGAGAGC	TTTCAGATTT	TGCAGATGCC	TGCATTTGTG
	550	560	570	580	590	600
	CAGCCAAGCA	GTTTGCACGT	GCTCCTTTGG	TTGCCAAACA	TGGAGAGCCT	GTAGGATATG
	610	620	630	640	650	660
	ATGGTCAGAT	TCANGATTTG	ATCGTCATTG	GTATGGGTAA	GCTAGGGGCA	CAAGAGCTGA
	670	680	690	700	710	720
	ACTCCATCCA	GTGATATTGA	TCTGATTGTT	GCCTATGATG	AGCAGGGCGA	AACAAATGGT
	730	740	750	760	770	780
	CGTAAATCAA	TTGATGTGCA	GCAGTGTGTT	GTATNCCCGT	GGGGACAAAA	GCTGATTTAT
	790	800	810	820	830	840
	TTGCTGGATC	ATATTACCGC	AGATGGTTTT	GTATTTTCGTG	TGGATATGCG	ATTACGTCCC
	850	860	870	880	890	900
	TGGGGTGATG	GTTCAGCTTT	GGCAATTAGC	CATATGGCAT	TAGAGAAAATA	TCTGATCCAG
	910	920	930	940	950	960
	CATGGACGCG	AATGGGAGCG	TTATGCGTGG	ATCAAAGCGC	GTATCATCAG	TGGTGGAAG
	970	980	990	1000	1010	1020
	CACGGCGATG	ACCTGCTGGA	AATGACCCGA	CCATTTGTGT	TTCGGCGCTA	TGTCGATTAT
	1030	1040	1050	1060	1070	1080
	TCCGCTTTTCG	CAGCCATGCG	TGAAATGAAA	AGTATGATCG	AACGTGAAGT	GGCACGTCGT
	1090	1100	1110	1120	1130	1140
	AATATCGCAG	ATGATATTAA	GCTAGGCGCG	GGAGGAATAC	GTGAAGTTGA	ATTCATTGTT
	1150	1160	1170	1180	1190	1200
	CAGGTATTTTC	AGCTTATCTA	TGGTGGATCG	AAACGTGAGT	TGCAAGATCG	CCAATGTTTG
	1210	1220	1230	1240	1250	1260
	GTCAGCCTAA	ATCATTTAGG	TCAGGCTGGC	TTACTTCAGT	CACAAGATGT	GATTGAGTTA
	1270	1280	1290	1300		
	GAAGATGCCT	ATTTGTTTTT	AAGACGTGTA	GAACATNCCA	3'	

Figure A-12: Sequence ID#12

FILE NAME : ID13.DNA

SEQUENCE : 446BP; 140 A; 92 C; 90 G; 117 T.

\*\*\* SEQUENCE LIST \*\*\*

(SINGLE)

5'	10	20	30	40	50	60
	CGATCTGTTT	GTTTNTANGA	CGTGTAGNAA	CATGCCATTC	AAGCCTTGCGN	ATGATCAGCA
	70	80	90	100	110	120
	AACCCAGATG	TTACCGATGG	AGCCTGAGCT	ACGCCAACGT	ATACTCAGAT	ACGCTTGAAT
	130	140	150	160	170	180
	ACCCAACCTG	GAACAATTTT	ATTGAGGCTT	TAAACGAAAA	ACGTCATAAA	GTGAGTGAAC
	190	200	210	220	230	240
	AGTTTAAAAA	ACTGATTCAG	GAAGAAGTCA	CTTCACCAGA	CGAAACCGAT	ACAGAGCTAG
	250	260	270	280	290	300
	AACAACAAC	TAATGCTATC	TTGGATGAGA	CAGCCCCAAA	TTTAGTGTCAT	GATGGCGGCA
	310	320	330	340	350	360
	GAGTAATGCA	TTAAAACGGC	TTCTTTCTAA	AGCGGNACAG	CGTCTAAAAG	ATTTCTGGCC
	370	380	390	400	410	420
	TCATTTTATT	GAAGCTATTT	TACAGNCTGA	ACATCCACAA	ATGGCATTTA	TGCGTNTGAT
	430	440				
	GCCTTGATTG	ATCTTGTCAT	GCGCCG	3'		

Figure A-13: Sequence ID#13

FILE NAME : ID14.DNA

SEQUENCE : 786BP; 202 A; 155 C; 198 G; 222 T.

\*\*\* SEQUENCE LIST \*\*\*

(SINGLE)

5'	10	20	30	40	50	60
	CCGACACTGG	CATCTAGCGT	NTGATGTCCT	TGATTGAATC	TGCCATGCGN	CGCACTGTAT
	70	80	90	100	110	120
	ATCTGGTGAT	GCTGNTGGAA	AGTCGAGGTG	CCATGCAGCG	ACTGGTCAAA	ATGGCCACCG
	130	140	150	160	170	180
	TGAGCCCCTG	GATTTGTGAG	GAGCTAACGC	AATATCCTGT	GTTACTGGAT	GAATTTCTTT
	190	200	210	220	230	240
	CTATGGATGG	TNGAACTGCC	ACAGCGNAAG	GATCTGGAAG	ATTCTTTACG	TCAGCAGCTT
	250	260	270	280	290	300
	CTTCGGATTG	AAATTGATCA	GGTCGAAGAC	CAGATGCGTG	TACTGCGGCT	GTTTAAGAAA
	310	320	330	340	350	360
	AGTAATGTCC	TTACCGTTGC	TGCAAGTGAT	GTTTTAGCCG	AAAGTCCTCT	CATGAAAGTT
	370	380	390	400	410	420
	TCAGATGCAT	CGACCGATAT	TGCTGAAGTC	AGTGTGCGAG	CAACCTTAAA	TTTGGCCTAT
	430	440	450	460	470	480
	CAGGCTGTTG	TTAAAAAACA	TGGTTATCCC	AAAGATGCCA	GTGGTGAACG	TTGCTCACTG
	490	500	510	520	530	540
	GAGCATACAG	GTTTTGCAGT	GATTGGTTAT	GGGAAGCTGG	GGGGGATTGA	GCTGGGTTAT
	550	560	570	580	590	600
	GGTTCTGATC	TGGACCTGGT	TTTTATTAC	TATTTTGATG	AACAGGCCGA	AACAGATGGA
	610	620	630	640	650	660
	TCAAAATCCA	TCACAGGTTT	TGAATTTGCC	ATGCGTGTGG	NACAAAAGTT	TTTATCACTC
	670	680	690	700	710	720
	ATGACAACTC	AAACCTTGGA	TGGTCGTGTG	TATGAAATTG	ATACTCGACT	TCGACCATCT
	730	740	750	760	770	780
	GGAGAAGCAG	GACTACTGGT	AACAAGTNTA	ANAGCATTTG	ACACCACCAC	TCAAAAGTNC
	ATCGCT 3'					

Figure A-14: Sequence ID#14

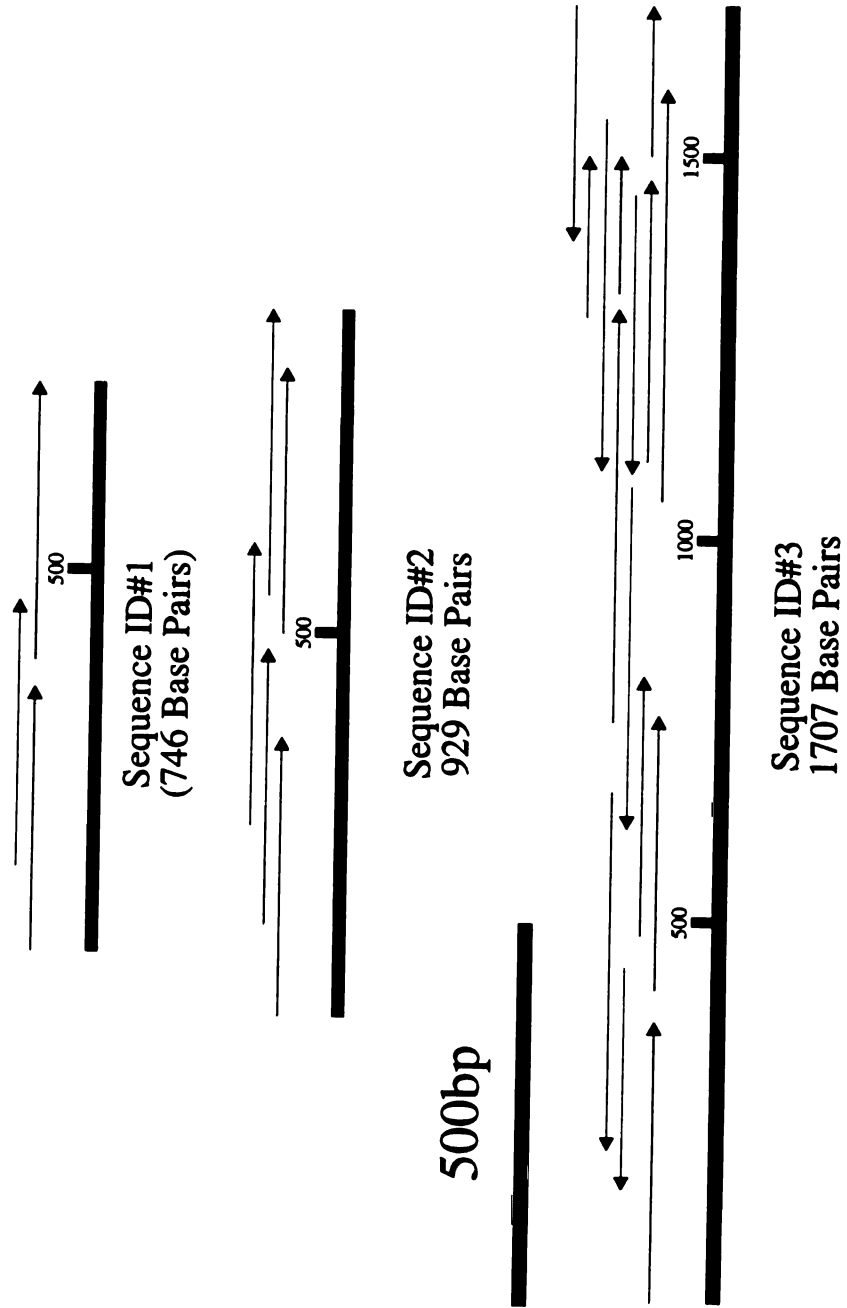


Figure A-15: Sequencing contigs of pSR6. Arrows show the direction of the sequencing run.



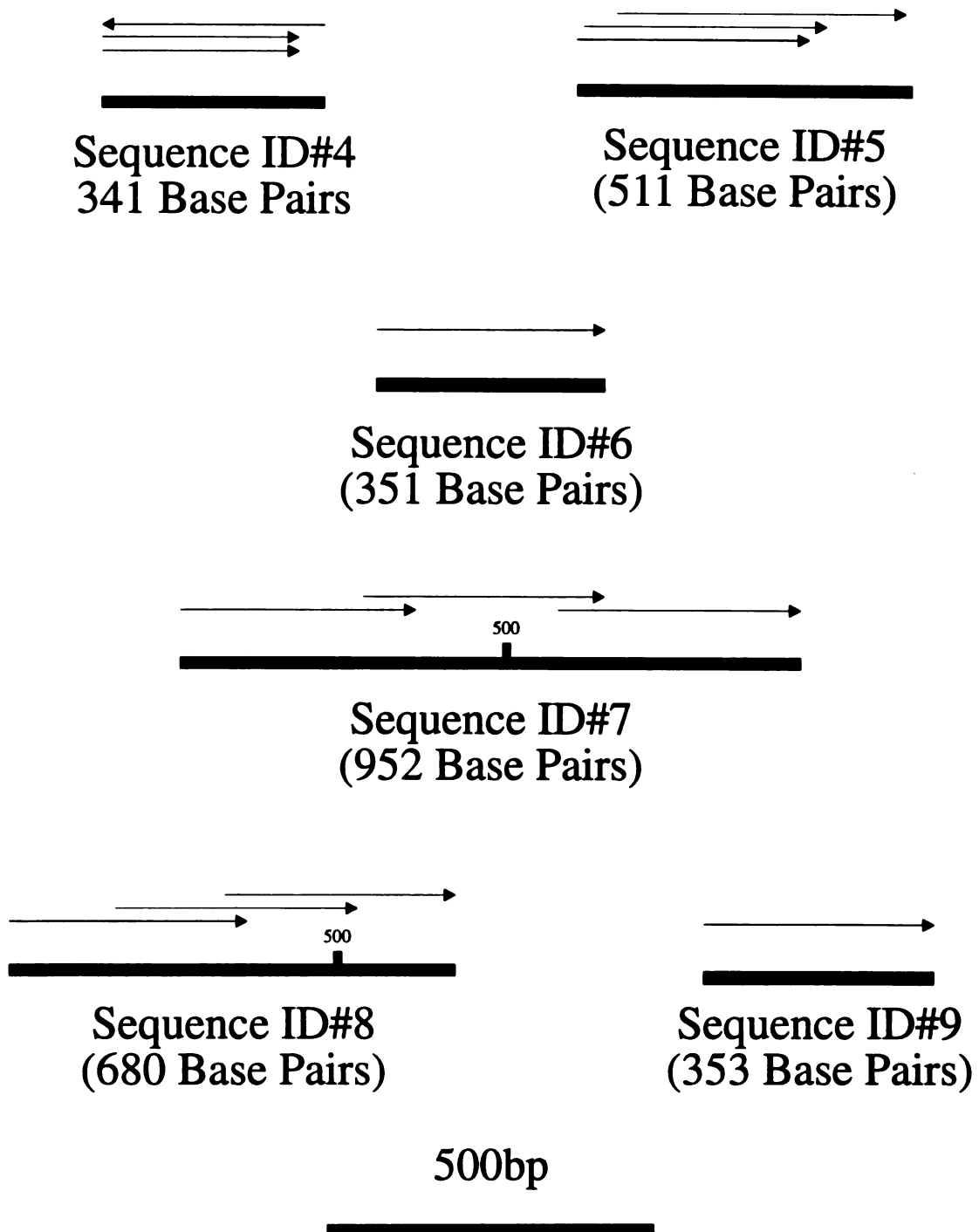
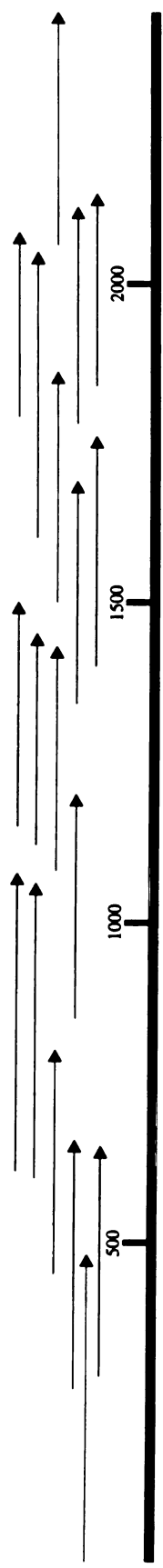


Figure A-16: Sequencing contigs of pSR2. Arrows show the direction of the sequencing run.

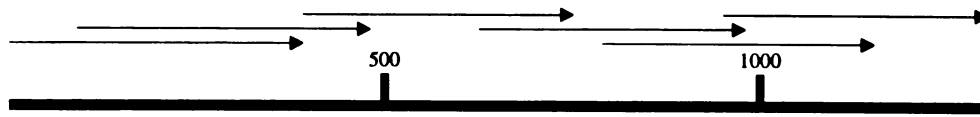


Sequence ID#10  
(2423 Base Pairs)

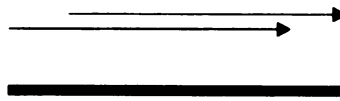


Sequence ID#11  
(325 Base Pairs)

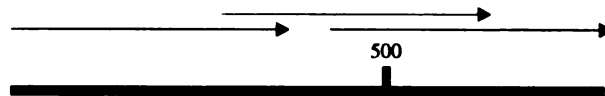
Figure A-17: Sequencing contigs of pSR11. Arrows show the direction of the sequencing run.



Sequence ID#12  
(1300 Base Pairs)



Sequence ID#13  
(447 Base Pairs)



Sequence ID#14  
(786 Base Pairs)

500bp



Figure A-18: Sequencing contigs of pSR12. Arrows show the direction of the sequencing run.

## **APPENDIX B**

## APPENDIX B

### CONSTRUCTION OF A TRANSCRIPTIONAL EXPRESSION VECTOR FOR *A. CALCOACETICUS* AND *E. COLI*

During the course of the examination of the wax ester and triacylglycerol mutants, a possibility existed that the gene or genes of interest might reside in an operon. To ascertain which of the genes had been affected by the chemical mutagenesis, and which was needed to complement the mutant phenotype, it would be necessary to express the genes outside of the operon. This would necessitate removing the gene from the environment of its promoter. Therefore to express the isolated gene, it would need to be expressed in some sort of transcriptional expression vector that was functional in *A. calcoaceticus*. Therefore, it was decided to construct such a vector using pSER2, a pBR322 derivative that is able to replicate in both *A. calcoaceticus* and *E. coli*. This appendix highlights the construction of pSER1 and pSER2 and their subsequent use in constructing pSER200-1 and pSER200-4. Table B-1 lists the plasmids used for this purpose.

An *A. calcoaceticus*/*E. coli* shuttle vector, pWH1274, was previously constructed by Hunger et. al. (Hunger et al., 1990). It is a pBR322 derivative containing ampicillin and tetracycline resistance markers and an *A. calcoaceticus* origin of replication in addition to the origin of replication from *E. coli* (Figure B-1).

Table B-1: Plasmid sources and derivations for Appendix B.

Plasmid	Description or Construction	Source or Reference
pWH1274	<i>A. calcoaceticus</i> / <i>E. coli</i> shuttle vector. pBR322 derivative containing <i>A. calcoaceticus</i> origin of replication (Tet <sup>r</sup> Amp <sup>r</sup> )	(Hunger et al., 1990)
pSER1	<i>A. calcoaceticus</i> / <i>E. coli</i> shuttle vector (Tet <sup>r</sup> Km <sup>r</sup> )	Figure B-1, this study
pSER2	<i>A. calcoaceticus</i> / <i>E. coli</i> shuttle vector (Tet <sup>r</sup> Km <sup>r</sup> )	Figure B-1, this study
pUC4k	Km <sup>r</sup> cloning vector	Dr. Lee McIntosh
pUC19	Source of MCS to give pSER200 derivatives	New England Biolabs
pPR13	Reporter construct containing full length <i>lacZYA</i> cassette	Dr. Frans DeBruijn (Ratet et al., 1988)
pSER100	pSER2 derivative with the EcoRI site filled in to destroy it	Figure B-2, this study
pSER110	pSER100 derivative containing <i>lacZYA</i> cassette from pPR13	Figure B-2, this study
pSER120-1	pSER110 derivative containing ~1200 bp insertion homologous to <i>pntA</i>	Figure B-2, this study
pSER120-4	pSER110 derivative containing ~500 bp insertion with homology to dihydrofolate reductase	Figure B-2, this study
pSER200-1	pSER120-1 derivative with <i>lacZYA</i> removed	Figure B-5, this study
pSER200-4	pSER120-4 derivative with <i>lacZYA</i> removed	Figure B-8, this study

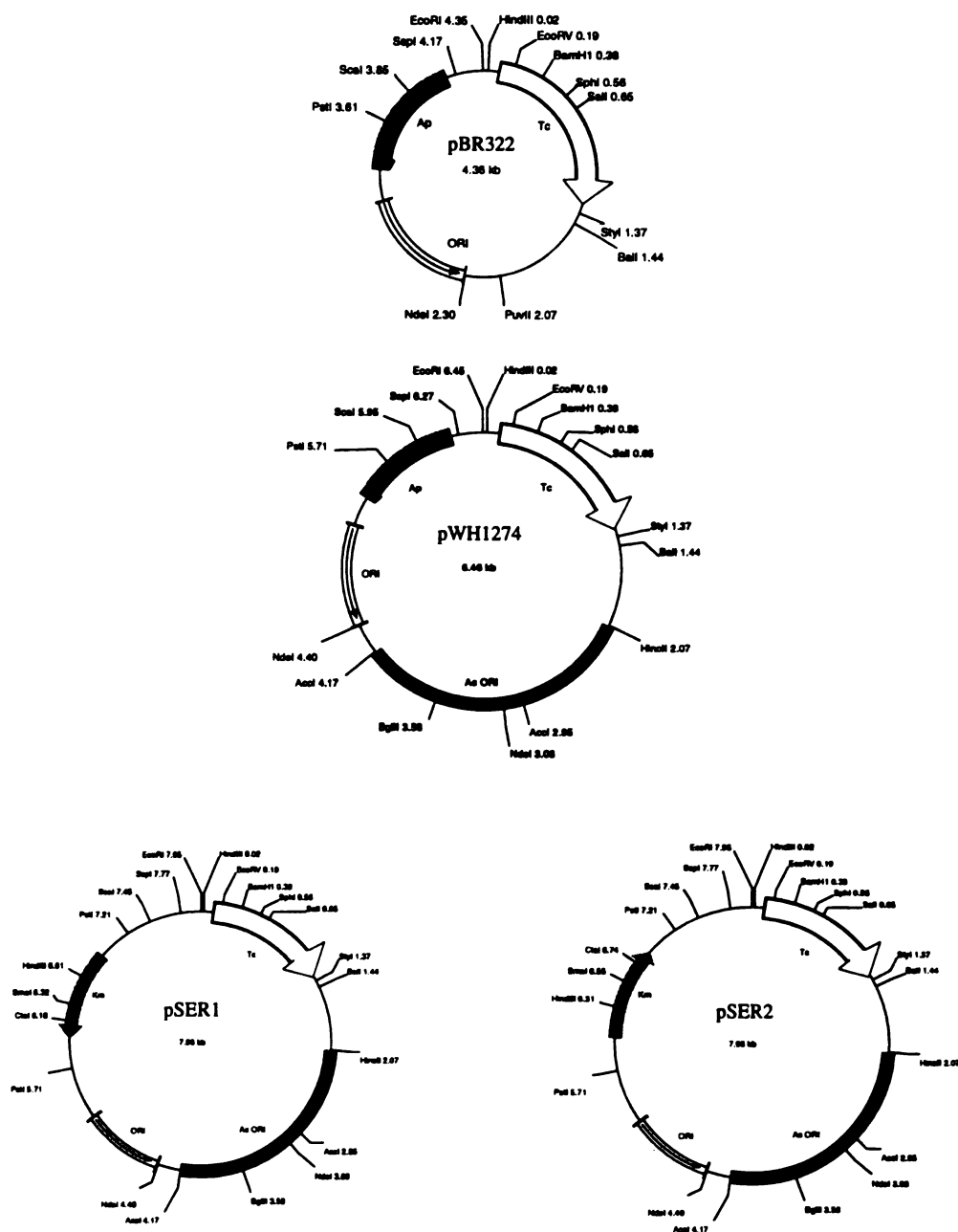


Figure B-1: Restriction maps of pBR322, pWH1274, pSER1 and pSER2. The original *A. calcoaceticus*/*E. coli* shuttle vector was derived from pBR322 (top) by the addition of an *A. calcoaceticus* origin of replication to give pWH1274 (middle). The plasmids at the bottom of the figure, pSER1 and pSER2 are derivatives of pWH1274 that contain the Km<sup>r</sup> cassette from pUC4K (probably derived from Tn903). The location of several restriction sites are listed by their positions in kb.

One problem with this vector is that *A. calcoaceticus* is naturally resistant to ampicillin, making selection with that particular marker difficult in this species. Therefore, it was decided to modify pWH1274 by inserting a kanamycin resistance marker taken as a PstI fragment from pUC4k into the PstI site of the ampicillin cassette of pWH1274, thus inactivating it. The kanamycin resistance marker from pUC4k is probably derived from Tn903 as evidenced by the lack of a BglII site and the locations of the HindIII and ClaI sites. The new vectors containing the kanamycin cassette in two different orientations were called pSER1 and pSER2 (Figure B-1).

pSER2 was then used to construct the transcriptional expression vector in the following manner. pSER2 was digested with EcoRI. The site was filled in using Klenow enzyme and dNTPs and the vector recircularized to produce pSER100. The full length *lac* cassette (containing *lacZYA*) was then removed from pPR13 (a kind gift from Dr. Frans DeBruijn) via a BamHI+Sall digestion (Ratet et al., 1988). This *lac* cassette was then directionally cloned into pSER100, removing the majority of the Tet<sup>r</sup> cassette, creating pSER110 (Figure B-2). This provided a unique BamHI site upstream of the *lac* cassette for the insertion of random fragments of DNA that might contain promoter activity. This promoter activity could be detected by the presence of  $\beta$ -galactosidase activity in *A. calcoaceticus*. SauIIA partials of the cosmid 1A-3F (the cosmid that complements the *wow1* phenotype) were carried out, and fragments of approximately 500 bp were size selected. The reason that it was decided to obtain a promoter element from this cosmid, as opposed to something from the genome, was in the hope of enriching for a promoter that would be inducible under low nitrogen conditions. This would allow the expression of the gene of interest under the same



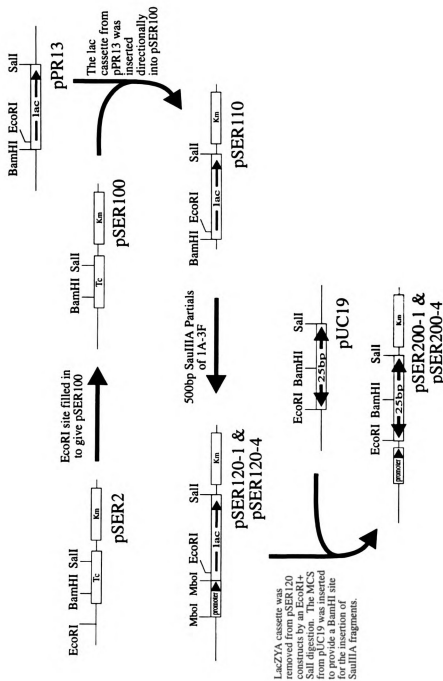


Figure B-2: Illustration of the steps taken to construct pSER200-1 and pSER200-4 transcriptional expression vectors for use in *A. calcoaceticus*. Major restriction sites are given for orientation.

conditions that they were needed for expression of the rest of the operon, all of which would presumably be induced under low nitrogen conditions.

The resulting products containing the *SauIIA* partials were transformed into *A. calcoaceticus* which was then plated onto medium containing 15 µg/ml Tetracycline and X-gal (40 µg/ml). Seven blue colonies were identified. These seven were replated onto low nitrogen selective medium containing X-gal and IPTG. Two of the seven seemed to be more heavily stained when grown under low nitrogen conditions, than when plated on LB. No colonies were identified that turned blue under low nitrogen conditions, that had previously been blue on LB. The two different plasmid constructs (presumably different because of their promoter fragments) were called pSER120-1 and pSER120-4 (Figure B-2).

The final products, pSER200-1 and pSER200-4 derived from pSER120-1 and pSER120-4 respectively, were the result of digesting the samples with *EcoRI*+*SalI* to remove the *lac* cassette and replace it with a polylinker from pUC19. This allowed the presence of a unique *Bam*HI site for cloning foreign fragments behind the promoter element. Restriction analysis of the pSER200 constructs indicated that the promoter element located in pSER200-1 is approximately 500 bp, while the one present in pSER200-4 is roughly 1200 bp.

To ascertain the relative strengths of the promoters, assays were conducted to measure the amount of  $\beta$ -galactosidase in the cells. Activity was measured in extracts of cells grown in minimal medium under both high and low nitrogen levels. Additionally, the constructs were transformed into *E. coli* strain DH5 $\alpha$  and  $\beta$ -galactosidase levels were measured for transformants cultured in LB medium. Assays

were carried out in the manner described by J. H. Miller (Miller, 1992). The number of units of  $\beta$ -galactosidase were calculated based on the absorbance reading of the sample at 420 nm resulting from the cleavage of OPNG and are presented in Table B-2.

From these data we see that wild type *A. calcoaceticus* strain BD413 does not exhibit any  $\beta$ -galactosidase activity. As a control, *A. calcoaceticus* was transformed with pSER110, the construct containing the *lac* cassette without any sort of promoter element. In this transformant,  $\beta$ -galactosidase levels are only slightly higher. Transformation and introduction of pSER120-1 into *A. calcoaceticus* resulted in the presence of 1817 units of  $\beta$ -galactosidase. *A. calcoaceticus* transformants containing pSER120-4 have approximately half the levels of pSER120-1 constructs at 950 units of  $\beta$ -galactosidase. Neither sample was induced to higher levels of  $\beta$ -galactosidase when grown under low nitrogen conditions, contradicting what appeared like a marked increase when the colonies were inspected visually on plates. Rather, there appears to be an approximately 10-20% decrease in the amount of  $\beta$ -galactosidase present in the cells.

Examination of the constructs in *E. coli* shows them to still be active, but at greatly different levels. Because of the genotype of the *E. coli* strain, it was not convenient to measure the amount of  $\beta$ -galactosidase under low and high nitrogen conditions, rather measurements were made after incubating the cultures in LB medium. Introduction of pSER120-1 in *E. coli* results in an almost 10 fold increase in  $\beta$ -galactosidase production, while there is a about a six fold decrease in levels of  $\beta$ -galactosidase production when pSER120-4 is expressed in *E. coli*.

Table B-2:  $\beta$ -Galactosidase content of cells transformed with pSER120 constructs.

Sample	Units of $\beta$ -Galactosidase
<b><i>A. calcoaceticus</i> strain BD413</b>	
<b>High nitrogen conditions</b>	
Wild type	3.13
Wild type with pSER110	13.65
Wild type with pSER120-1	1817.03
Wild type with pSER120-4	950.48
<b>Low nitrogen conditions</b>	
Wild type	7.37
Wild type with pSER110	15.03
Wild type with pSER120-1	1600.54
Wild type with pSER120-4	759.77
<b><i>E. coli</i> strain DH5<math>\alpha</math></b>	
Wild type	27.96
Wild type with pSER110	39.19
Wild type with pSER120-1	10127.3
Wild type with pSER120-4	167.78

To get some sense of the origin of subcloned promoter elements, a single stranded sequence read into both ends of the promoter element was performed. The promoter of pSER200-1 was found to have 100% sequence identity with a pyridine nucleotide transhydrogenase (*pntA*) from *E. coli* (Figure B-3). The only explanation for this result is that the cosmid DNA that was partially digested and used to identify promoter elements must have been contaminated with *E. coli* genomic DNA. This is easily explainable since cosmid DNA was routinely prepared using Promega's Wizard DNA preparation kits. These kits employ a resin that the DNA binds to and is later removed from via salt exchange. Because the cosmid DNA was routinely extracted from *E. coli* strain HB101, where it is present in a very low copy number, it is likely that there was sufficient room on the column for genomic DNA fragments to bind, resulting in contamination of the DNA sample. Although this is rather unfortunate and sloppy, it still does not detract from the fact that this promoter element is completely active in *A. calcoaceticus*. It also serves to explain the 10 fold increase in  $\beta$ -galactosidase accumulation when the construct is introduced into *E. coli* in comparison to *A. calcoaceticus*. The known sequence of the upstream region of *pntA* starts approximately 200 bp upstream of the *lac* cassette. Additionally, the gene is oriented in such a way that it is being transcribed in the opposite direction to the *lac* cassette. This implies that the transcriptional activity of the subcloned fragment resides in the 200 bp just upstream of the *lac* cassette and is oriented away from the *pntA* gene toward the cassette. Possible promoter elements are highlighted in Figure B-4. Finally, the best known restriction map for pSER200-1 is illustrated in Figure B-5.

DNA sequencing of the promoter element in pSER200-4, found it to be

FILE NAME : 200-1-5'.DNA

SEQUENCE : 347BP; 70 A; 103 C; 86 G; 72 T.

\*\*\* SEQUENCE LIST \*\*\*

(SINGLE)

```

      10      20      30      40      50      60
5' GATCCCCAGC GCGCCATCGC TATTGAATTC CGCGCCCATA CTTTGAAC TTCTTTTCAC
      70      80      90     100     110     120
   TTCCGGGNGG GTGTCGAATG CACGCACAAT CGCGCCGAGA CTGNTTGCTG CGCCAATGGC
      130     140     150     160     170     180
   GGCCAGACCT GCAACACCCG YACCAATCAC CATCACTTTT GCCGGTGGCA CTTTCCCGGN
      190     200     210     220     230     240
   CGCAGTAATT TGCCCGGTWA AGAAGCGCCC AAATTCATGT GCCGCTTCAA CAATGGNGCG
      250     260     270     280     290     300
   ATAACCGGNG ATGTNCGCCA TCGAGCTTAG NGNGTCCAGC GNATTGTGCG NGTGANATAC
      310     320     330     340
   GCGGCACAGA GTCCATCGCC ANCACGGTCA NGTTANGTTC CGCAAGT 3'

```

Figure B-3: Sequence ID#15. Sequence of the 5' region of the promoter cloned into pSER200-1. This sequence was found to be 100% identical to *pntA* from *E. coli*.

FILE NAME : 200-1-3'.DNA

SEQUENCE : 414BP; 117 A; 99 C; 85 G; 109 T.

\*\*\* SEQUENCE LIST \*\*\*

(SINGLE)

```

      10      20      30      40      50      60
5' CAACATAAAA AGAGGCGGCA CCTTCTTTAT CTGCGCGACG AGAAACGGCT TTCACCGCTT
      70      80      90     100     110     120
   CGCCAATAGC ATTAAACGA CCGGTAACCA CTACACGGTC AAAAGGTTTA ACCGCTGCCG
      130     140     150     160     170     180
   CTTGCTCCGG TGTCAGTTCT GTTGCTGCGT TAACGGAGAA TGCCATAGCA GAAAGCAGTG
      190     200     210     220     230     240
   CCGACGCCAG GAGGGTGTTT TTAAGCTTCA TAAAAATAAT CCTTCGCCTT GCGCAAACCA
      250     260     270     280     290     300
   GGTACTGGTA TTGTTATTAA CGAGAAACGT GGCTGATTAT TGCATTTAAA CGGTGTAAGT
      310     320     330     340     350     360
   GTCTGCGTCA TTTTTCATAT CACATTCCTT AAGCCAATTT TAATCCTGCT CAAATGACGN
      370     380     390     400     410
   CTATGCTTAA AAAACAGCCG NNTCAGCATC ATTACTACTG AAGCAACTGN ATTG 3'

```

Figure B-4: Sequence ID#16. Sequence of the 3' region of the promoter cloned into pSER200-1. This sequence was found to be 100% identical to *pntA* from *E. coli*. Base pair 209 through the end of the sequence represents *pntA* 5' untranslated region, as it was deposited in GenBank. A possible -10 and -35 boxes are highlighted in bold type.

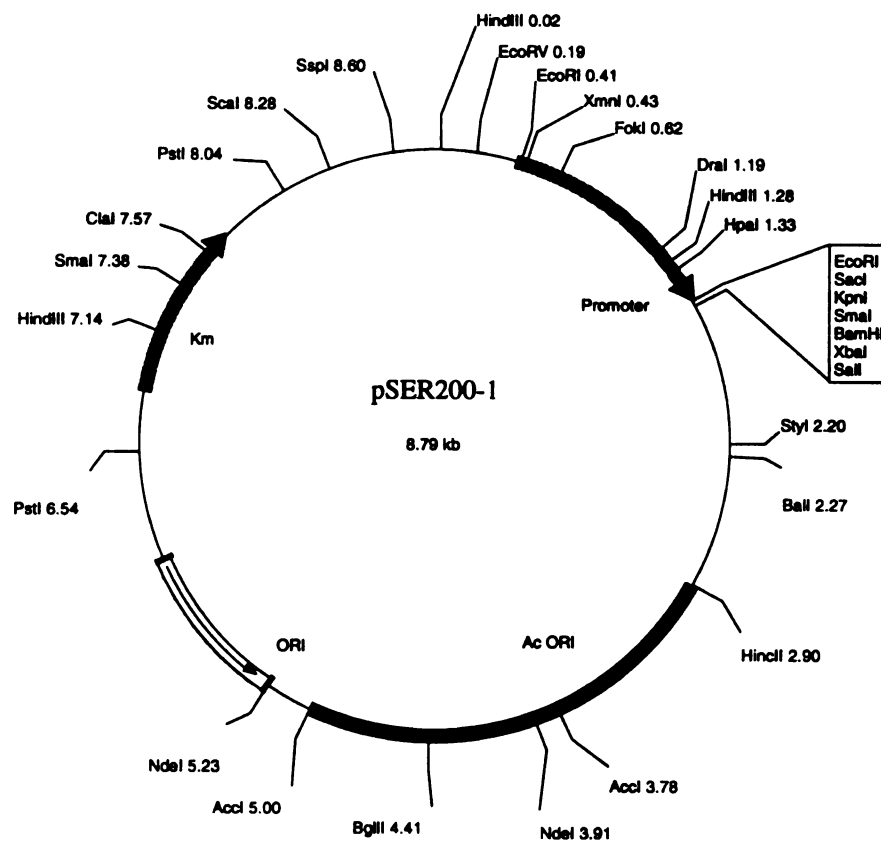


Figure B-5: Best known restriction map of *A. calcoaceticus*/*E. coli* transcriptional expression vector pSER200-1. The region between 0.62 kb and 1.19 kb was not sequenced so restriction sites in this area are currently unknown. Features include Km<sup>r</sup> from the Km<sup>r</sup> cassette, probably derived from Tn903, *Acinetobacter* and *E. coli* origins of replication, a promoter that is active in both *E. coli* and *Acinetobacter* (10x higher expression in *E. coli*) and polylinker with several possible cloning sites. DNA sequence information for the promoter region of this vector can be found in this text as sequence ID#15 and ID#16.

strongly similar to dihydrofolate reductase (BLAST score of 175, Figure B-6), which has been cloned from several different organisms. The sequence of this promoter element is shown in Figure B-7. A strong blast score to dihydrofolate reductase starts approximately 330 bp upstream of the *lac* cassette and continues up to the *lac* cassette. This would most likely place the promoter element in approximately the first 170 bp of the fragment, about 330 bp away from the *lac* cassette. Possible promoter elements in this region are highlighted in Figure B-7. This explains the rather weak accumulation of  $\beta$ -galactosidase in samples containing this promoter element. However, the possibility of a cryptic promoter element in the coding sequence of dihydrofolate reductase cannot be ruled out. Finally, the best known restriction map for pSER200-4 is illustrated in Figure B-8.

Neither of these transcriptional expression vectors was modified any further. It would be nice to streamline them by eliminating the excess sequence that is present in both of the vectors. Approximately 1.1 kb could probably be cut out of pSER200-1 without any adverse affect. Similarly, the 300 bp of sequence that separates the promoter from the potential cloning sites in pSER200-4 could also be removed. In this case it might even improve transcriptional expression. Regardless of these minor imperfections, both of these constructs are new and important tools that could be used in studying *A. calcoaceticus*.



```

>sp|P12833|DYS3_SALTY DIHYDROFOLATE REDUCTASE TYPE III. >pir|S|RDEBDT
dihydrofolate reductase (EC 1.5.1.3) type III - Salmonella
typhimurium plasmid pAZ1 >gp|J03306|PAZDHFRA_1 Plasmid pAZ1 type
III dihydrofolate reductase gene, complete cds. [Plasmid pAZ1]
Length = 162

Minus Strand HSPs:

Score = 235 (109.3 bits), Expect = 2.6e-27, P = 2.6e-27
Identities = 42/79 (53%), Positives = 57/79 (72%), Frame = -1

Query: 297 VVAMDQKQCIGKGNALPWHIPADLKHFKBITQDGVVIMGRKTLSEMGRTLPKRVNWVITR 118
      + A+      IGK N +PWH+PADL+HFK +T      V+MGR+T ES+GR LP R N V++R
Sbjct: 6 IAALAHNNLIGKDNLIPWHLPADLRHFKAVTLGKPVVMGRRTFESIGRPLPGRRNVVVS 65

Query: 117 DPNWQFEGAKVASSIEAAL 61
      +P WQ EG +VA S++AAL
Sbjct: 66 NPQWQAEGVEVAPSLDAAL 84

```

Figure B-6: Results of BLASTX alignment using sequence ID#17 as a query sequence. Based on this homology, the promoter element for pSER200-4 was found to be derived from the promoter of dihydrofolate reductase from *A. calcoaceticus* strain BD413.

FILE NAME : 200-4-5'.DNA

SEQUENCE : 478BP; 128 A; 108 C; 113 G; 119 T.

```

*** SEQUENCE LIST ***                               (SINGLE)

      10          20          30          40          50          60
5' CGGAGCNNTA TCGACTACGC GATCATGGCG ANCACACCCG TCCTGTGGAT CTGTTTGATT
      70          80          90         100         110         120
TTAAATTTGA AGATATTGAA ATTGTGGATT ATCAATCCCA CCCTGCAATC AAAGCCCCTG
      130         140         150         160         170         180
TTGCCGTATA AGGAAGCTCA GCAATGGCAT TTCAAGATTT AGAAGTCGTG CATGTGGTTG
      190         200         210         220         230         240
CGATGGATCA AAAACAATGT ATTGGTAAAG GCAATGCATT ACCTTGGCAC ATTCCTGCCG
      250         260         270         280         290         300
ATCTCAAACA TTTTAAGGAA ATCACTCAAG ATGGCGTCGT GATTATGGGT CGTAAGACAC
      310         320         330         340         350         360
TTGAATCCAT GGGGCGCACG CTCCCTAAAC GTGTCAACTG GGTGATTACC CGNGATCCTA
      370         380         390         400         410         420
ATTGGCAGTT TGAAGGCGCC AAAGTTGCAT CCAGCATAGA AGCTGCACTT NAAAGGCGCA
      430         440         450         460         470
GCTCAGGATC CSGNGAATTC GAGCTCGGTA CCCSGNGNAT CCTCTAGTAG AGTCGACC

```

Figure B-7: Sequence ID#17. DNA sequence of the promoter element used in the construction of pSER200-4. Possible -10 and -35 boxes are shown in bold faced type. Sequence similarity to dihydrofolate reductase begins at base pair 172 and extends to the end of the sequence.

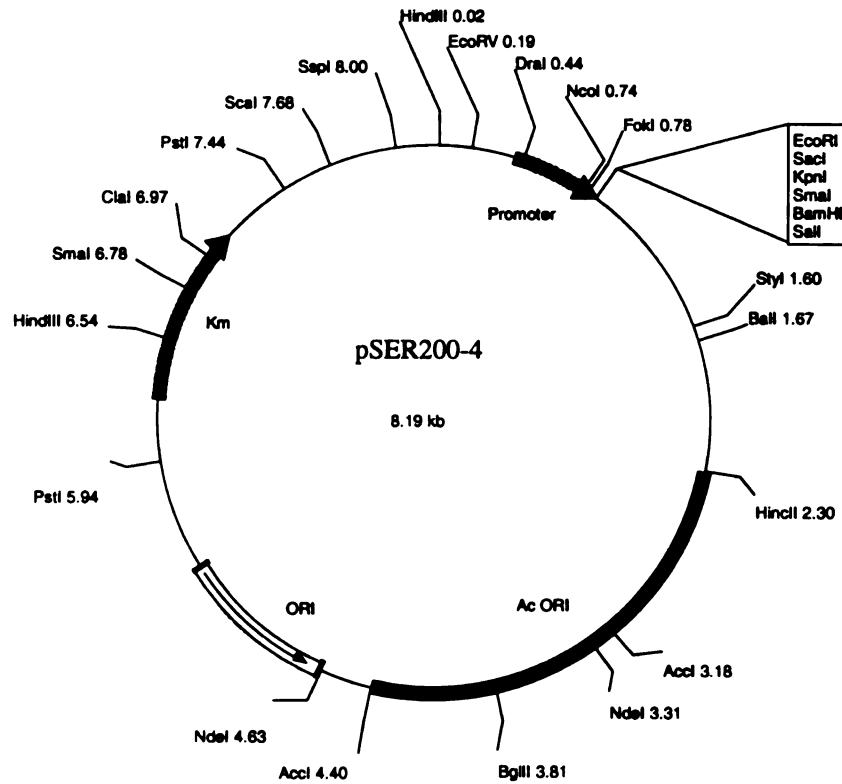


Figure B-8: Best known restriction map of *A. calcoaceticus*/*E. coli* transcriptional expression vector pSER200-4. Features include Km<sup>r</sup> from the Km<sup>r</sup> cassette, probably derived from Tn903, *Acinetobacter* and *E. coli* origins of replication, a promoter that is active in both *E. coli* and *Acinetobacter* and a polylinker with several possible cloning sites. DNA sequence information for the promoter region of this vector can be found in this text as sequence ID#17.

**REFERENCES**

- Hunger, M., Schmucker, R., Kishan, V. and Hillen, W.. 1990. Analysis and Nucleotide Sequence of an Origin of DNA Replication in *Acinetobacter calcoaceticus* and its use for *Escherichia coli* Shuttle Plasmids. *Gene*, 87:45-51.
- Miller, J. H.. 1992. Procedures for Working with *lac*. In A Short Course in Bacterial Genetics: A Laboratory Manual and Handbook for *Escherichia coli* and Related Bacteria. Cold Spring Harbor Laboratory Press, Plainview, New York.
- Ratet, P., Schell, J. and de Bruijn, F. J.. 1988. Mini-Mulac Transposons with Broad-Host-Range Origins of Conjugal Transfer and Replication Designed for Gene Regulation Studies in *Rhizobiaceae*. *Gene* 63:41-52.

## APPENDIX C

## APPENDIX C

### CLONING OF A PARTIAL DNA FRAGMENT OF SN-1 ACYLTRANSFERASE FROM *A. CALCOACETICUS*

Another attempt at isolating DGAT (diacylglycerol acyltransferase) involved an approach using degenerate oligonucleotides and PCR. It was our belief that DGAT might be isolated by constructing degenerate primers based on consensus sequence generated from other known acyltransferases. Several acyltransferases have been isolated from a number of different organisms. A careful comparison of those sequences was done using the GCG sequence analysis program by Dr. Joe Ogas. In his pileup of the different sequences, Dr. Ogas was able to identify two different region that were conserved among the acyltransferases. These are shown in Figure C-1.

Degenerate oligos based on the conserved regions highlighted in Figure C-1 were constructed based on the preferred codon usage table published by White et. al. (White et al., 1991). These primers and their degeneracy are listed in Table C-1. PCR was carried out under the following conditions. A total of 100 ng of genomic DNA from *A. calcoaceticus* strain BD413 was mixed with 50 pmols of each primer, 2.5  $\mu$ l of 2 mM dNTP's 2.5  $\mu$ l of 10x buffer (660 mM Tris-HCl (pH 7.6), 50 mM MgCl<sub>2</sub>, 10 mM dithioerythritol and 10 mM ATP (pH 7.5)) and 1.25 units of TAQ

	1				50
A. calco.	.....HR	WMDYLLLSY	VIYKRGLM..	VPYIAAGDNL	
Yst-Sn1-p1	KNHPEIIKGR	SKNPQTTPVN	FTKRFSAKSL	LGLPDYLS..	NAQIKEIPDD
Yst-Sn1-p2	K.....R	VIGHDT...H	FLTDCMPKGL	IGLPKSMG..	FGEIQSIESD
E.coli-Sn1	ERVRLAHDG	HELVVVPCHR	SHMDYLLLSY	VLYHQGLV..	PPHIAAGINL
MousMitSn1	EMVKAATETN	LPLFLPVHR	SHIDYLLLT	ILFCHNIK..	APYIASGNL
E.coli-Sn2	KPTDAESYGN	A..IYIANHQ	NNYDMVTASN	IVQPPTVT..	...VGKKSLL
Yst-Sn2-p1	KVVGEENLAK	KPYIMIANHQ	STLDIFMLGR	IFPPGCTV..	...TAKKSLK
Maize-Sn2	RSMGKEHA..	...LIISNHR	SDIDWLIGWI	LAQRSGCLGS	TLAVMKKSSK
Yst-Sn2-p2	LSHLKSNS..	...VAICNHQ	IYTDWIFLWW	LAYTSNLGAN	VFIILKKSLA
Consensus		HR	SHMDY		
	51				100
A. calco.	NLPFVGQLLR	GGGAFFIRRS	FRGNGLYTSV	FK.....	
Yst-Sn1-p1	ETIILSSPFR	TSKSKVVELL	TNGTNFKYAE	KI.....	
Yst-Sn1-p2	TSLTLRKEFK	MAKPEIKTAL	LTGTTYKYAA	KV.....	
E.coli-Sn1	NFWPAGPIFR	RLGAFFIRRT	FKG.....N	KL.....	
MousMitSn1	NIPVFSTLIH	KLGGFFIRRR	LDETPDGRKD	IL.....	
E.coli-Sn2	WIPFFGQLYW	LTGNLLIDRN	NRTKAHGTIA	EV.....	
Yst-Sn2-p1	YVPFLGWFMA	LSGTYFLDRS	KRQEAIDTLN	KG.....	
Maize-Sn2	FLPVIGWSMW	FAEYLFLEERS	WAKDEK.TLK	WGLQ.....	
Yst-Sn2-p2	SIPILGFGMR	NYNFIIFMSRK	WAQDKI.TLS	NSLAGLDSNA	RGAGSLAGKS
	101				150
A. calco.	.....EYLYS	ILSRNTPLEY	FPEGTRS...		
Yst-Sn1-p1	.....D	NTETFQSVFD	HLHTKGCVGI	FPEGGSHDRP	SL..LPIKAG
Yst-Sn1-p2	.....D	QSCVYHRVFE	HLAHNNCIGI	FPEGGSHDRT	NL..LPLKAG
E.coli-Sn1	.....Y	STVFREYLGE	LFSRGYSVEY	FVEGGRSRTG	RL..LDPKTG
MousMitSn1	.....Y	RALLHGHVVE	LLRQQQFLEI	FLEGTRSRSRG	KT..SCARAG
E.coli-Sn2	.....VNH	FKKRRISIWM	FPEGTRSRRGR	GL..LPFKTG	
Yst-Sn2-p1	.....LEN	VKKNKRALWV	FPEGTRSYSYS	ELTMLPFFKG	
Maize-Sn2	.....RLK	DFFRPFWLAL	FVEGTR....	...FTPAKLL	
Yst-Sn2-p2	PERITEEGES	IWNPEVIDPK	QIHWPNLIL	FPEGTN....	...LSADTRQ
Consensus			FPEGTRS		
	151				199
A. calco.	.....	.....	.....	.....	
Yst-Sn1-p1	VAIMALGAVA	ADPTMKVAVV	PCGLHYFHRN	KFRSRVLEY	GEPIVVDGK
Yst-Sn1-p2	VAIMALGAMD	KHPDVNVKIV	PCGMNYFHPP	KFRSRVVEF	GDPIEIPKE
E.coli-Sn1	TLSMTIQAML	RGTRPITLI	PIYIGYE...	.....HVMEV	G...TYAKE
MousMitSn1	VLSVVVNTLS	SENTIPDILVI	PVGISYD...	.....RIIE	G...HYNGE
E.coli-Sn2	AFHAAIAAGV	P.....II	PVCVSTTSNK	I..NLNRLHN	G...LVIVE
Yst-Sn2-p1	AFHLAQQSKI	P.....IV	PVVVSNTSTL	VSPKYGVFNR	G...CMIVR
Maize-Sn2	AAQE.YAASQ	GLPAPRNVL	PRTKG.FVSA	VS.....	
Yst-Sn2-p2	KSAK.YAAKI	GKKPFKNVLL	PHSTGLRYSL	QKLKPSI..ES	LYDITIGYS

Figure C-1: Pileup of known and putative acyltransferases. Regions used to construct the degenerate oligos are highlighted with the predicted consensus sequence underneath the pileup. The consensus sequence used for the construction of oligo 3'-3' is actually 5'-F(P,V,L)EG(T,G)RS-3'. The DNA sequence of the cloned fragment is illustrated above. The sequences used for the pile up are: (A. calco.), the determined *A. calcoaceticus* sequence appearing in sequence ID#18, (Yst-Sn1-p1), a putative Yeast Sn1-acyltransferase, (Yst-Sn1-p2), another putative Yeast Sn1-acyltransferase, (E.coli-Sn1), an *E. coli* Sn1-acyltransferase, (MousMitSn1), Mouse mitochondrial Sn1-acyltransferase, (E.coli-Sn2), *E. coli* Sn2-acyltransferase, (Yst-Sn2-p1), Yeast Sn2-acyltransferase, (Maize-Sn2), Maize Sn2-acyltransferase and (Yst-Sn2-p2), another Yeast Sn2-acyltransferase. Alignment was constructed by Dr. Joe Ogas using the PILEUP program from the GCG software package.

Table C-1: Synthetic degenerate oligonucleotides used in Appendix C.

<b>Name of primer</b>	<b>Sequence (5'-3')<sup>a</sup></b>	<b>Degeneracy</b>
Primer 5'-1	CA(T/C) CG(T/C/A) (T/A)(C/G)N CA(T/C) ATG GA(T/C) TA(T/C)	768
Primer 3'-3	N(G/C)(A/T) (A/G/T)CG N(G/C)(T/C) (A/G/T)CC (T/C)TC N(G/A)(G/C/A) (A/G)AA	221184

<sup>a</sup>Bases in parenthesis represent degeneracy at that position

polymerase (Boehringer Mannheim) in a total volume of 25  $\mu$ l. The reaction was cycled under the following conditions:

- Step 1: 94°C for 1 minute
- Step 2: 65°C for 1 minute -1°C per cycle
- Step 3: 72°C for 2 minutes
- Step 4: Repeat steps 1-3 ten times
- Step 5: 94°C for 1 minute
- Step 6: 55°C for 1 minute
- Step 7: 72°C for 2 minutes
- Step 8: Repeat steps 5-7 30 times
- Step 9: 72°C for 5 minutes
- Step 10: hold at 4°C

Following the PCR reaction the products were separated on a 1.2% agarose gel and visualized by staining using ethidium bromide. An expected band of approximately 250 bp was observed. This DNA was removed from the agarose by electroelution and subcloned into pGEM-T to produce the construct p51-33. The subcloned region was sequenced and is shown in Figure C-2. BLASTX alignment of this sequence against the GenBank database indicated a strong (BLASTX score of 255 with a probability score of  $2.2 \times 10^{-28}$ , 51 out of 84 (60%) amino acids were identical) similarity to sn-glycerol-3-phosphate acyltransferase from *E. coli* (accession number K00127) (Figure C-3) (Altschul et al., 1990).

At this point the experiment was drawn to a close. The probability of success was highly doubtful since it appeared that the degenerate oligos that were synthesized,



```

*** INPUT INFORMATION ***

FILE NAME : ACYL.DNA

SEQUENCE : 252BP; 51 A; 56 C; 57 G; 88 T.

*** SEQUENCE LIST *** (SINGLE)

      10      20      30      40      50      60
5' CATCGCTGGC ATATGGATTA TTTGCTGTTG TCCTATGTCA TTTACAAACG CGGCTTGATG
      70      80      90     100     110     120
   GTTCCGTACA TTGCAGCGGG TGACAATCTT AACTTGCCAT TCGTTGGTCA GCTATTGCGT
     130     140     150     160     170     180
   GGTGGTGGTG CATTCTTCAT TCGACGTTCT TTCCGTGGTA ATGGCTTATA TACTTCGGTT
     190     200     210     220     230     240
   TTAAAGAAT ATCTATACAG TATTTTGTCA CGTAACACGC CGCTTGAATA TTTCCCCGAG
     250
   GGCACACGCT CC 3'

```

Figure C-2: Sequence ID#18. Sequenced region of p51-33 that was found to contain homology to Sn-1 acyltransferase from *E. coli*.

```

>gp|K00127|ECOPLSB_2 sn-glycerol-3-phosphate acyltransferase [Escherichia coli]
      Length = 807

Plus Strand HSPs:

Score = 255 (117.3 bits), Expect = 2.2e-28, P = 2.2e-28
Identities = 51/84 (60%), Positives = 63/84 (75%), Frame = +1

Query:   1 HRWHMDYLLLSYVIYKRLMVPYIAAGDNLNLPFVGQLLRGGGAFFIRRSFRGNGLYTSV 180
          HR HMDYLLLSYV+Y +GL+ P+IAAG NLN   G + R GAFFIRR+F+GN LY++V
Sbjct:  306 HRSHMDYLLLSYVLYHQGLVPPHIAAGINLNFWPAGPIFRRLGAFFIRRTFKGNKLYSTV 365

Query:  181 FKEYLYSILSRNTPLEYFPEGTRS 252
          F+EYL  + SR  +EYF EG RS
Sbjct:  366 FREYLGELFSRGYSVEYFVEGGRS 389

```

Figure C-3: BLASTX alignment between a putative acyltransferase from *A. calcoaceticus* and Sn-1 acyltransferase from *E. coli*. Sn-1 acyltransferase from *A. calcoaceticus* is labelled as Query and the Sn-1 acyltransferase from *E. coli* is the sequence labelled Sbjct.

would most likely result in the amplification of known acyl-transferases. This might have been predicted since it was acyl-transferase sequences that the consensus sequences were based on. Therefore subsequent experiments in this direction were abandoned.

## REFERENCES

Altschul, S. F., Gish, W., Miller, W., Myers, E. W. and Lipman, D. J.. 1990. Basic Local Alignment Search Tool. *J. Mol. Biol.* 215: 403-410.

White, P. J., Hunter, I. S., and Fewson, C. A.. Codon Usage in *Acinetobacter* Structural Genes. In The Biology of *Acinetobacter*: Taxonomy, Clinical Importance, Molecular Biology, Physiology, Industrial Relevance. Plenum Press, New York, New York. 1991. Eds. Towner, K. J., Bergogne-Bérézin, E., and C. A. Fewson.

MICHIGAN STATE UNIV. LIBRARIES



31293013904408